

Construction and use of cDNA arrays in studying barley seed development and foxtail millet salt tolerance

Dissertation

zur Erlangung des akademischen Grades

Doctor rerum naturalium (Dr. rer. nat)

vorgelegt der

Mathematisch-Naturwissenschaftlich-Technischen Fakultät
der Martin-Luther-Universität Halle-Wittenberg
Fachbereich Biologie

von Nese Sreenivasulu
aus Anantapur, India

Gutachter: Prof. Dr. U. Wobus (IPK, Gatersleben)
Prof. Dr. C. Wasternack (IPB, Halle)
Prof. Dr. K. Breunig (Institut für Genetik, alle)

Datum der Verteidigung: 11.11.2002

urn:nbn:de:gbv:3-000004223

[<http://nbn-resolving.de/urn/resolver.pl?urn=nbn%3Ade%3Agbv%3A3-000004223>]

Preface

The phenomenon of seed development remains an intriguing problem and much effort has been directed toward its understanding. In this thesis, particular attention is drawn to early seed development and the process that lead up to the phase of storage product accumulation in barley by an integrative approach including genomics, biochemistry, physiology and histology. In addition, close inspection of early seed development in the *seg8* mutant of barley, which is defective in endosperm development, is carried out by genomic studies to understand the importance and complexity of maternal and filial tissue interactions during early caryopses development. By using the EST-array resources generated in this project we conducted gene expression analysis in foxtail millet cultivars differing in salt sensitivity by cross-hybridization experiments. The foxtail millet experimental system has been chosen because of the availability of two different genotypes differing in their sensitivity to salinity, which is absent in barley.

The thesis is comprised of four chapters. Chapter-1 is dealing with a general introduction of the main technology used; macroarrays based on expressed sequence tags (ESTs). A results and discussion section deals with construction and employment of an EST-based macroarray and its quality control. Chapter-2 consists of early seed development studies in the cultivar Barke of barley. Chapter-3 deals with early seed development in the *seg8* mutant of barley and chapter-4 with gene expression during salinity stress in foxtail millet. Each chapter (2, 3 and 4) starts with an introduction into the specific research area, describes the obtained results and discusses the relevant problems. To avoid repetitions Materials and Methods adopted are described in one section at the end of the thesis.

Contents

0 ABSTRACT.....	1
0 ZUSAMMENFASSUNG.....	4
CHAPTER 1: Expressed Sequence Tags (ESTs) and cDNA arrays as tools for global gene expression analysis in barley.....	8
1.1 AN INTRODUCTION TO EXPRESSED SEQUENCE TAGS (ESTs).....	8
1.1.1 EST-based gene discovery - its merits and inherent limitations.....	9
1.1.1.1 <i>cDNA library generation</i>	10
1.1.1.2 <i>EST sequencing and quality check</i>	10
1.1.1.3 <i>EST clustering/Gene content</i>	11
1.1.1.4 <i>Employing bioinformatic tools for annotation of ESTs</i>	11
1.1.2 High throughput transcript profiling by EST arrays.....	13
1.1.2.1 <i>Data mining</i>	14
1.1.2.2 <i>Array development</i>	15
1.1.2.3 <i>Probe synthesis/hybridization</i>	16
1.1.2.4 <i>Data analysis</i>	16
1.1.3 Biological interpretation of expression data.....	18
1.2 RESULTS AND DISCUSSION.....	19
1.2.1 EST generation from developing caryopsis library (0-15 DAF)	19
1.2.2 Annotation and functional classification of barley ESTs from developing caryopses....	19
1.2.3 Preparation of an EST macroarray	22
1.2.4 Performance of an EST macroarray containing 711 clones.....	23
1.2.5 Performance of an EST macroarray containing 1412 clones.....	26
1.2.6 Expression analysis of selected genes.....	27
CHAPTER 2: A Genomic approach to barley seed development.....	31
2.1 INTRODUCTION.....	31
2.1.1 Aspects of seed development.....	31
2.1.2 Molecular physiology of caryopses development during early stage.....	33
2.1.3 Carbohydrate metabolism and its role in seed development.....	34
2.1.3.1 <i>Role of sucrose / hexose transporters in seed development</i>	34
2.1.3.2 <i>Catabolism of sucrose to hexoses during seed development</i>	35
2.1.3.3 <i>Sugar sensing mechanisms during seed development</i>	36
2.1.3.4 <i>Sugar-regulated genes during seed/plant development</i>	36
2.1.4 Genomic approaches in seed development.....	37
2.2 RESULTS.....	39
2.2.1 Barley seed development: seed morphology and tissue preparation.....	39
2.2.2 Identification of 16 clusters representing tissue – and development-specific expression profiles during early caryopses development.....	40

2.2.3 Identification of functional classes of genes expressed specifically in pericarp tissue during caryopses development.....	43
2.2.4 Identification of functional classes of genes expressed in filial tissue during pre-storage and initial storage phase of developing caryopses.....	47
2.2.5 Carbohydrate metabolism during seed development	55
2.2.5.1 <i>Expression patterns of starch metabolic pathway genes in maternal and filial tissues..</i>	55
2.2.5.2 <i>Expression patterns of glycolysis metabolic pathway genes in maternal and filial tissues</i>	58
2.3 DISCUSSION.....	60
2.3.1 Pericarp specific expression during the development of barley caryopses (0-12 DAF)...	61
2.3.2 Gene expression map of the filial tissue during caryopses development (0-12 DAF).....	62
2.3.3 Interaction of maternal and filial tissues with reference to starch storage function	64
2.4 SUMMARY.....	66
CHAPTER 3: <i>seg8</i> mutant analysis during seed development	67
3.1 INTRODUCTION.....	67
3.2 RESULTS.....	70
3.2.1 Fresh weight of developing caryopses of <i>seg8</i> and wild type.....	70
3.2.2 Starch content in caryopses of <i>seg8</i> and wild type.....	71
3.2.3 Characteristic changes in sugar and metabolite concentrations in <i>seg8</i> and Bowman during pre-storage and storage phase in pericarp and embryo sac fractions.....	71
3.2.4 Anatomy and starch distribution pattern in developing grains of <i>seg8</i> mutant and wild type.....	73
3.2.5 Characteristic changes of gene expression in developing caryopses of <i>seg8</i> and Bowman	74
3.2.6 Different expression profiles of genes encoding enzymes of the sugar-to-starch pathway monitored in maternal and filial fractions of developing <i>seg8</i> mutant and Bowman wild type grains.....	76
3.2.7 mRNA expression of some transporter genes is drastically reduced in the filial fraction of developing <i>seg8</i> grains, as compared to the wild type.....	78
3.3 DISCUSSION.....	79
3.3.1 The <i>seg8</i> genomic environment integrated in "Bowman" displays the same features described for the original mutant identified in "Klages".....	79
3.3.2 Low mRNA expression of genes encoding key enzymes in the starch biosynthesis pathway may cause the reduced starch content of the mutant grain.....	79
3.3.3 High sucrose levels in the maternal and filial fraction during storage phase hint to a delay in sugar utilization and reduced starch accumulation in mutant's endosperm.....	80
3.3.4 A defect in starch accumulation can be expected for the developing gynoecium.....	81
3.4 SUMMARY	81

CHAPTER 4: Expression analysis of foxtail millet genotypes differing in salt tolerance.	82
4.1 INTRODUCTION.....	82
4.2 RESULTS.....	87
4.2.1 Growth attributes.....	87
4.2.2 Sodium content measurements.....	87
4.2.3 Effect of salinity on electrolyte leakage.....	88
4.2.4 Effect of salinity on malonaldehyde content.....	89
4.2.5 High-throughput expression analysis of salt stress responsive genes.....	89
4.2.6 Hydrogen peroxide scavenging enzymes.....	91
4.2.7 Isolation and identification of a full-length cDNA coding for a PHGPX from millet.....	91
4.2.8 Identification of PHGPX gene family in millet.....	93
4.2.9 Salt-specific induction of the PHGPX protein (25 kD).....	94
4.2.10 Purification of the salt-induced 25 kD PHGPX protein.....	95
4.2.11 Amino acid sequence analysis of salt-induced 25 kD protein.....	96
4.3 DISCUSSION.....	96
4.3.1 Application of barley macroarrays to foxtail millet.....	96
4.3.2 Differential response of physiological parameters to salinity stress in salt-tolerant and salt sensitive seedlings of foxtail millet.....	97
4.3.3 The possible role of hydrogen peroxide scavenging enzymes in salt-mediated oxidative stress tolerance.....	97
4.4 SUMMARY.....	100
5. MATERIALS AND METHODS SECTION.....	101
5.1 Methodology adopted for genomic studies in barley seed development and <i>seg8</i> mutant analysis.....	101
5.1.1 Plant material.....	101
5.1.2 EST identification, annotation and metabolic pathway assignment.....	101
5.1.3 Macroarray preparation.....	102
5.1.4 RNA extraction and synthesis of ³³ P-labelled cDNA probes.....	103
5.1.5 Procedure for cDNA macroarray hybridization.....	104
5.1.6 Array evaluation.....	104
5.1.7 Data filtering.....	105
5.1.8 Clustering algorithmic.....	105
5.1.9 Northern blotting.....	105
5.1.10 Extraction and determination of metabolic intermediates.....	106
5.1.11 Determination of starch.....	106
5.2 Methodology adopted for salinity response studies in foxtail millet.....	107
5.2.1 Plant material and salinity treatments.....	107
5.2.2 Growth parameters.....	107
5.2.3 Determination of sodium content.....	107
5.2.4 Electrolyte leakage.....	107
5.2.5 Estimation of malonaldehyde (MDA) concentration.....	108
5.2.6 cDNA arrays.....	108

5.2.6.1 Array design.....	108
5.2.6.2 Synthesis of ³³ P hybridization cDNA probe, hybridization and data normalization	108
5.2.7 RT-PCR mediated cloning of PHGPX cDNA.....	109
5.2.8 Southern hybridization.....	109
5.2.9 Northern blot analysis.....	109
5.2.10 Characterization of the salt-induced 25 kD protein.....	109
5.2.10.1 Protein extraction and estimation of protein content.....	109
5.2.10.2 SDS-PAGE analysis.....	110
5.2.10.3 Purification of 25 kD protein.....	110
5.2.10.4 Amino acid sequencing.....	110
6. REFERENCES.....	111
7. ACKNOWLEDGEMENTS.....	123

Index of Tables

Table 1: Expressed sequence tags of major cereals in dbEST.....	9
Table 2: Web sites useful for EST annotation.....	13
Table 3: Design principles of arrays used for expression analysis.....	16
Table 4: Analytical tools with application to gene expression and worldwide web addresses of softwares for array data analysis from the public domain as well as the private sector	17
Table 5 cDNA clones that are preferentially expressed in pericarp.....	25
Table 6 cDNA clones preferentially expressed in the embryo sac.....	26
Table 7 Members of cluster 1_1, 1_2 and 1_3 showing higher expression in pericarp tissue....	45
Table 8 Members of cluster 2_1, 2_2 and 2_3 showing higher expression in the filial tissue during the pre-storage phage.....	48
Table 9 ESTs included in cluster 3_2 showing up regulation of expression in the intermediate phase of development in filial tissues.....	50
Table 10. ESTs included in cluster 4_1, 4_2, 4_3 and 4_4 showing up regulation of expression in the storage phase of the filial tissues.....	52
Table 11 Members of cluster 5 showing high expression especially in the storage phase of the filial tissues.....	55
Table 12: ESTs belongs to the sugar to starch pathway are preferentially down regulated in developing caryopses of <i>seg8</i> mutant.....	75
Table 13 cDNA clones that are preferentially expressed in salt-treated tolerant seedlings.....	90

Index of Figures

Fig. 1 A diagrammatic representation of EST-array technique.....	14
Fig. 2 Scatter plot representation of EST annotation data.....	20
Fig. 3a Annotation of 1400 ESTs from developing caryopses (0-12 DAF).....	21
Fig. 3b Functional classification of ESTs from developing caryopses (0 to 12 DAF).....	21
Fig. 4 Segment of a cDNA macroarray.....	23
Fig. 5 Comparison of the normalized signal intensities obtained from two independently spotted arrays hybridized with the same labelled cDNA (A) and from one array hybridized successively with labelled cDNA from embryo sac and pericarp tissues of the developing barley grain 1-7 DAF (B).....	24
Fig. 6 Levels of transcripts differentially accumulated in pericarp and embryo sac of developing caryopses measured by northern analysis	29
Fig. 7 Comparison of expression levels of selected genes resulting from cDNA array and Northern blot analyses.....	29
Fig. 8 Schematic representation of the histological organization of a barley caryopsis.....	35
Fig. 9 Developing caryopses and hand-dissected maternal (pericarp) and the filial (endosperm and embryo) fractions.....	40
Fig.10 Tissue and development-specific expression profiles identified by k-mean cluster analysis.....	42
Fig. 11 Groups of genes specifically expressed in the maternal tissue (0-12 DAF).....	44
Fig. 12 Up regulation of gene expression (cluster 1_2 and 1_3) in the maternal fraction demonstrated by the Eisen method.....	44
Fig. 13 Groups of genes specifically expressed in filial tissues (0 to 12 DAF).....	47
Fig. 14 Expression of photosynthetic genes in the filial fraction of the caryopsis during 4 to 8 DAF.....	51
Fig. 15 Schematic representation of the sucrose-starch pathway and mRNA level of the respective enzymes as determined by expression analysis in both maternal pericarp (p) and filial tissue containing endosperm and embryo (e).....	57
Fig. 16 Schematic representation of the glycolysis pathway and mRNA level of the respective enzymes as determined by expression analysis in both the maternal fraction containing mainly pericarp (p) and filial tissues containing endosperm and embryo (e).....	59

Fig. 17 After separation of maternal (pericarp) from the filial part (embryo sac), fresh weight of both fractions was estimated and the fresh weight ratio was calculated. On X-axis the developmental scale 2-14 DAF (Days After Flowering) is given in every two day intervals...	70
Fig. 18 Starch content in caryopses of <i>seg8</i> and wild type.....	71
Fig. 19 Sugar and metabolite measurements determined in maternal and filial fraction of <i>seg8</i> and wild type of developing caryopses.....	72
Fig. 20 Starch distribution pattern of <i>seg8</i> caryopses shown in median-transversal sections (8-12 DAF) by Iodine staining.....	73
Fig. 21 Comparison of the normalized signal intensities obtained from two independent experiments (experiment 1 and 2).....	74
Fig. 22 Expression data of EST clones with homology to genes coding sugar to starch pathway were selected.....	77
Fig. 23 Expression profiles of transporter genes in filial fraction of mutant (a) and wild type (b) during early and mid caryopses development.....	78
Fig. 24 A proposed model for pathways leading to the induction of reactive oxygen species (superoxide radical, hydrogen peroxide and hydroperoxides) during NaCl treatment and the role of the protective antioxidative enzymes superoxide dismutase (SOD), ascorbate peroxidase (APX) and phospho glutathione peroxidase (PHGPX) in scavenging superoxide, hydrogen peroxide and hydroperoxide radicals respectively.....	84
Fig. 25 Differences in root and shoot length of 5-day old seedlings of a salt-tolerant (P – Prasad) and a salt-sensitive (L – Lepakshi) foxtail millet cultivar grown under control conditions (CP – control Prasad; CL – control Lepakshi) and at different NaCl concentrations (SP – salt-treated Prasad; SL – salt-treated Lepakshi).....	87
Fig. 26 Na ⁺ accumulation in 5-day-old seedlings of the tolerant and sensitive foxtail millet cultivar grown at different NaCl concentrations.....	88
Fig. 27 Electrolyte leakage rate measured in cells of 5-day-old seedlings of the tolerant and sensitive foxtail millet cultivars grown at different salt concentrations.....	88
Fig. 28 Variation in the MDA content of salt-tolerant and salt-sensitive seedlings of foxtail millet grown under different concentrations of NaCl.....	89
Fig. 29 Northern blot analysis of PHGPX mRNA accumulation following salt treatment (250 mM NaCl) in the tolerant foxtail millet cultivar as compared to the salt-sensitive cultivar.....	91
Fig. 30 Amino acid sequence alignment of cDNA clone isolated from <i>Setaria italica</i> PHGPX (SiGPX) with PHGPX sequences from other species.....	92
Fig. 31 Southern blot analysis of <i>Setaria italica</i> PHGPX gene.....	94

Fig. 32 Protein patterns of 5-day-old tolerant seedling samples grown under control (Ct) conditions and different types of stress such as 150 mM NaCl (S), drought (D), high temperature (H) and cold (C) depicted on a 12-15% gradient acrylamide gel..... 94

Fig. 33 Purification of the salt-induced 25 kD protein from NaCl-treated tolerant seedlings by DEAE-Sepharose and FPLC..... 95

ABSTRACT

Single-pass sequencing of randomly chosen cDNA clones is currently the most efficient method for the discovery of many genes from cereals with large genomes. Management and analysis of the enormous amount of low-quality sequence data requires great care and powerful computational methods for annotation. In order to study the network of gene expression underlying seed development during the pre-storage (0 to 4 days after flowering, DAF) and the initial storage phase (6 to 12 DAF) in barley, we employed EST-based macroarrays. Radioactive labelled cDNA probes were prepared from pericarp and post-fertilization embryo sac preparations of developing caryopses (0 –12 DAF) in two-day intervals and hybridized to cDNA macroarrays containing 1412 cDNA inserts, which represent 1184 unique sequences. Grouping of genes by K-mean cluster analysis according to gene expression patterns resulted in 16 gene sets, which can be arranged into 6 cluster groups. Most of the genes up regulated in the pericarp encode proteases, hormonal regulated proteins, and proteins involved in energy production and carbohydrate and lipid metabolism (cluster group1). In the embryo sac probe unique developmental stage specific transcript profiles were identified. During the pre-storage phase, 25% of genes up regulated in embryo sac probe are related to cell division and cell elongation (cluster group 2). In the intermediate phase, photosynthetic genes are up regulated in embryo sac (cluster group3). During the onset of storage phase the embryo sac fraction mainly represents genes belonging to specific metabolic pathways, for instance, the starch (cluster group 4) and storage protein (cluster group 5) biosynthetic pathways including several protease and amylase/trypsin inhibitor genes. On the basis of annotated ESTs and global expression analysis an attempt was made to unravel the complex metabolic and regulatory networks involved during barley seed development. A detailed examination of gene expression patterns related to sucrose to starch and sucrose to pyruvate metabolism pathways provides interesting results of gene networking. Some of the differentially regulated genes detected by expression analysis were studied and further characterized by northern analysis and *in situ* hybridizations.

seg8, a barley mutant defective in seed development, provides a unique opportunity to study the influence of the maternal tissue on endosperm development and storage product accumulation. In order to gain deeper insight into the complex regulatory and metabolic control of maternal and filial tissues and their interaction we analysed *seg8* mutant by expression analysis and metabolite profiling. During pre-storage phase of early caryopsis development no obvious difference were found in seed fresh weight between wild type and

mutant; mutant seeds weighed approximately 43% of normal 'Bowman' wild type during storage phase. Microscopic studies revealed that *seg8* mutant shows massive growth of nucellar projection tissue (maternal) with abnormal shrunken endosperm at 4 days after flowering. The failure of proper endosperm development in *seg8* that was evident already during 4 DAF became a prominent event at 10 DAF onwards with two lobes of endosperm with professed nucellar projection touching the dorsal crease. In the present study we used the 1412 cDNA array to analyse expression of genes involved in different metabolic pathways during early stages of development (2-14 DAF, days after flowering) between '*seg8*' mutant and its corresponding wild type 'Bowman'. A comparison of *seg8* versus Bowman during 0-14 DAF at whole caryopsis level as well as in maternal and filial fractions hinted that key genes of carbohydrate metabolism from sugar to starch pathway are down regulated in *seg8* mutant. The results provide evidence that genes encoding the UDP-glucose metabolising enzymes are specifically down regulated in *seg8*. As expected a decrease in the ADP-glucose content was registered in the filial fraction containing endosperm. On the other hand transcripts coding for storage proteins did not yield any considerable differences between mutant and wild type. The reason for maternal inheritance of the abnormal endosperm mutant is not clear, since there is no differences found among transcripts expressed in maternal tissue in the very early stages except at 0 DAF. Characteristic irregularities occur in the endosperm tissue itself with lower expression of carbohydrate metabolic genes immediately before storage activity starts in endosperm. The observed major changes in the expression of starch biosynthetic pathway genes in *seg8* mutant result in less starch accumulation. In addition, we observed decreased transcript levels of some transporters in filial fraction of mutant during 4 to 14 DAF.

Using cDNA macroarray encoding stress genes selected from a barley EST library, we identified transcripts differentially expressed in salt (NaCl)-treated tolerant and sensitive seedlings of foxtail millet. Transcripts of unknown genes and hydrogen peroxide scavenging enzymes such as phospholipid hydroperoxide glutathione peroxidase (PHGPX) and, additionally, ascorbate peroxidase (APX) and catalase 1 (CAT1) were found to be up regulated during salinity treatment in five-day-old salt-tolerant foxtail millet seedlings (Cv. Prasad). In order to understand the protection mechanism induced in salt-treated tolerant seedlings at the molecular level, we cloned and characterized a foxtail millet cDNA encoding a PHGPX homologue, which shows 85% and 95% homology to one stress-induced member of the small barley PHGPX gene family coding for non-selenium glutathione peroxidases at

the DNA and protein level, respectively. As shown by Southern blot analysis, a small family of PHGPX genes exists in foxtail millet, too. The expression of the PHGPX gene is markedly induced in tolerant seedlings by high salt concentrations, suggesting that its product plays a role in defence against salt-induced oxidative damage. To analyse this process further at the protein level we examined protein expression patterns under various stress conditions. A 25 kD protein was found to be induced prominently under high salt concentrations (250 mM). The salt-induced 25 kD protein has been purified and identified as PHGPX protein based on its peptide sequence. The increase of the PHGPX protein level induced under salt stress conditions only in tolerant seedlings parallels the result found for the PHGPX mRNA in the comparative expression analysis (see above). Most likely, this non-selenium glutathione peroxidase is one of the components conferring resistance against salt to the tolerant foxtail millet cultivar. The tolerant five-day-old seedlings grown during high salinity treatment (200 mM NaCl) contained a lower amount of Na⁺ ions and showed a lower electrolyte leakage than sensitive seedlings. In conclusion, our comparative studies indicate that at least in part, salt-induced oxidative tolerance is conferred by an enhanced compartment specific activity of antioxidant enzymes (Sreenivasulu *et al.*, 2000).

Zusammenfassung

Gegenwärtig ist die Sequenzierung großer Cerealien-Genome vor allem aus Kostengründen nicht möglich. Eine effiziente alternative Methode zur Identifizierung von Genen ist die unidirektionale Sequenzierung zufällig ausgewählter cDNA-Klone. Die enorme Anzahl und die Qualitätsmängel der entstehenden Primärsequenzen (ESTs – Expressed Sequences Tags) erfordern während des Annotationsprozesses sorgfältige Analysen unter Verwendung leistungsfähiger Software.

Die Entwicklung von Gerstensamen wird durch Netzwerke von Genexpressionsprogrammen gesteuert. cDNA-Makroarray-Filter, basierend auf Karyopsen-spezifischen ESTs, wurden verwendet, um Genexpressionsprogramme während der Vorspeicher- (0 – 4 Tage nach der Blüte, Days After Flowering, DAF) und der Speicherphase der Gerstensamen (6 – 12 DAF) zu analysieren. Zur cDNA-Makroarray-Analyse wurden Filter mit 1412 cDNA-Inserts (repräsentieren 1184 unikale Sequenzen) mit radioaktiv markierten cDNA-Proben hybridisiert. Zur Amplifikation der cDNA wurde mRNA verwendet, die in 2-Tages-Abständen sowohl aus dem maternalen als auch aus dem filialen Teil des sich entwickelnden Gerstenkorns isoliert wurde. Die Anwendung der *K mean* Cluster Analyse auf die Expressionsanalyse-Ergebnisse ergab 16 Gruppen von Genen (Cluster) mit ähnlichem Expressionsprofil, die in 6 Clustergruppen zusammengefaßt werden können. Gene mit höherer Expression im maternalen Teil des Korns (*cluster group 1*) codieren Proteasen, hormonell regulierte Proteine und Proteine, die Funktionen in Energieproduzierenden Prozessen und im Kohlehydrat- und Lipid-Metabolismus besitzen. Den filialen Teil des Korns charakterisieren für das Entwicklungsstadium spezifische Expressionsprofile. 25% der während der Vorspeicherphase hochregulierten Gene können mit Zellteilungs- und -streckungsprozessen in Verbindung gebracht werden (*cluster group 2*). In der intermediären Phase (8 – 10 DAF) hochexprimierte Gene codieren für Photosynthese-assoziierte Genprodukte (*cluster group 3*). Zu Beginn der Speicherphase werden in der filialen Fraktion Gene exprimiert, deren Produkte spezifischen Biosynthesewegen zugeordnet werden können, so z.B. der Akkumulation von Stärke (*cluster group 4*) und Reserveproteinen (*cluster group 5*) sowie der Expression von Genprodukten, die den Abbau der Speicherstoffe verhindern (verschiedene Protease- und Amylase/Trypsin-Inhibitoren). Ausgehend von der Annotation der ESTs und der Gesamtheit der Expressionsanalyse-Ergebnisse wurde

der Versuch unternommen, das komplexe Netzwerk von Regulations- und Biosynthesewegen während der Gerstensamen-Entwicklung im Zusammenhang darzustellen. Die detaillierte Auswertung der für den Stärkebiosynthese- und Glykolyse-Stoffwechselweg spezifischen Genexpressionsprofile ergab interessante Ergebnisse in Bezug auf das Netzwerk der Genexpression. Einige der differentiell exprimierten Gene wurden mittels Northernblotting und *in situ*-Hybridisierung näher untersucht, auch um die Ergebnisse der Expressionsanalyse zu bestätigen.

Seg8, eine Mutante mit Defekten in der Endospermentwicklung des Gerstenkorns, bietet exzellente Möglichkeiten, den Einfluß der maternalen Gewebe auf Endosperm-Entwicklung und Speicherstoff-Akkumulation zu untersuchen. Um die komplexe regulatorische und metabolische Wechselwirkung zwischen maternalen und filialen Geweben näher zu untersuchen, wurden für die Samenentwicklung der Mutante *seg8* Expressions- und Metabolitprofile erstellt. Während der Vorseicherphase wurden keine Unterschiede im Frischgewicht der Mutanten- und Wildtypsamen gefunden. Jedoch zeigten mikroskopische Untersuchungen einen verzögerten Abbau des Nucellus-Gewebes und einen abnormen Aufbau der nucellaren Projektion (beide Gewebe sind maternalen Ursprungs) während der frühen Entwicklung (2 – 4 DAF) der Mutantenkörner. Abweichungen von der normalen Endospermentwicklung sind bereits 4 DAF nachweisbar, werden jedoch 10 DAF deutlich sichtbar anhand der Ausbildung zweier Endospermhälften, die von der nucellaren Projektion getrennt werden, die den gegenüberliegenden Rückenbereich des Korns berührt. In dieser Arbeit wurde der 1440 cDNA-Fragmente enthaltende Makroarray-Filter benutzt, um Genexpressionsprogramme verschiedener Biosynthesewege während der frühen Entwicklung (2 – 14 DAF) von Mutanten- und Wildtyp-Körnern vergleichend zu untersuchen. Sowohl bei der Verwendung von ganzen Körnern als auch bei der Analyse der maternalen und filialen Fraktion zeigte sich, dass die Expression der Schlüsselgene des Stärke-Biosyntheseweges in *seg8* auf einem niedrigeren Niveau erfolgt als im Wildtyp „Bowman“. Besonders die Expression der UDP-Glukose metabolisierenden Enzyme ist in *seg8* reduziert. Wie erwartet, konnte eine Erhöhung des ADP-Glukosegehaltes in der filialen Fraktion der Mutantenkörner nachgewiesen werden. Jedoch unterscheidet sich die Transkription der Speicherprotein-Gene in *seg8* und Wildtyp-Körnern nicht. Die maternale Vererbung des *seg8*-Phänotyps kann auf der Grundlage der bisher vorliegenden Ergebnisse nicht erklärt werden. Die

Expressionsanalyse zeigte keine Unterschiede in den Transkriptmengen, die während der Bestäubung (0 DAF) in den maternalen Geweben von *seg8* und Wildtyp exprimiert werden. Charakteristisch ist die Verringerung der Expression der Gene des Kohlenhydratmetabolismus unmittelbar vor Beginn der Stärkeakkumulation im Endosperm der Mutantenkörner. Die beobachtete Verringerung der Expressionsraten führt zu einer Verringerung der Stärkeakkumulation. Weiterhin konnte eine Verringerung der Expression mehrerer für Transport-Proteine codierenden Gene in der filialen Fraktion der Mutantenkörner nachgewiesen werden.

Unter Verwendung eines Makroarray-Filters, der für Stress-Gene codierende cDNA-Fragmente aus einer Gersten-cDNA-Bank enthielt, wurden Transkripte identifiziert, die differentiell in Salz-toleranten und –sensitiven Varietäten der Fuchsschwanz-Hirse (*Setaria italica* L.) unter NaCl-Stress exprimiert werden. Transkripte unbekannter Gene und Wasserstoffperoxid-abbauender Enzyme, wie z.B. Phospholipid Hydroperoxid Glutathion Peroxidase (PHGPX), Ascorbat Peroxidase (APX) und Katalase 1 (CAT1) wurden in der 5-Tage-alten Keimlingen der toleranten Varietät (Cv. Prasad) unter Salz-Stress in erhöhter Menge nachgewiesen. Um den unter Salz-Stress in den toleranten Keimlingen initiierten Abwehrmechanismus auf molekularer Ebene zu verstehen, wurden cDNAs aus Fuchsschwanz-Hirse isoliert und charakterisiert, die für ein PHGPX-Homologes codieren. Die cDNA zeigt 85% (DNA) und 95% Homologie (Protein) zu einem Mitglied einer kleinen Stress-induzierten PHGPX-Genfamilie aus Gerste, die für nicht-Selen Glutathion Peroxidasen codiert. Mittels Southernblot-Analyse konnte gezeigt werden, dass auch in Fuchsschwanz-Hirse eine kleine Genfamilie existiert. Die Expression des PHGPX-Gens wird unter Salz-Stress in den Keimlingen der toleranten Varietät deutlich induziert, woraus abgeleitet werden kann, dass das Genprodukt eine Rolle in der Abwehr der Salz-induzierten oxidativen Zerstörung spielt. Um diesen Prozess auch auf Protein-Ebene zu verstehen, wurden Protein-Expressionsmuster unter verschiedenen Stress-Bedingungen untersucht. Bei hohen Salzkonzentrationen (250 mM) wurde besonders ein 25 kD-Protein induziert. Dieses Protein wurde gereinigt und anhand seiner Peptid-Sequenz als PHGPX identifiziert. Die Erhöhung der Konzentration des PHGPX-Proteins unter Salz-Stress in Keimlingen der toleranten Varietät entspricht der für die PHGPX-mRNA in der vergleichenden Expressionsanalyse nachgewiesenen Expressionserhöhung. Wahrscheinlich ist diese

nicht-Selen Glutathion Peroxidase eine der Komponenten, die in Fuchsschwanz-Hirse Resistenz gegen Salz vermittelt. Die 5-Tage-alten Keimlinge der toleranten Varietät, die unter Salz-Stress (200 mM) angezogen wurden, enthielten geringere Na⁺-Mengen und zeigten einen geringeren Elektrolyt-Verlust als sensitive Keimlinge unter vergleichbaren Bedingungen. Gemeinsam mit bereits publizierten Ergebnissen (Sreenivasulu et al., 2000) zeigen diese Untersuchungen, dass Toleranz gegen Salz-induzierten oxidativen Stress durch eine verstärkte Kompartiment-spezifische Aktivität antioxidativer Enzyme vermittelt wird.

CHAPTER 1

Expressed Sequence Tags (ESTs) and cDNA arrays as tools for global expression analysis in barley

1.1 AN INTRODUCTION TO EXPRESSED SEQUENCE TAGS

The discovery, characterization, and exploitation of agriculturally important genes is critical to further increase productivity and to meet the food security needs of mankind because of the ever increasing population and the hardship being faced by the agriculture. Prime targets are the genes of crop plants like rice, wheat, maize, barley and sorghum, which belong to the ten most important crop plants worldwide. Traditionally, gene discovery programs followed a "one gene at a time" approach, which is both costly and time consuming. In the present era of genomics, scientists are taking global approaches such as genomic sequencing. Among cereals, rice has the smallest genome with a size of only 430 Mbp. Consequently, the complete set of genes and their genomic locations could be identified *via* genomic sequencing with an acceptable investment. The genomes of the other species are considerably larger, sorghum 800 Mbp, maize 2,500 Mbp, barley 5,500 Mbp and wheat 16,000 Mbp, which precludes this approach. As an alternative to a genomic sequencing program, an EST based approach, which is an unedited sequence generated from single-pass sequencing read of a cDNA clone chosen randomly from a library at all stages of plant growth and life cycle allows fast and affordable gene identification at a large scale (Adams *et al.*, 1992; Rounsley *et al.*, 1996). This approach greatly assists in the identification and isolation of economically important genes among cereals. Large EST programs for the grasses and other crop species are currently under way in many research groups worldwide. The ESTs from wheat, barley, maize, sorghum, or other closely related Triticeae species are being produced to maximize the access to all genes in the cereal genomes (Table 1). Currently, the EST database (<http://www.ncbi.nlm.nih.gov/dbEST>) contains 684,838 EST entries from monocotyledonous

plants, out of which 163,282 are reported from wheat, 155,288 are reported from maize, 155,287 from barley, 104,880 from rice, and 107,278 from different species of sorghum.

Table 1: Expressed sequence tags of major cereals in dbEST

species	ESTs	cDNA libraries	low quality	≤100 b/≥800 b	<i>E. coli</i>
<i>Triticum aestivum</i>	163,283	38	4,068	82 / 1,793	198
<i>Zea mays</i>	155,288	31	3,850	186 / 1,352	16
<i>Hordeum vulgare</i>	155,287	31	5,043	637 / 24,916	178
<i>Oryza sativa</i>	104,880	27	8,889	140 / 1,464	289
Sorghum bicolor	84,712	10	132	349 / 18	132
Sorghum propinquum	21,387	2	41	10 / -	31
Sorghum halepense	1,179	1	-	- / -	10

For the major cereals the number of entries in dbEST (05-2002) and the number of cDNA libraries from which more than 500 ESTs were derived is listed. Critical quality parameters include the number of ESTs containing low quality segments (≥ 3 ambiguities/25 bases), short (≤ 100 bases) and overly long ESTs (≥ 800 bases) as well as contaminations, e.g. sequences showing homology to *E.coli* sequences (>100 bases with $\geq 95\%$ identity).

The large-scale EST projects provided an extensive reservoir of sequences in cereals. To accomplish further biological knowledge the available sequence information of respective genes has to be converted into biologically significant knowledge with respect to putative identification of functional role of genes and relative abundance of transcripts belonging to different cells, tissues, developmental stages and stress treatments. Proper annotation of EST data is crucial to integrate the various kinds of data into a higher level of biological knowledge. The EST approach is inexpensive and efficient in gene-discovery that can be used to identify novel cDNAs encoding enzymes of specific plant metabolic pathways. Collections of ESTs from metabolically active tissues during different developmental stages of plant growth and seed set provide a platform for quantitative estimates of gene expression levels and thus to unravel plant metabolic and regulatory networks.

1.1.1 EST-based gene discovery - its merits and inherent limitations

Gene discovery *via* ESTs is comprised of four steps which include (i) the construction of cDNA libraries, (ii) single-pass sequencing of (randomly) selected clones and EST quality

check, (iii) the alignment of ESTs to identify the number of genes represented and (iv) the annotation of these partial sequences or genes which are available thereof.

(i) cDNA library generation

The production of ESTs starts with the construction of cDNA libraries. Within a certain tissue of defined developmental and physiological status, only a specific fraction of the entire set of genes of an organism is expressed and the level of abundance of mRNAs for different genes varies widely. This makes it less likely to identify low expressed genes and leads to redundant sequencing of the ones that are highly expressed. In addition to the construction of several cDNA libraries to cover a wider spectrum of expressed genes, various strategies have been applied to circumvent or minimize redundant sequencing. cDNA libraries can be normalized either during their synthesis by subtractive hybridization or related approaches (Kohchi *et al.*, 1995) or afterwards by techniques such as oligonucleotide fingerprinting (Guerasimova *et al.*, 2001). The identification and exclusion of already sequenced cDNAs or even complete libraries when redundant sequencing exceeds a certain limit, provides another valid alternative to minimize the cost of uncovering new genes. Table 1 provides an overview for the number of relevant cDNA libraries employed in these programs. Despite these efforts it can be shown for species with completely sequenced genomes that the number of genes represented by ESTs is significantly smaller as the number of predicted genes. For instance more than 113,000 ESTs from *Arabidopsis* represent less than 16,200 genes out of the 25,556 genes, which are predicted in the genome.

(ii) EST sequencing and quality check

After the isolation of cDNA clones, plasmid preparation and single-pass sequencing, several quality issues have to be addressed. Vector and low quality sequences as well as bacterial sequences or other contaminations need to be removed from the non-processed sequence data. No generally accepted standards exist for these procedures so that the quality of submitted sequences does depend on the submitting laboratory. Wrong bases as well as small insertions and deletions (indels) go undetected in single-pass sequences. Especially indels occur frequently at short homo polymer stretches at greater read length. For that reason, sequences should be trimmed at a certain read length. This has not been done for many database entries, as can be seen by the large number of ESTs with more than 800 bases (Table 1). Furthermore, handling errors or lane tracking problems in gel-based sequence analysis lead to wrong assignments of clones and sequences. Such errors can not be recognized in databases, but will

become apparent when the cDNA clones have to be used, e.g. for the construction of cDNA arrays (see below).

(iii) EST clustering / Gene content

The assembly of gene sequences or parts thereof from a collection of ESTs to determine the number of represented genes is a non-trivial task. Above-mentioned problems with sequence quality and possible sequence errors together present huge challenges for EST clustering. Special program packages such as the Phred/Phrap/Consed system (<http://www.phrap.org/>), UniGene (Boguski *et al.*, 1995), Genexpres Index (Houlgatte *et al.*, 1995), TIGR_ASSEMBLER (ftp://ftp.tigr.org/pub/software/TIGR_assembler/), STACK_PACK (Christoffels *et al.*, 1999; Miller *et al.*, 1999), CAP3 (Huang and Madan, 1999), PCP/CAP4 (www.paracel.com/products), HarvESTer (<http://mips.gsf.de/proj/gabi/news/bioinformatics.html>) and others have been and continue to be developed for the assembly of large EST collections. The result of the assembly process can be divided in so-called singletons, sequences which do not assemble with any other sequence, and groups of assembled sequences which might be called clusters, contigs, tentative consensus, tentative genes, unique genes (unigenes), etc.

Several institutions provide pre-calculated assemblies of ESTs, sometimes including completely sequenced cDNA clones and genomic sequences to improve the results. Prominent examples are the gene indexes at The Institute of Genomic Research (TIGR; <http://www.tigr.org>), which provide an overview of gene indices of various species. Even so certain quality issues of ESTs are addressed by TIGR, one should keep in mind that the number of unique sequences should not be interpreted as the number of genes identified in a certain species.

(iv) Employing bioinformatic tools for annotation of ESTs

In addition to the number of genes represented by ESTs, it is important to collect information about their (potential) function and to associate this information with the respective clones. This process, called annotation will help to identify promising targets for further research and to interpret results of downstream applications which employ these clones, respectively their sequences, e.g. global expression analysis. The annotation process has to face the same difficulties as the annotation of unknown genes in genomic sequences (except splice site prediction), but is further complicated by the partial information and the high, yet undefined

error content of ESTs. To minimize these problems, consensus sequences of aligned ESTs should be used whenever available, because they contain more information of increased reliability with respect to individual ESTs. The primary question, which needs to be addressed from the annotation point of view, is if the EST is identical or similar to a known gene. The possible approach is comparing its sequence with appropriate databases using Blast or FASTA programs. Comparisons at the nucleotide level will identify closely related database entries, whereas comparisons at the amino acid level, after translation of the EST in all (meaningful) reading frames, can be used to uncover less related genes. The public availability of databases and the Blast (Altschul *et al.*, 1997) and FASTA (Stoesser *et al.*, 2002) programs as well as the low price of high computing power make it feasible to run many thousand comparisons at low costs within a moderate time. Yet, the incomplete sequence information with respect to the cDNA clone itself and with respect to the gene content of the genome usually precludes a precise answer. Usually the description and references contained in a database entry related to an EST provide a quick access to the relevant information, but several problems are associated with this approach. Mainly as a result of genomic sequencing, many hypothetical genes will be encountered for which no functions could be assigned. The description of a database entry might be outdated or even worse it may propagate annotation errors. To obtain a higher level of confidence specialized databases, which are curated and providing more detailed information can be used for sequence comparisons, e.g. SwissProt (Bairoch and Apweiler, 2000), TRANSFAC for transcription factors (Wingender *et al.*, 2000), BRENDA for enzymes (Schomburg *et al.*, 2002; Schoof *et al.*, 2002).

In case no related genes could be identified for an EST or if the related gene does not provide information with respect to function, attempts shall be made to identify functional motifs, which may guide further investigations. The identification of protein patterns from the PROSITE database (Falquet *et al.*, 2002), Pfam (Bateman *et al.*, 2002) and other databases, the prediction of targeting signals and transmembrane helices as well as the prediction of open reading frames provide several opportunities. In general computational annotation of ESTs is still in its infancy (Table 2). Software tools have to be improved significantly to meet the challenges provided by a rapidly increasing number of ESTs and to cope with their specific problems. Especially for cereals with large genomes EST development will be important because complete genomic sequences are not expected to be available in the near future.

Table 2: Web sites useful for EST annotation

programs	purpose	URL
BLAST	sequence comparison	http://www.ncbi.nlm.nih.gov/BLAST/
FASTA	sequence comparison	http://www.ebi.ac.uk/fasta33
SWISSPROT	protein sequence comparison	http://www.expasy.org/sprot/
PFAM	protein sequence comparison	http://www.sanger.ac.uk/Software/Pfam/
PROSITE	protein pattern findings	http://www.expasy.ch/prosite/
TRANSFAC	transcription factor detection	http://transfac.gbf.de/TRANSFAC/
BRENDA	enzyme functional data collection	http://www.brenda.uni-koeln.de/
TMPRED	trans membrane prediction	http://www.ch.embnet.org/software/TMPRED_form.html
TMHMM	trans membrane helice prediction	http://www.cbs.dtu.dk/krogh/TMHMM/
FRAMED	GC content	http://www.toulouse.inra.fr/FrameD/cgi-bin/FD
GENEMARK	prediction of ORF	http://genemark.biology.gatech.edu/GeneMark/
GENESCAN	prediction of ORF	http://202.41.10.146/
BESTORF	prediction of ORF	http://genomic.sanger.ac.uk/gf/gf.html

The table presents the tools, which are useful for the annotation of ESTs. Some of the publicly available tools are listed, which might be used to annotate translated ESTs with respect to functional motifs, but none of them has been designed or adjusted to handle ESTs specifically and to take care of associated problems.

1.1.2 High throughput transcript profiling by EST arrays

A popular new approach for the examination of global changes in gene expression is the use of high-density cDNA / EST arrays (PCR amplified inserts of full-length or partial sequence cDNAs), which allow to study genome-wide expression levels in parallel (Skena *et al.*, 1995). ESTs provide the main resource for the construction of cDNA arrays in cereals, because genomic sequences are not available, except for rice. The rapidly growing EST databases allow the detection of regions showing sequence homology in functionally related gene products even from distantly related organisms. Thus, it is increasingly possible to assign putative functions for a large proportion of anonymous cDNA clones/ ESTs. Such type of ESTs, once annotated by BLAST search, are being used as resources for the analysis of gene expression with the help of high-density arrays as demonstrated in *Arabidopsis* (Skena *et al.*, 1995; Girke *et al.*, 2000). It is also important to note that array-based results identify novel genes most worthy of detailed characterization. It is often interesting to look into genes belonging to different metabolic pathway that show a dramatic induction or repression in their expression, which in turn provide an integrative view of physiological information of a plant's response during developmental studies.

The construction and use of such EST arrays for high-throughput transcript profiling can be divided into four general steps, which are depicted in Figure 1. These steps comprise (i) the identification of a non-redundant set of cDNA clones, (ii) the synthesis and deposition of hybridization targets on an appropriate surface, (iii) preparation of mRNA from the tissue of interest, labelling of the hybridization probe and hybridization of the array and (iv) data acquisition and evaluation.

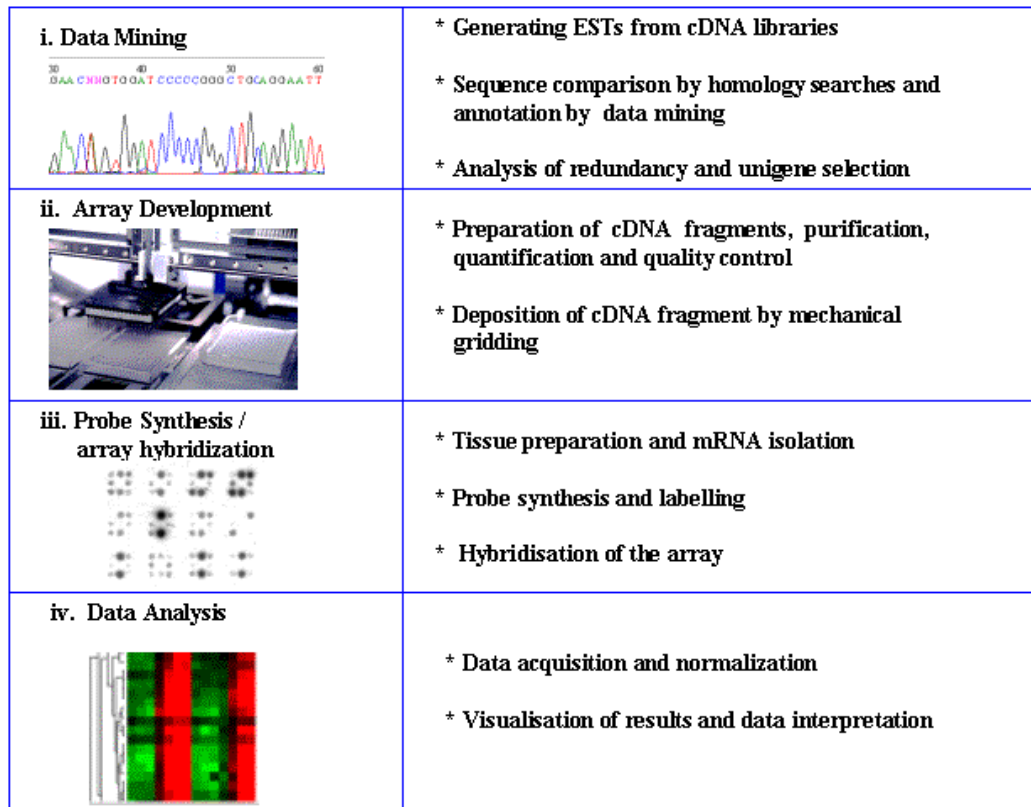


Fig. 1 A diagrammatic representation of EST-array technique.

Four major steps involved in EST-array production technology are i. Database mining; ii. Array development; iii. Probe synthesis/array hybridization; iv. Data analysis. The sub-steps followed in every major step have been provided with a star mark on the right side of the diagram.

(i) *Data mining*: The development of a non-redundant unigene set from ESTs has been covered in the above section. It serves the purpose to minimize the number of samples on a cDNA array mainly for technical reasons, even so a low degree of redundancy will provide data for quality control (Herwig *et al.*, 2001).

(ii) *Array development*: Several different approaches, which are summarized in Table 3, could be taken for the construction of a cDNA array. The least expensive approach is the PCR amplification of cDNA fragments using vector primers and their spotting on Nylon membranes or chemically modified glass or plastic surfaces (for review specifically on plant cDNA arrays see Richmond and Sommerville, 2000). For that purpose the cDNA clones from the EST project have to be available and all handling errors with respect to the clones will be reflected on the array. The second approach uses long oligonucleotides (50 – 80mers), which can be synthesized and spotted instead of cDNA fragments. The advantage of this approach is that oligonucleotides can be designed to distinguish members of gene families, that cDNA clones need not to be available and that handling errors with respect to the clones will not affect the array. The third approach is the on-chip synthesis of short oligonucleotides (25mers), which is offered by Affymetrix (<http://www.affymetrix.com/>). Set-up costs are high; furthermore, the array design is rather static with respect to the gene content, because a new design would require a completely new set-up. Therefore, construction of these types of arrays is thought to be useful, if a genomic sequence is available to identify most of the genes or parts thereof with a high degree of reliability. Except for Affymetrix arrays, the oligonucleotides or cDNA fragments need to be transferred and permanently attached to the array surface. Usually this is accomplished by solid or slit pins which pick-up the samples from microtiter plate wells and transfer them to the target locations on the array. Spot distances on the order of 100 to 400 μm , up to several thousand spots per array and transferred volumes in the picolitre-range require high precision, high speed moving devices which perform this task in an environment with precisely controlled temperature and humidity. For the permanent bonding of cDNA fragments gene products are immobilized on to the solid support such as nylon or nitrocellulose membrane defined as macroarrays or onto glass surface usually called microarrays. Array designs used for expression analysis differ widely with respect to the hybridization targets, the solid support, the method of application of hybridization targets and their density, as well as the label which is used to detect hybridization intensities.

Table 3: Design principles of arrays used for expression analysis

target on array	array surface	target application	features cm ⁻²	label
cDNA fragments	Nylon membrane	spotting	100	³³ P
cDNA fragments		spotting	4,000	fluorescent dye
Oligonucleotides (50 – 80mers)	modified glass or plastic	spotting	4,000	fluorescent dye
oligonucleotides (25 mers)		on-chip synthesis	300,000	fluorescent dye

(iii) *Probe synthesis / hybridization*: The next step in cDNA array analysis involves the isolation of mRNA, probe synthesis and labelling as well as the hybridization with the array. To synthesize a labelled hybridization probe various protocols are available (Gupta *et al.*, 1999). Generally, ³³P-labelled nucleotides are employed when membrane based macroarrays are hybridized, because incorporation rates are high and sensitive phosphoimagers can be used for signal detection. Radioactive labels cannot be used for any kind of microarray, because the spatial resolution of phosphoimagers is not sufficient to separate signals of neighboring spots. Usually, fluorescent dyes are incorporated either directly using dye modified nucleotides (CyDye™ fluorescent dyes: Amersham/Pharmacia) or indirectly *via* aminoallyl-modified dUTP (Molecular Probes, Stratagene). Alternative strategies employ for example the incorporation of biotinylated nucleotides and labelling with phycoerythrin-conjugated streptavidin after the hybridization was performed (Affymetrix). Hybridizations are performed under the most stringent conditions possible to prevent cross-hybridization.

(iv) *Data analysis*: Afterwards signals are detected using specialized scanners for microarrays and phosphoimagers for macroarrays. Resulting images are processed with software for automatic spot detection to derive a list of signal intensities for all features on array. This raw data has to be processed to gain biological knowledge. Important steps include (a) the critical assessment of data reliability and normalization to allow the comparison of different experiments as well as (b) the categorizing of gene expression profiles and their biological interpretation.

(a) Depending on the type of experiment, various procedures can be employed to normalize raw data for comparison with a series of other experiments. These procedures range from

mathematical methods, which assume that the intensity distribution of signals does not change between experiments to the use of reference signals, which are derived from housekeeping genes or foreign mRNAs included in probe synthesis. The choice of a method will often influence the experimental design and has to be made before an array is constructed. Based on the comparative results with macroarray experiments and Northern blot controls for many differentially expressed genes lead to the conclusion that mathematical methods are sufficiently accurate (Sreenivasulu *et al.*, 2002; Potokina *et al.*, 2002). Equally important is a careful evaluation of signal and array quality. Most often the initial dataset will be reduced to

Table 4: Analytical tools with application to gene expression and worldwide web addresses of software's for array data analysis from the public domain as well as the private sector.

Organization	Primary function	URL
Academic software's:		
Array Viewer	Multi experiment viewer,	http://www.tigr.org/softlab/
Image/J	Image processing	http://rsb.info.nih.gov/ij/
Spot finder	Spot detection	http://www.tigr.org/softlab/
Scan Alyze	Spot detection	http://rana.lbl.gov/EisenSoftware.htm
Cluster	Data filtering/ clustering	http://rana.lbl.gov/EisenSoftware.htm
Tree View	Cluster visualisation	http://rana.lbl.gov/EisenSoftware.htm
Xcluster	Clustering, visualisation	http://genome-www.stanford.edu/~sherlock/cluster.html
J-Express	Clustering, visualisation	http://www.ii.uib.no/~bjarted/jexpress/
Genesis	Clustering, visualisation	http://genome.tugraz.at
Amanda	Clustering, visualization	http://xialab.hku.hk/software
Data explorer	Data flow visual program	http://www.opendx.org/
The R language	Comprehensive statistical Analysis, clustering, etc	http://cran.us.r-project.org/
Cyber T	t-test variants for gene expression datasets	http://genomics.biochem.uci.edu/genex/cybert/
Commercial softwares:		
Array-Pro	Spot detection	http://www.mediacy.com/arraypro.htm
Array Vision	Image visualization, Spot detection	http://imaging.brocku.ca/products/Arrayvision.htm
Array Explorer	Clustering and visualization	http://www.spotfire.net/
Expressionist	Clustering, visualisation	http://www.genedata.com/products/expressionist/
Gene Maths	Clustering, visualisation	http://www.applied-maths.com/ge/ge.htm
Gene Sight	Clustering, visualization	http://www.biodiscovery.com/products/genesight/genesight.html
Gene Spring	Clustering, visualisation and normalization	http://www.sigenetics.com/cgi/SiG.cgi/index.smf
JMA Viewer	calls KEGG, BLAST,	http://sequence.aecom.yu.edu:8000/jmaviewer/
Partek	Clustering, visualisation 3D gene expression data	http://www.partek.com/

a much smaller dataset of differentially expressed genes within this selected dataset. Experimental artifacts, which lead to large differences in signal intensity, will specifically accumulate and cause misleading interpretations. In addition, the biological variability will significantly influence the data and it is good practice to repeat each experiment with hybridization probes from independently obtained tissue samples. It seems to be very difficult or even impossible to control all environmental variables to such an extent that no significant variation in gene expression is observed in such repeats.

(b) As a consequence of the large number of data points obtained from just a few moderately sized experiments, evaluation of the data has to be supported by computational methods. For these purposes several software packages are available commercially and in the public domain. An overview is given in Table 4. To categorize expression profiles, several methods from multivariate statistics can be employed, such as hierarchical clustering (Eisen *et al.*, 1998), K-mean clustering (Tavazoie *et al.*, 1999), principal component analysis, self-organizing maps (Tamayo *et al.*, 1999) and others. If they are used on a carefully controlled reliable dataset, they will yield similar, but not identical results.

1.1.3 Biological interpretation of expression data

Finally, expression data are expected to yield insights into metabolic and regulatory processes during plant development. To reach that goal, it is necessary to compare the preprocessed array data with known models of metabolic and regulatory networks as depicted in KEGG (Goto *et al.*, 1997, <http://www.genome.ad.jp/kegg/metabolism.html>), the Boehringer biochemical pathway database (Michal, 1993; <http://www.expasy.ch/cgi-bin/search-biochem-index>) or the general literature and to confirm or reject specific hypotheses. Many successful examples have been provided already, e.g. the analysis of seed development (White *et al.*, 2000, Ohlrogge and Benning, 2000) or phytochrome A signalling (Teppermann *et al.*, 2001) in *Arabidopsis* and the analysis of salt stress in rice (Kawasaki *et al.*, 2001).

Until now, most of this interpretation process is a manual task, which requires the simultaneous integration of many different information resources. Software tools to support this complicated process are still in their infancy. Implementation of powerful interactive simulation environments for metabolic and regulatory networks, such as Metabolika (Hofestädt and Scholz, 1998), with integrated access to the information about related genes, proteins and metabolites as well as the actual expression data will be a next important step.

Until such tools are available the development of new hypotheses from the data of expression analysis will continue to depend on human ingenuity.

1.2 RESULTS AND DISCUSSION

1.2.1 EST generation from developing caryopses library (0-15 DAF)

A program aimed at the functional genomics of barley seed development was started with the synthesis of cDNA libraries from developing caryopses. In the Institute of Plant Genetics and Crop Plant Research (IPK) cDNA libraries from developing caryopses (0-15 DAF) were constructed and cloned into λ -ZAP Express (Stratagene) according to the manufacturers instructions (W. Weschke). In total 6,319 ESTs were generated from developing caryopses libraries either from 3' or 5' ends. Sequence cleaning and quality check has been performed under high-stringent conditions. Comparisons to other plant EST-sequences and redundancy within the EST collection has also been performed (Michalek *et al.*, 2002). The EST sequence of all clones along with clustering information is available at our web site <http://pgrc.ipk-gatersleben.de>.

1.2.2 Annotation and functional classification of barley ESTs from developing caryopses

We examined the cDNA clones associated with pre-storage and initial storage phase of developing barley caryopses by EST approach. Clones were selected preferentially from a cDNA library of developing caryopses (1235 clones) and smaller numbers were chosen from etiolated seedlings (70) and roots (104) library. ESTs were annotated with reference to gene function using the results of BlastX2 comparisons with the SwissProt protein database. SwissProt was used instead of TrEMBL to prevent the occurrence of a large number of functionally non-informative database matches with putative or hypothetical proteins from genomic sequencing projects. Information regarding score, length of the aligned sequence segment and other parameters were extracted from the results using a custom made Perl script. EST sequences were grouped in three categories based on the score and the length of the aligned sequence segment with the top database hit after BlastX2 comparison with SwissProt. Two straight lines, which separate the three categories, were defined on a scatter plot of score versus aligned length by manual annotation of approximately 700 sequences.

These lines run through a common point defined by the minimal alignment length of 12 amino acids (aa) and a corresponding score of 27 bits. The "Secure" and "potential" assignments were separated by a straight line with the slope of 1.36 bits/aa and "potential" and "unassigned" sequences were separated at 0.62 bits/aa. In case, 5'- and 3'-end sequences were available the highest category was assigned to the cDNA clone of top hit. All cDNA clones on our array were categorized by using these criteria. Out of 1421 cDNA fragments 1309 unique ESTs were identified based on BlastX2 assignment. ESTs were grouped in three categories, called "secure" (509 clones, 38.9%), "potential" (308 clones, 23.5%) and "unassigned" (492 clones, 37.6%) (Fig. 3a), based on the ratio between score and length of the aligned sequence segment as described above.

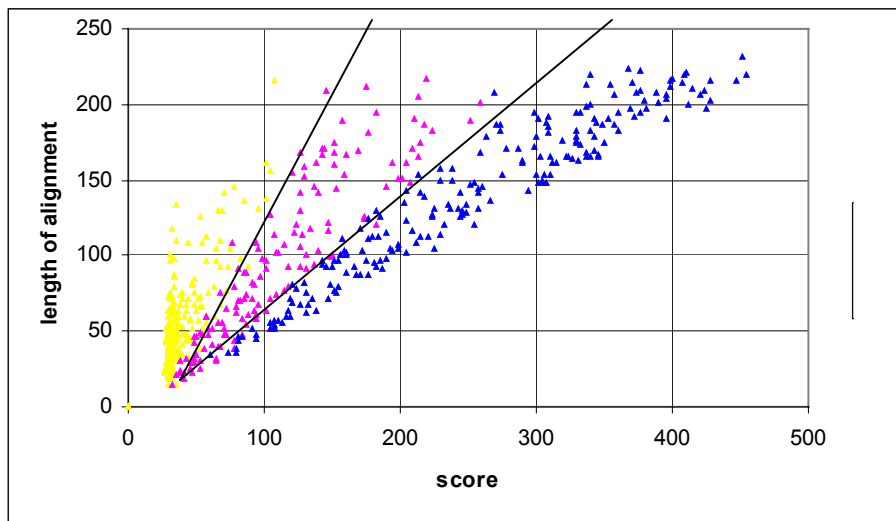


Fig. 2 Scatter plot representation of EST annotation data

Plotting of score value and length of alignment of 700 ESTs on X and Y axis respectively. 'Secure' class is represented by blue colour, 'potential' class by pink colour and 'unassigned' class by yellow colour.

A second, independent approach was taken to estimate the number of genes represented on the cDNA array, which is independent of known genes in databases. For that purpose sequences of a larger set of ESTs (Michalek *et al.*, 2002) from which clones on the array had been selected were clustered using StackPack. Depending on the use of 5'- or 3'-end sequence data, the ESTs on the array represent between 1176 and 1199 consensus sequences and singeltons. Of those approximately 410 (404 [5'], 426 [3']) belong to the "secure", 300 (300 [5'], 299 [3']) to the "potential" and 470 (472 [5'], 474 [3']) to the functionally unassigned group of ESTs.

To allow the placement of EST encoded genes on metabolic pathway charts, as provided by KEGG (www.tokyo-center.genome.ad.jp/kegg), EC-numbers were extracted from the description line of a matching SwissProt entry for "secure" and "potential" assignments (62.4% of the clones present on our array). The remaining 37.6% with no assignment were placed in non-significant homology section (Fig. 3a). In the total cDNA set, sequences assigned to carbohydrate metabolism (No. 1 in Fig. 3b; 6.94%), amino acid metabolism (No. 5; 6.85%) and genes involved in energy metabolism (No. 3; 6%) dominate, followed by groups of metabolism of miscellaneous substances (No. 8, 2.3%), cell division and cell cycle genes (No. 13, 1.57%) and genes involved in transcription (No. 14; 3.05%) and translation (No. 16; 4.6%). The largest group (No. 17; 11.8%) contains non-classified genes (Fig. 3b). The complete list of genes and their classification along with sub-classes for all unique clones on our cDNA-macroarray is available on-line at <http://pgrc.ipk-gatersleben.de/sreeni>.

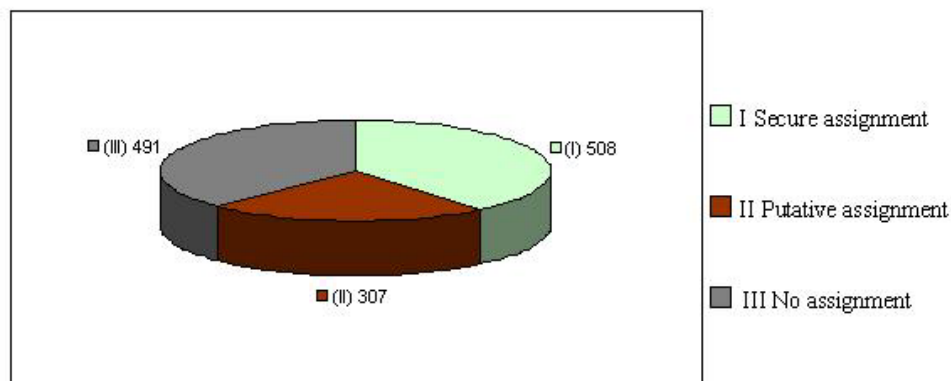


Fig. 3a Annotation of 1400 ESTs from developing caryopses (0-12 DAF)

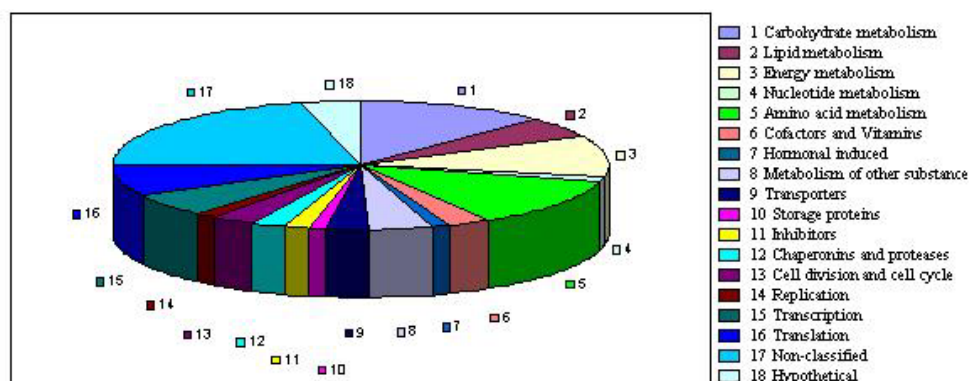


Fig. 3b Functional classification of ESTs from developing caryopses (0 to 12 DAF)

1.2.3 Preparation of an EST macroarray

DNA array technology is an attractive and ideal tool to investigate expression profiles in developmental studies in a large-scale fashion (Tanaka *et al.*, 2000). In comparison, among the available array techniques, the use of nylon membranes and radioactively labelled probes seems to be especially reliable (Herwig *et al.*, 2001). In this study, high-density nylon arrays together with a ^{33}P radioactive probe based hybridization technique have been employed. During the early phase of this program 711 clones representing more than 620 unique genes were selected to construct a cDNA array. Among them 517 clones from a cDNA library of developing caryopses, 70 clones from etiolated seedlings and 104 clones from roots were selected. To produce a larger array, inserts of 1412 cDNA clones containing 1184 unique clones and additionally, some internal control cDNAs were amplified. The same EST amplified independently or different ESTs representing the same gene were used as controls. A complete list of these clones as well as BlastX2 results and other data relevant to this chapter are available from our WWW-server (<http://pgrc.ipk-gatersleben.de/sreeni>). Based on current sequence and clustering data these clones represent more than 1184 unique genes and therefore comprise the largest collection used for expression analysis of barley reported so far. The cDNA inserts of all clones used for array preparation were amplified with vector specific primers, purified, analyzed on agarose gels, adjusted to concentrations between 2.0 and 1.8 $\mu\text{g}/\mu\text{l}$, and spotted in duplicate onto nylon membranes as described in Materials and methods. The resulting 711-cDNA array (5 x 9 cm) consists of 10 x 18 subarrays with square of nine spots (see Fig. 4). The 1412-cDNA array (8 x 12 cm) consists of 16 x 24 subarrays, each being a square of nine spots. The central spot of each subarray provides a blank control, while the remaining eight spots contain four different amplification products, each of them represented twice. After hybridization with ^{33}P -labelled second strand cDNA and three washing steps under highly stringent conditions the signals on the array were detected using a phosphoimager. Resulting images were processed with a specialized software package for spot detection, and data files were exported to a standard spreadsheet program. To allow the comparison of data sets from different experiments, signals were normalized with respect to the total amount of radioactivity bound to the array after background subtraction in case of 711-cDNA array. To allow comparison of signal intensities across experiments the median of the logarithmically scaled intensity distribution for each experiment was set to zero in case of 1412-cDNA array (median centering of arrays, Eisen *et al.*, 1998).

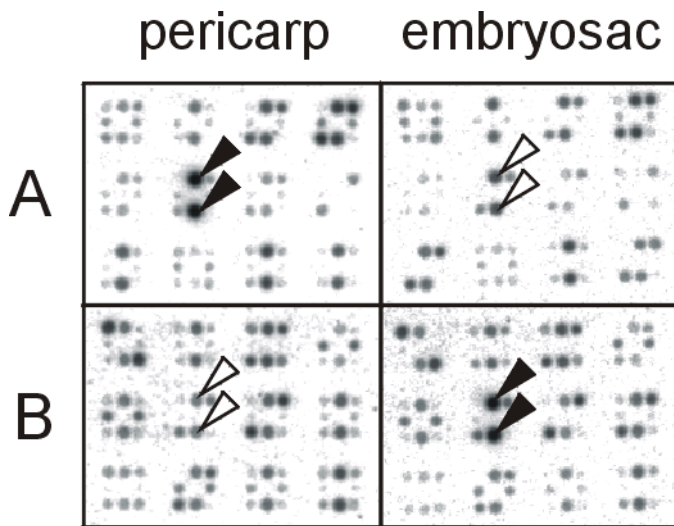


Fig. 4 Segment of a cDNA macroarray

A cDNA macroarray containing 711 clones was hybridized with ^{33}P -labelled second-strand cDNAs derived from pericarp and embryo sac tissues of the developing barley grain 1-7 DAF. Each panel shows 12 subarrays in a 4 x 3 arrangement, which are made up of a blank spot in their center and eight surrounding spots representing four different cDNA-fragments, spotted in duplicate. Hybridization signals for the cDNA clones HY05K19 (A) and HY09L21 (B) which were used for Northern analysis and *in situ* hybridization are marked. The filled triangles indicate strong signals, the open triangles, weaker signals.

1.2.4 Performance of an EST macroarray containing 711 clones

It is important to note here that most of the technical aspects of array preparation and its performance has been dealt with two different cDNA arrays, one with 711 ESTs (620 unique genes) and second one with 1412 (1184 unique genes). In order to get primary insights into pericarp and embryo sac tissue specific expression and to look into the technical details of performance of macroarray, we pooled pericarp (0-7 DAF) and embryo sac probes (0-7 DAF), labelled the probes and hybridized to the macroarray containing 711 ESTs. The probes were synthesized from two completely independent preparations of pericarp and embryo sac tissues (tissue preparations 1 and 2) and used for hybridization first with array 1. In addition, tissue preparation 2 was hybridized to a second membrane (array 2) to check the consistency of results between different arrays. A comparison of the results is shown in a scatter plot (Fig. 5A) which clearly demonstrates that relevant deviations between the two arrays occur only at low signal intensity when the accuracy of the spot finding algorithm diminishes and the influence of background noise increases considerably. Fig. 5B shows the plotted results of a representative experiment (tissue 2/array 1) in which the membrane was hybridized first with cDNA from pericarp and then, after probe removal, with cDNA from embryo sac tissue. cDNAs with a more than two-fold difference in signal intensity between the two tissues can be identified as being outside of the two parallel lines in Fig. 5B. In this experiment, 48 cDNAs appeared to be expressed preferentially in the pericarp and 42 genes were more highly expressed in the embryo sac that gave a signal intensity above 5 arbitrary units (au) in at least

one of the two tissues examined and at levels at least two-fold higher than in the other tissue. If all three experiments (tissue 1 / array 1; tissue 2 / array 1; tissue 2 / array 2) are taken into consideration, 38 clones, representing 34 different genes, consistently showed a more than two-fold difference between the two tissues (Tables 5 and 6). The ratio between the highest and the lowest signal, defined as the average background intensity plus three standard deviations, was used to approximate the dynamic range of our array experiments. With background values ranging from 0.05 – 0.25 au (arbitrary units; standard deviation 0.08 – 0.12 au) and the most intense signals between 450 and 1000 au, the dynamic range has been greater than 1000 in all our experiments. As a consequence of the weak influence of intense signals on neighboring spots (data not shown), we did not fully exploit this dynamic range, but rather restricted our interpretations to clones which had a signal intensity above 5 au in at least one of the two tissues examined (see Fig. 5B).

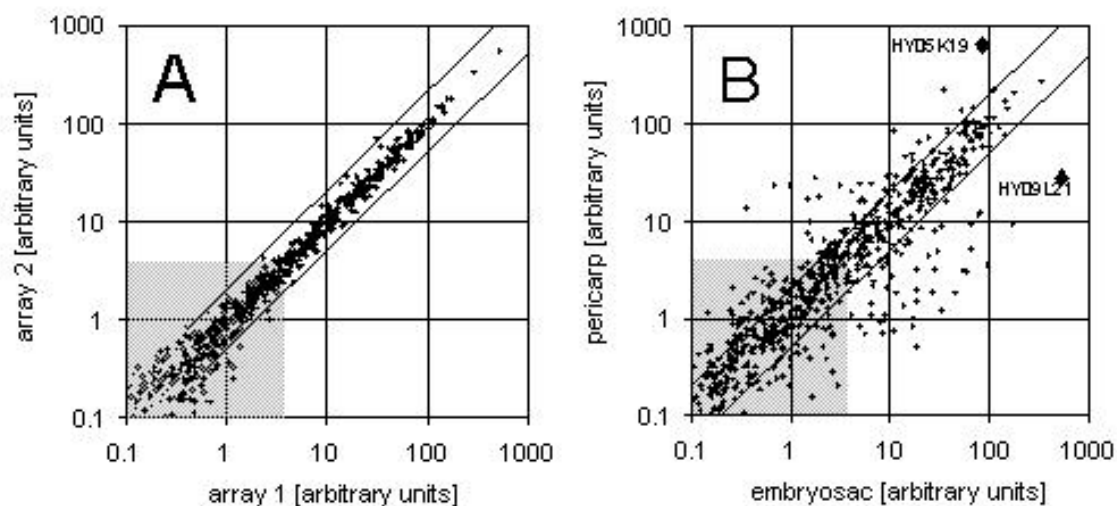


Fig. 5 Comparison of the normalized signal intensities obtained from two independently spotted arrays hybridized with the same labelled cDNA (A) and from one array hybridized successively with labelled cDNA from embryo sac and pericarp tissues of the developing barley grain 1-7 DAF (B).

Signals outside the diagonal lines differ by more than a factor of two between the two hybridization experiments. The cDNA clones HY05K19 and HY09L21 (enlarged symbols in B) were used for Northern analysis and *in situ* hybridization. Signals within the shaded areas were excluded from further evaluation because of their low signal intensities.

Internal controls of genes represented twice on the array but amplified independently (for example, in Table 5, HK03G06) or derived from different cDNA clones of the same gene (HY03B06 and HY10J06; HK03G06 and HW01G04 in Table 5) showed that expression

ratios between pericarp and embryo sac can be reproduced with considerable accuracy within an array. In contrast to the ratios, the signal intensities should not be used as reliable indicator of the expression level of a certain gene, because their values depend strongly on the amount and quality of the spotted amplification product. Reproducibility from array to array was evaluated by hybridizing two independently spotted arrays with the same labelled cDNA. In addition, several cDNAs that showed wide variability between hybridizations with tissue preparations 1 and 2 have been observed, e.g. clone HY10J06 and HY03B06, both are derived from the one gene, pericarp/embryo sac ratios vary from 11 to 40, see Table 5) between tissue preparations. We confirmed that this variability is not a result of hybridization artifacts, but rather a consequence of differences between the two tissue preparations (for further explanation, see below).

Table 5 cDNA clones that are preferentially expressed in pericarp

Clone ID	Tissue 1 /array 1			Tissue 2 / Array1			Tissue 2 / Array 2			BlastX2 result	Score
	peri	emb	ratio	peri	emb	ratio	peri	emb	ratio		[bits]
HY10J06	21	1.9	11	24	0.7	34	20	0.5	38	filamentous flower protein FIL, arabidopsis	68
HY03B06	15	1.4	11	14	0.3	40	12	0.4	34	filamentous flower protein FIL, arabidopsis	133
HY01A03	17	3.0	5.8	23	1.0	23	25	1.1	22	β -amylase	446
HY02E15	20	3.5	5.8	17	1.9	9.0	29	2.1	14	lipoyxygenase 2	416
HY05B22	12	2.9	4.1	17	1.5	12	18	1.7	10	probable NADP-dependent	205
HK04H17	19	3.2	6.0	28	1.8	16	21	2.0	10	nonspecific lipid-transfer protein	80
HY05O10	223	44	5.1	219	34	6.4	270	41	6.7	fructokinase	254
HY05K19	459	126	3.6	644	84	7.6	549	87	6.3	methyltransferase/methionine synthase	357
HY03J19	19	5.0	3.8	23	3.1	7.4	20	3.3	6.0	(hypothetical protein T8P19.200,	166
HK03G06	15	3.7	4.0	10	1.6	6.2	8.7	1.6	5.4	cysteine proteinase 1	114
HK03G06	8.9	2.0	4.4	7.4	1.5	5.0	6.4	1.3	5.1	cysteine proteinase 1	114
HY03G16	7.8	2.1	3.8	6.5	1.6	4.1	7.7	1.9	4.1	(hypothetical protein F26G5.50,	122
HW01K18	9.1	3.9	2.3	8.0	3.5	2.3	9.0	2.5	3.5	(rna polymerase beta subunit, virus strain)	40
HW02F11	28	8.3	3.4	20	4.1	5.0	18	5.3	3.4	vacuolar invertase	247
HY08P04	14	4.6	3.0	11.5	4.2	2.7	7.5	2.3	3.2	(oncogene protein, chicken)	30
HY04F24	47	16	3.0	72	24	2.9	67	22	3.0	(p-selectin precursor, mouse)	37
HY04H09	31	11	2.8	30	9.5	3.1	43	15	3.0	auxin-responsive protein	184
HY04N15	57	23	2.5	65	20	3.2	67	24	2.9	probable NADP-dependent	102
HY07C03	37	12	3.0	33.8	17.4	2.0	40	16	2.6	glucan endo-1,3-beta-glucosidase	83
HY03C16	63	18	3.5	45	14	3.1	49	15	2.6	acyl-coa-binding protein	117
HW01G04	48	21	2.3	29	12	2.4	22	9.3	2.3	cysteine proteinase 1	282
HW01F04	11	4.2	2.7	5.2	2.1	2.4	5.1	2.2	2.3	UDP-glucose 4-epimerase	86
HY04F14	20	7.6	2.6	16	5.0	3.2	17	7.4	2.4	glycine dehydrogenase	287
HY10D17	32	8.4	3.8	21	8.7	2.4	31	14	2.2	(web1 protein, baker's yeast)	28
HY08K19	18	8.9	2.0	16	6.0	2.8	17	7.7	2.2	(growth factor receptor-bound protein 7,	32
HY09N04	50	23	2.2	49	17	2.9	29	13	2.2	(hypothetical protein, arabidopsis)	46

Table 6 cDNA clones preferentially expressed in the embryo sac

Clone ID	Tissue 1 / Array			Tissue 2 / Array 1			Tissue 2 / Array 2			BlastX2 result	Score [bits]
	peri	emb	ratio	peri	emb	ratio	peri	emb	ratio		
HY03M02	1.3	5.4	4.2	3.5	96	27	4.2	114	27	α -hordothionin	272
HY09L21	100	932	9.4	28	541	19	20	518	26	(nuclear transition protein 2, pig)	38
HY06E14	4.8	16	3.4	1.8	46	26	2.0	50	24	flower-specific gamma-thionin	70
HY09N16	14	34	2.5	9.4	174	18	11	169	16	sucrose synthase 2	331
HY04N22	6.1	17	2.8	2.9	58	20	4.0	63	15	(none)	0
HY04E07	19	73	3.9	1.8	26	14	1.5	23	15	vacuolar processing enzyme	211
HY01O19	6.5	21	3.2	3.1	54	17	3.3	48	15	α -amylase / subtilisin inhibitor	69
HY07E21	25	141	5.7	9.1	64	7.0	8.2	67	8.2	replication factor C 38kD subunit	142
HY03O04	1.4	9.4	6.6	1.0	8.6	8.9	1.5	11	7.2	(monocarboxylate transporter 8, human)	29
HY09L18	22	110	4.9	12	77	6.6	12	65	5.5	probable aspartic proteinase	296
HY02B16	6.8	35	5.1	1.8	11	6.4	2.4	11	4.6	serine carboxypeptidase I precursor	390
HY02F04	57	122	2.1	12	82	6.8	27	84	3.2	(hypothetical protein F3A4.230,	65

Table 5: Clones that are preferentially expressed in the pericarp are defined as those that give pericarp/embryo sac signal intensity ratios larger than 2 and absolute signal intensities greater than 5 au in three array experiments. Normalized signal intensities for pericarp (Peri) and embryo sac (Emb) tissues, as well as the corresponding Peri/Emb (P/E) ratios are listed for three experiments involving two different tissue preparations (Tissues 1 and 2) for probe synthesis, and two different array filters (Arrays 1 and 2). Top scores from a BlastX2 search against the protein databases Swissprot and PIR provide hints as to the potential functions of the respective genes.

Table 6: Clones preferentially expressed in the embryo sac are defined as those with embryo sac to pericarp signal intensity ratios larger than 2, and absolute signal intensities greater than 5 au in three array experiments. Normalized signal intensities for embryo sac (Emb) and pericarp (Peri) tissues, as well as the corresponding Emb/Peri (E/P) ratios are listed for three experiments. For further details see legend of Table 5.

1.2.5 Performance of an EST macroarray containing 1412 clones

The 1412-cDNA array (8 x 12 cm) represent approximately 1184 unique genes of which 63% can be annotated with respect to gene function using the available partial sequences. To gain biological knowledge of pericarp and embryo sac development during pre-storage and storage phase we used cDNA array of 1412 clones. Details of the results were presented in Chapter 2. To allow comparison of signal intensities across experiments in case of 1412-cDNA array, the median of the logarithmically scaled intensity distribution for each experiment was set to zero (median centering of arrays, Eisen *et al.*, 1998). We would like point out that technical detail of array performance has been performed also with cDNA array containing 1412 (1184 unique) clones. The reproducibility of expression patterns of internal controls of some genes represented twice on the array (amplified independently) was evaluated on 1412-cDNA macroarray during pericarp and embryo sac development. The same EST clones amplified

independently showed similar expression patterns and reproduced with considerable accuracy e.g. (Table 7: pericarp-specific expression HK03G06, HY05B22, HY03G16) and (Table 10: embryo sac specific expression pattern during initial storage phase HY07C09, HY04I11, HY10G16, HY05G12, HY02B16, HY03H23). The EST derived from different cDNA clones represents the same gene (Table 7: HY07K19 and HW01G04 represent for cysteine proteinase 1) showed pericarp-specific expression pattern. Further the EST clones (Table 10: HY10G10, HY07L04, HY01H24, HY07F09, HY10F20, HW08D05, HY03P12 represent sucrose synthase 1; HY09L14, HY09N16, HY07C09, HY06C06, HY09N15, HY07H01, HY10D14, HY04D17, HY03J05 represent sucrose synthase 2; HY01D18 and HY04D04 represent ADP-glucose pyrophosphorylase large subunit 1; HY10G16, HY08N11 and HK03F04 represent ADP-glucose pyrophosphorylase small subunit; HY06L03 and HY02N15 represent aspartate aminotransferase, cytoplasmic; HY08O12, HW06P12 and HW03P06 represent 6-phosphofructokinase beta subunit) showed embryo sac specific expression pattern during initial storage phase (6-12 DAF).

In case of gene families, it is expected that homologous sequences will lead to cross-hybridization which may obscure the data for individual members. Even so the overall sequence identity might be as low as 70%, more highly conserved segments do result in considerable cross-hybridization signals (Girke *et al.*, 2000). For that reason we do not know how cross-hybridization influences our data set in general and in special cases where we have clearly identified gene families, e.g. the two different members of the sucrose synthase (SUS) family present on our cDNA array (Table 10: sucrose synthase 1 and sucrose synthase 2). On the other hand based on expression data sucrose synthase 1 and 2 groups are well resolved into different clusters (compare Fig. 10 clusters 4_1 and 4_2).

1.2.6 Expression analyses of selected genes

Based on cDNA macroarray results the methionine synthase (HY05K19) and the unknown 'Nucpro' gene (HY09L21), depict abundant expression in pericarp and embryo sac tissues, respectively (Fig. 5 A, B). To validate the array data, expression of HY05K19 and HY09L21 ESTs was monitored by *in situ* hybridizations. In accordance with expression data, HY05K19 expression was localized mainly in the outer part of the pericarp, especially in the micropylar region but also in endospermal transfer cells (Sreenivasulu *et al.*, 2002). Clone HY09L21 localization by *in situ* hybridization revealed expression exclusively in the cells of nucellar projection (Sreenivasulu *et al.*, 2002), leading to the provisional name 'Nucpro'. This

unexpected result can be explained by the tissue organization of the developing caryopsis, which leads to the adherence of maternal nucellar projection cells to the filial embryo sac (see Sreenivasulu *et al.*, 2002). The sequence of HY09L21 did not exhibit significant homology to any gene of known function, i.e. we regard the BLASTX2 result “nuclear transition protein 2” (score bits 38) as fairly low. The *in situ* localization confirms tissue-specificity seen on the macroarray for the two selected clones. It also points to the importance of using techniques with high spatial resolution, such as *in situ* hybridization, in gene expression studies.

To further validate the macroarray data we selected additional 4 clones for RNA-gel blot analyses. HY03B06 (FIL) shows the highest ratio of pericarp to embryo sac expression (see Table 5), HY09L21 (Nucpro) shows one of the highest ratio of embryo sac to pericarp expression, HY09N16 (HvSUS2) shows unexpected major differences in the ratios between the two independent experiments (see Table 6) and HW02F11 (vacuolar invertase, HvVCINV) shows a rather low expression level but a fairly constant pericarp to embryo sac ratio in all three experiments (see Table 5). Among the genes with low transcript levels but highly specific expression in the pericarp is one represented by two ESTs, HY10J06 and HY03B06 (see Table 5). The sequence is related to that of an *Arabidopsis* gene coding for the transcription factor FIL (*FILAMENTOUS FLOWER*). FIL shows homology to the *CRABS CLAW* genes, founding members of the *Arabidopsis* *YABBY* gene family (Bowman and Symth, 1999). Northern analysis with an HY03B06 probe (see Fig. 6) in principle confirmed the array data. Northern analysis verified specific expression of HW02F11 in the maternal pericarp with especially high levels at 0 DAF and very low levels at 8 DAF (Fig. 6, 7A). Northern blot analysis of HvSUS2 (HY09N16) expression during early grain development (Fig. 6, 7B) revealed that mRNA levels in the embryo sac tissues rose from undetectable (2DAF) to relatively low (4 and 6 DAF) and eventually very high levels (8 DAF). This increase can be correlated with the enzyme activity profile described earlier (Weschke *et al.*, 2000). A comparison of the mRNA profile of Fig. 7B with the different values obtained for HvSUS2 expression in cDNA array experiments 1 (ratio 2.4) and 2/3 (ratio 18/16, see Table 6) points to a problem in our 711 array analysis which becomes evident for genes like sucrose synthase 2. We studied early seed development from 1 to 7 DAF. Since HvSUS2 mRNA levels rise dramatically at around 7 DAF (see Fig. 6, 7B), the signal intensity in the array is critically dependent on the exact developmental stage of the material collected for analysis. Generally, day 7 after flowering marks the beginning of an exponential increase in sucrose

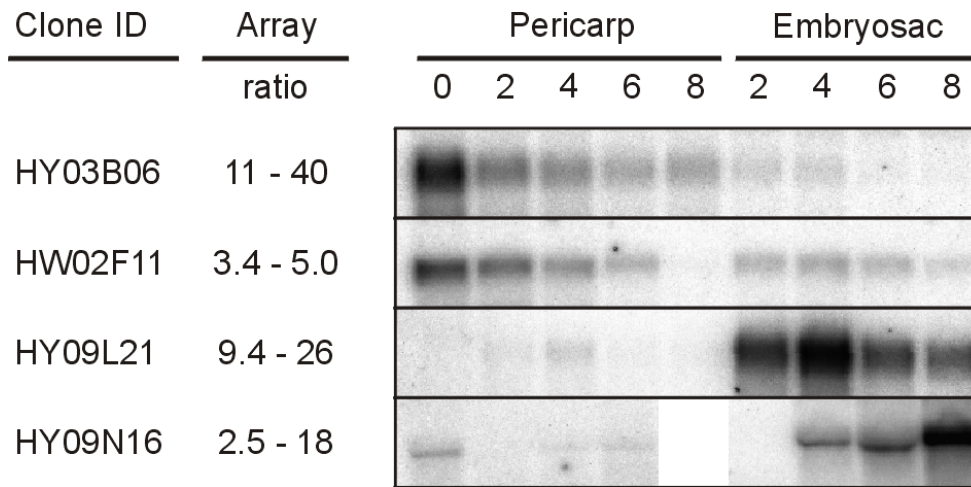


Fig. 6 Levels of transcripts differentially accumulated in pericarp and embryo sac of developing caryopses measured by northern analysis

Differentially expressed clones pericarp to embryo sac ratios (HY03B06 and HW02F11) or embryo sac to pericarp ratios of expression (HY09L21 and HY09N16) as determined by cDNA array analysis were compared by northern blot analysis. The numbers 0, 2, 4, 6 and 8 indicate the time (in days after flowering) at which tissues samples were taken for the isolation of total RNA. HY03B06: FIL-related transcription factor; HW02F11: vacuolar invertase (Hv VCINV); HY09L21: gene of unknown function termed Nucpro; HY09N16: sucrose synthase isoform 2 (HvSUS2)

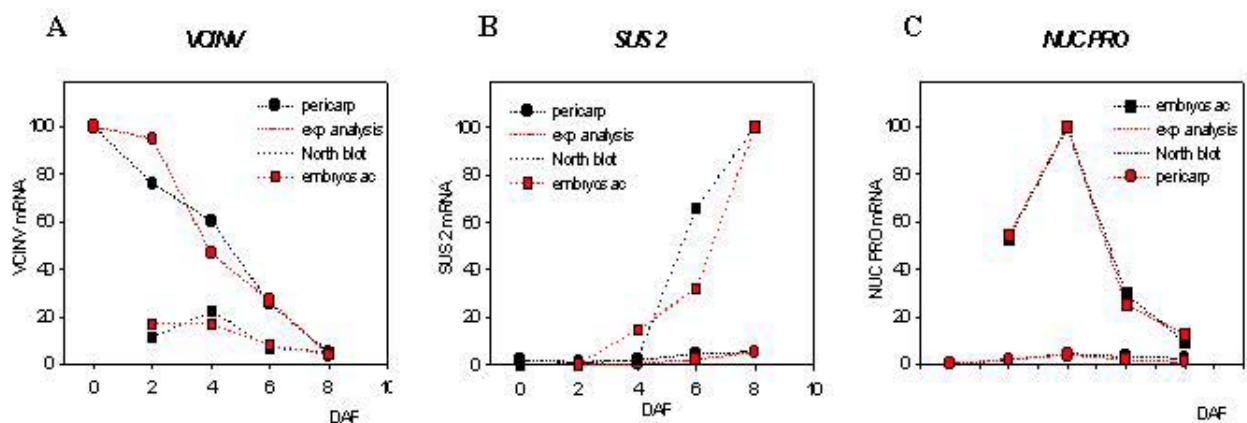


Fig. 7 Comparison of expression levels of selected genes by cDNA array (containing 1412 clones) and northern blot experiments

Transcripts differentially expressed in pericarp and embryo sac tissues of developing caryopses (0 to 12 DAF) were selected based on expression data of 1412-cDNA array and verified expression data by northern blot analysis. For every gene, the highest signal intensity value is considered to be 100% across the developmental scale. The intensity of northern blot

signals was quantified by using the BioImage Analyser and the signal intensity is given in percentage of the most intensive signal (100%). The numbers 0, 2, 4, 6 and 8 indicate the time (in days after flowering) at which tissue samples were taken for the isolation of total RNA. HW02F11: vacuolar invertase (Hv VCINV); HY09L21: gene of unknown function termed Nucpro; HY09N16: sucrose synthase isoform 2 (HvSUS2)

concentration in the whole caryopsis, a remarkable increase in the expression of the caryopsis-specific sucrose transporter HvSUT1 and a linear increase in sucrose synthase activity (Weschke *et al.*, 2000). All these parameters indicate the beginning of starch accumulation in the starchy endosperm. Therefore, small age difference between the caryopses used for pericarp and embryo sac tissue preparation will result in large differences in expression levels observed for genes related to carbohydrate metabolism, as was found for HvSUS2 (see above). Further, we demonstrated the nicely correlated expression patterns of SUS2 during 0 to 8 DAF between array (containing 1412 cDNA clones) and northern blot experiments.

1.3 CONCLUSIONS

In our first attempt we annotated ESTs generated from early stages of developing caryopses and used these resources to establish the cDNA macroarray technique to analyse the complexity of developing processes in the early stages of barley grain. Performance and evaluation of macroarray results originating from replicated experiments enhanced our ability to confirm the standardisations. Further, our results provide correlative evidence for expression data of selected gene candidates by using independent methods such as Northern blotting and *in situ* hybridization. Results presented in Chapter 1 can be used as starting point for isolation of tissue specific promoters. Given the drive to the more focused analysis, we used larger array for detailed studies of the timing of expression patterns in seed development (see Chapter 2) and, further, *seg8* mutant analysis during seed development (see Chapter 3).

CHAPTER 2

A genomic approach to seed development

2.1 INTRODUCTION

Seed development is a very complex phenomenon crucial for plant survival and the yield and quality of the economically important grain. Hence, the events in seed development and the associated metabolism becomes an attentive subject, in particular during the seed-filling phase in which photosynthates are converted into storage reserves. Cereals are among the very important crops, as they constitute the staple food for human population worldwide. Barley seeds have traditionally been used in malting and brewing industry. Recent biotechnological advancement allows us to alter specific processes to produce seeds with more desirable properties. In order to fulfil desire, thorough and proper understanding of seed development in barley is necessary. With this clear intention, genomic approaches as for instance macroarray analyses has been taken up to study global expression analysis and to understand the events during seed development in barley.

2.1.1 Aspects of seed development

The plant life cycle alternates between gametophytic (haploid) and sporophytic (diploid) generations. In plants, meiosis process results in haploid spores, which undergo differentiation to develop into male and female gametophytes. Male gametophyte germinates to form a pollen tube and delivers two sperm cells into the female gametophyte, and as a process of “double fertilization” embryo and endosperm formation takes place (Maheshwari, 1950). After fertilization, genes expressed in the female gametophyte participate in inducing seed development (Chaudhury *et al.*, 1997). Seed development is a sequential process, which involves cell division, followed by cell differentiation, storage accumulation and maturation. Seeds are complex organs containing diploid embryo and triploid endosperm. In barley, these filial organs are surrounded by maternal tissue (pericarp), which possess a main vascular

bundle in the ventral region and two lateral vascular bundles. The main and lateral vascular bundles download nutrients into specialized maternal cells where these are further mobilized into the underlying filial tissues (Murray, 1987). The import of sucrose, amino acids, certain mineral ions and macromolecules from sieve elements into maternal tissues of developing seeds has been the subject of reviews in the recent years (Patrick and Offler 1995; Patrick 1997; Weber *et al.*, 1997). Recently, Patrick and Offler (2001) discussed the compartmentation of transport and transfer events in developing seed sink tissues. The interaction between the various tissues of a seed, viz pericarp versus endosperm and endosperm versus embryo, is believed to be important in developmental events. The coordinated gene expression and networking regulations between maternal and filial tissues during the early phase of seed development is mostly unknown. Among cereals, aspects of endosperm development were studied in maize, rice and barley. The vast majority of published research has been devoted to the endosperm and its specialized tissue the aleurone (for review, see e.g. Ritchie *et al.*, 2000) but only little is known about the maternal seed fraction which makes up most of the early seed weight in caryopses before the onset of storage phase. Brown *et al.* (1994), described the major events of barley endosperm development, which include three main stages: syncytial stage (0-6 DAF), cellularization stage (6-8 DAF) and differentiation stage (8-20 DAF). During syncytial stage, the dominating mitotic division without cytokinesis results in a multinucleate endosperm. During 5 to 6 DAF, the nuclei were evenly spaced in the cytoplasm, which still remained undivided. The cellularization phase was marked by vacuolation, shaping of the cytoplasm and deposition of the first anticlinal walls of the endospermal cells. During 8 DAF, the cellularization was completed and the mitotic division frequency diminished. Aftermath of syncytial and cellularization process, the endosperm cells enter the maturation phase. The maturation process begins with formation of elongated polyhedral starchy endosperm cells and aleurone differentiation. In the later phase of the maturation phase the mitotic activity stops and storage product deposition initiates first at central regions and proceeds slowly towards the periphery of the starchy endosperm (Olsen *et al.*, 1992; Weschke *et al.*, 2000). In barley, the endosperm stores complex carbohydrates and proteins, which represent a major source of nutrients for mankind. At the end of the seed filling stage, the starchy endosperm reaches the end of its life by programmed cell death. The programmed cell death in the endosperm appears to be linked to ethylene production, which is evidenced in *shrunken2* mutant, which produces high levels of ethylene and undergo precocious cell death in comparison to wild type (Young *et al.*,

1997). However, it remained unclear whether programmed cell death of endosperm is autonomous or linked to signals provided by other parts of the seed.

2.1.2 Molecular physiology of early caryopses development

The filial part of the barley seed consists of embryo and endosperm, whose development is regulated by genes of both the maternal parent through the egg cell and the paternal parent through the pollen. After the onset of fertilization, the filial part of the seed develops within maternal tissue, the ovule, and the ovule may influence the coordinated development of embryo and endosperm in growing caryopses. The main challenge is to understand how the process of development of these different tissues is regulated in a coordinated manner. The interaction between the various tissues of the seed and the coordination of gene expression between maternal (pericarp) and filial (endosperm and embryo) seed fractions during the early phase of seed development in barley is unknown. During the pre-storage phase, the maternal pericarp represents a major portion of the caryopsis and serves nutrients to the filial embryo/endosperm. The importance of maternal tissue in endosperm development of barley caryopsis is shown in *seg* mutants. These maternal influenced mutants show a less developed endosperm but the embryo is not affected (Felker *et al.*, 1985).

Sucrose is the long-distance transport form of photosynthate, which gets transported to storage sink tissue such as the developing barley seed. Developing seeds convert imported sucrose into hexoses, which will be used for instance in starch biosynthesis during storage phase. In addition to the importance of sugars in metabolism, these molecules can also act as regulatory signals that control aspects of seed development. Nutrients from source tissues destined for the grain reach the pericarp through the main vascular bundle, which runs across the whole length of the grain at the bottom of the crease. After unloading from the vascular tissue they are further transported symplastically through the maternal pericarp tissues to the nucellar projection cells. A second unloading step into the endospermal cavity is required to allow uptake of the nutrients by the filial endosperm tissue (Patrick and Offler, 1995; Weschke *et al.*, 2000). During early seed development, the embryo sac is only a weak sink for nutrients probably causing the pericarp to function as a transient storage tissue, but details of this process are unknown in monocotyledonous plants. In the ongoing storage phase (6 DAF onwards), the endosperm tissue occupies the most prominent part of the seed and acts as strong sink, which converts imported assimilate into storage products. Accumulation of

storage compounds (starch and storage proteins) is based mainly on imported sucrose and amino acids.

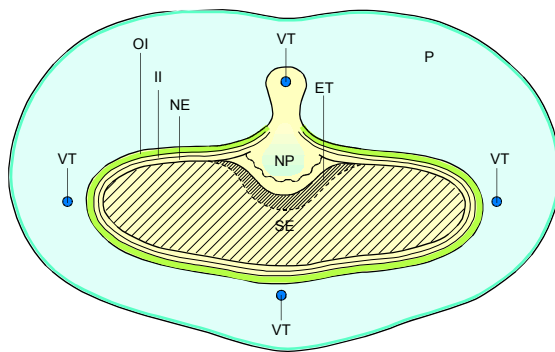
In earlier investigations, it was demonstrated that the changes in sucrose/hexose ratio are important for the transition between the prestorage and storage phase of seed development in both legumes and barley (Wobus and Weber 1999; Weschke *et al.*, communicated). The regulatory mechanism of sucrose import, catabolism of sucrose to hexoses, its distribution into the different parts of the seed and the expression of genes regulating sucrose to starch biosynthetic pathway during pre-storage and storage-phases provides valuable data in order to understand the mechanism of starch production.

2.1.3 Carbohydrate metabolism and its role in seed development

In cereals the photoassimilate sucrose is produced primarily by source leaves and is destined to the seed during caryopses development. Since developing seeds are strong sinks importing sucrose from the phloem and using it for growth and further storage activities during seed development it has been considered as an important event in seed biology, which need much attention. Sugars such as sucrose and its cleavage products, glucose and fructose have important functions in the synthesis of complex carbohydrates such as starch and cellulose, but are also used in energy production via glycolysis. In addition, sugars can also act as building blocks in amino acid and fatty acid biosynthesis during seed filling, and it has been proposed that sugars can act as signal molecules in altering gene expression patterns (Koch, 1996; Wobus and Weber, 1999).

2.1.3.1 Role of sucrose / hexose transporters in seed development

In cereals, the developing embryo and endosperm is symplastically separated from maternal tissues, and the supply of carbohydrates for caryopses development and deposition of storage compounds in endosperm is possible by action of sugar transporters in the maternal-filial boundary. Weschke *et al.* (2000), reported expression of barley sucrose transporters 1 and 2 in the cells of the nucellar projection and the endospermal transfer layers, indicating that especially HvSUT1 plays a possible role as control elements of sucrose flux to endosperm cells. Similarly, the role of hexose transporters in controlling sugar ratios between maternal and filial tissues of barley caryopses was investigated (Weschke *et al.*, submitted). Takeda *et al.* (2001), has also reported on the role of a sugar and a hexose transporter in early grain development of rice.



Median cross-section of a developing caryopses at 6 DAF (taken from Weschke *et al.*, 2000)

The different parts of the caryopsis are indicated as follows: ET, endospermal transfer cells; II, inner integument; NE, nucellar epidermis; NP, nucellar projection cells; OI, outer integument; P, pericarp; SE, starchy endosperm; VT, vascular tissue

Fig. 8 Schematic representation of the histological organization of a barley caryopsis

2.1.3.2 Catabolism of sucrose to hexoses during seed development

Sucrose cleavage is the first step in carbon usage of the seed, which is mediated by two enzymes invertase and sucrose synthase. The role of invertase and sucrose synthase genes in plant development and sucrose partitioning is discussed and reviewed by Sturm (1999) and Sturm and Tang (1999). The existence of different gene families coding for invertases and sucrose synthases are reported in many species (Koch, 1996). Regulation of these enzymes depends on the availability of sucrose, and the expressed genes were localized within a broad range of sugar importing tissues in developing kernels of maize (Doehlert and Felker, 1987; Doehlert, 1990). Since invertases can cleave sucrose into glucose and fructose, seed invertases are expected to play a major role in generating of high hexose pools. On the contrary, the activity of sucrose synthases, which generates fructose and UDP glucose opens the sucrose-to-starch pathway. Increasing sucrose levels and / or the increasing sucrose / hexose ratio and the distribution of sugars among different tissues is an important determinant of cellular events during seed development. In maize, it has been demonstrated that high hexose / sucrose ratios mediated by invertase activity are important for endosperm development. In *miniature1* maize seed mutant, lack of invertase activity in both pedicel and endosperm result in poor endosperm development. Genetic evidence suggests that the *mn1*-locus encodes an endosperm-specific isoenzyme of a cell wall-bound invertase (Cheng *et al.*, 1996). In legume (dicotyledonous) seeds a close interrelationship between carbohydrate metabolism in maternal tissues and embryo development has been shown convincingly.

Specifically during early development of faba bean seeds a cell wall-bound invertase is active only in the maternal seed coat, where the enzyme controls the glucose level, a key determinant of embryo development (Weber *et al.*, 1995; Wobus and Weber, 1999). If the tightly regulated glucose levels are disturbed, embryo development is distorted (Weber *et al.*, 1998). Later during seed development the increasing sucrose level is crucial for initiating starch accumulation (Weber *et al.*, 1996).

2.1.3.3 Sugar sensing mechanisms during seed development

As discussed above, sugars can also provide signals and are sensed by the cell. At least two different sensing systems have been found being either hexokinase-dependent or hexokinase-independent (Smeekens, 2000). The hexoses released as a result of sucrose catabolism will enter into a phosphorylation process by the action of hexokinases, which is an important sugar sensing mechanism in plants controlling many processes and metabolic pathways. On the other hand, the function of hexokinase as hexose sensor has not been generally accepted from the studies at whole plant level. Herbers *et al.* (1996), suggested that hexose sensing occurs in association with Golgi-ER system. Based on the existence of different forms of monosacharides (hexoses) there are several kinases reported in addition to hexokinases, which are fructokinase, glucokinase, galctokinase, arabinose kinase and SNF1. The function of these different kinases is not clear until now. However, based on recent investigation of *Arabidopsis* fructokinase 2 and its involvement in the metabolite-mediated regulation of gene expression some aspects of fructokinase 2 functions are understood. In addition, other kinases and phosphatases and further on, calmodulin protein phosphorylases have been identified that could control activity of enzymes such as sucrose synthase, sucrose phosphate synthase, β -amylase, small subunit of AGPase and sporamin (Mita *et al.*, 1995; Ohto *et al.*, 1995; Takeda *et al.*, 1994). The sugar-sensing and sugar-signalling pathways, which operate in cellular regulatory networks during seed development, are highly complex and unknown (for reviews see Wobus and Weber, 1999; Smeekens, 2000).

2.1.3.4 Sugar-regulated genes during plant / seed development

Sugars act as signals for developmental switches in seed development. It is known that specific sets of genes are positively regulated by sugars and a survey on sugar-regulated genes in plant development has been reported by Koch (1996). Carbohydrate catabolism results in high hexose accumulation; the process in turn up regulates genes for photosynthesis in plant tissues, which includes Rubisco large and small subunit, PEP carboxylase, triose-phosphate

translocator, pyruvate kinase and glycolytic genes (Koch, 1996). The other class of genes induced by sugar depletion includes invertase, sucrose synthase, sucrose phosphate synthase, α -amylase, phosphoglucomutase, malate synthase, starch phosphorylase and proteases (Koch, 1996). High sucrose levels exert opposite effects by inducing genes related to storage reserve synthesis. These changes result in increased starch levels and storage protein accumulation. The key enzymes involved in starch biosynthesis like ADP glucose pyrophosphorylase, starch synthase and branching enzymes are shown to be sugar responsive in developing seeds and tubers (Kobmann *et al.*, 1991; Weber *et al.*, 2000). Genes encoding storage proteins such as sporamin in sweet potatoes also have been reported to be sugar-responsive (Hattori *et al.*, 1990). In addition, vegetative storage proteins encoding phosphatase (Sadka *et al.*, 1994) and lipoxygenase activity (Grimes *et al.*, 1993) have also been found to be sugar-modulated. However, soluble sugars are not the only components in the large regulatory network that exists within seed tissues and affects its interactions (Wobus and Weber, 1999; Cowan *et al.*, 2001). Most likely this regulatory network will be reflected by the expression pattern of genes, which can be studied easily at the mRNA level. Therefore, extensive gene expression analysis is an important experimental approach, which will allow us to gain more intimate understanding of seed development.

2.1.4 Genomic approaches in seed development

Over the last few years, “Plant Genomics” has emerged as a high-throughput molecular approach to discover genes and measure their expression. A popular new approach for the examination of global changes in gene expression is the use of high-density cDNA / EST arrays, which allow to study genome-wide expression levels in parallel (Schena *et al.*, 1995). However, this powerful technique has not been used until recently to analyse seed development in detail, because of the lack of cDNA clones derived from plant seeds. Lately, a first large set of randomly chosen, partially sequenced cDNAs from seeds has been reported from *Arabidopsis* (White *et al.*, 2000), and a microarray with approximately 2600 seed-expressed genes has been generated and utilized to analyse their expression levels in seeds versus leaves and roots (Girke *et al.*, 2000). A small set of ESTs has also been reported from developing seeds of castor (Van de Loo *et al.*, 1995), which store carbon in the form of oil in oil bodies synthesized through the triacyl glycerol pathway. Genes coding for enzymes involved in ricinoleic acid and fatty acids biosynthesis have been identified clearly in castor and *Arabidopsis* seeds respectively. Array-based expression analyses from developing cereal

seeds, which in contrast to *Arabidopsis* store mainly carbohydrates in the endosperm instead of oil in the cotyledons, have not been reported yet. Therefore, we used cDNA clones from developing barley caryopsis and EST (expressed sequence tag) data derived thereof (Michalek *et al.*, 2002) to establish the cDNA array technology and analysed gene expression in maternal and filial tissues during the pre-storage and the ongoing storage phase of the barley grain. The initiatives of transcriptome analysis with large scale EST program specific for barley seed development will help to understand the developmental events and catalogue genes expressed in different tissues of barley caryopsis during developmental processes. By using barley caryopses ESTs as resource, expression patterns were studied during early caryopsis development based on 700 EST macro array (see Chapter 1; Sreenivasulu *et al.*, 2002). Although some glimpse were obtained from pre-storage phase of caryopsis development, the biosynthetic pathways responsible for accumulation of major seed storage components have to be studied with reference to the coordination of gene networks existing between maternal and filial tissues during early seed development, which is largely unknown. The foregoing discussion clearly demonstrates the need to understand the biological events of early seed development at the molecular level.

Considering these, the objectives of the present study have been considered as follows:

- (i) To identify a cluster of genes co-expressed during specific phases in maternal and filial tissues of caryopses development (0-12 DAF).
- (ii) To analyse the network of gene expression between maternal and filial tissues during the early and mid phase of barley seed development special emphasis has been given for the analysis of transcripts encoding enzymes of the glycolysis and sucrose to starch pathway during these phases of barley seed development.

2.2 RESULTS

2.2.1 Barley seed development: seed morphology and tissue preparation

After fertilization the developing barley caryopsis increases in length between 0 to 7 DAF (days after flowering). From 7 DAF onwards, the fresh weight increases drastically. The developing caryopsis consists of the maternal tissue mainly the pericarp and the filial endosperm and embryo. During early development, the caryopsis consists predominantly of maternal tissues starting their development before anthesis. Conspicuous elements of the pericarp (see Fig. 8) are the main vascular tissue bundle (VT), through which assimilates reach the grain, the nucellar projection cells (NP) releasing the assimilates into the endospermal cavity, the maternal outer and inner integuments, each composed of two cell layers, and the mono layered nucellar epidermis. These cell layers surround the diploid embryo and the triploid endosperm. Two cuticles placed between the two integuments as well as the inner integument and the nucellar epidermis separate the filial endosperm/embryo from the maternal tissue, except at the area of the main vascular bundle. To allow uptake of assimilates into the filial tissues, specific endospermal transfer cells (ET) are differentiated beginning at 4 DAF (for an electron microscopical characterization see Weschke *et al.*, 2000). These cells, localized in front of the nucellar projection are part of the maternal-filial boundary of the caryopsis. The maternal tissues, especially those surrounding the filial tissue grow very rapidly in the longitudinal direction during early grain development and in more transversal orientation during filling phase (Fig. 9). Parallel to the growth of the maternal tissues, the filial starchy endosperm expands very rapidly; later in development it accumulates storage products. During the early phase of storage product accumulation in endosperm the pericarp tissue reduces drastically. The caryopsis development of the barley variety “Barke” as well as hand-dissected maternal and filial tissue fractions from 0-12 DAF (ie from the pre-storage until initial storage phase) is depicted in Fig. 9. The upper panel shows the pollinated female gametophyte (0 DAF) and developing caryopses (2-12 DAF). In the lower panel, the two tissue fractions the maternal (pericarp) and the filial fraction (containing endosperm and embryo) are shown (Fig. 9). During 0 and 2 DAF, the filial tissue (left) is completely free of any adherent parts of chlorophyll-containing tissue; 4 DAF, parts of the chlorophyll-containing cell layers are included in the maternal as well as the filial fraction; 6-12 DAF, the green cell layers are nearly exclusively part of the filial fraction. Only the style region of the maternal fraction (always right-hand site of the dissection result) contains small loose patches of green tissue. A detailed knowledge of the tissue and cell types present in the two samples is

of special importance for the proper evaluation of hybridization results (see Sreenivasulu *et al.*, 2002).



Fig. 9 Developing caryopses and hand-dissected maternal (pericarp) and the filial (endosperm and embryo) fractions

The upper panel demonstrates developing caryopses. The lower panel represents hand-dissected maternal and filial tissue fractions of the respective developmental stage next to each other. The days after flowering (DAF) are numbered from 0 to 12. The bar on left side composed of 2.5 mm and on the right side 5mm.

2.2.2 Identification of 16 clusters representing tissue- and development-specific expression profiles during early caryopsis development

To gain deeper insight into the tissue development of barley caryopses we profiled expression data of developing maternal and filial tissues during 0 to 12 DAF. To get the relevant dynamical data and to restrict false positives, the measurements of normalized array data from all experiments were pre-processed by filtering, which show differential expression across the experiments and log transformed (see Chapter 5.1.7 materials and methods section). cDNA fragments in this reduced dataset were selected based on two criteria. To exclude cDNA fragments with signals always close to the background, the normalized non-logarithmic signal intensity had to exceeded 3 arbitrary units (au) for at least one experiment. This value may be compared with the normalized average background of 0.3 au and the maximal signal of 433 au. As second criteria, the ratio between the minimal and the maximal signal for a cDNA fragment across all experiments had to exceed the factor of 10. The filtered data set is comprised of 337 cDNA fragments (approximately 25% of the total clones present on the macroarray), which fulfil both criteria.

To get first insights into interaction processes co-ordinately regulating the development of both, the maternal and the filial part of the caryopsis during early development (0 to 12 DAF), we analyzed all expression values obtained from those 337 cDNA clones, which varied in expression with respect to developmental time and/or tissue in a total of 28 macroarray experiments. Expression profiles of the 337-cDNA fragments in the reduced dataset were clustered using K-means (J-Express; <http://www.molmine.com>) in order to identify the types of expression patterns. 16 clusters (Fig. 10) were selected after initial testing with higher and lower numbers of clusters. This cluster number represents a compromise between the aggregation of unrelated expression profiles and a separation in too many clusters with similar expression profiles. As a consequence of this compromise it was possible to group these clusters with respect to similar expression behaviour but with quantitative differences (compare Fig. 10 clusters 4_1 and 4_2). As a result, six higher order groups could be assembled, and are identified by the first number in the cluster designations given in Figure 11 and Tables 7 - 11. 3 out of 16 clusters (1_1, 1_2 and 1_3) represent genes showing higher expression in pericarp tissue. The remaining 10 clusters represent developmental stage specific expression in filial tissue. Clusters 2_1, 2_2 and 2_3 comprise approximately 59 genes, which show a peak of expression in the pre-storage phase in filial tissue with slight changes in pattern among the three clusters. Up regulation of gene expression in intermediate phase of filial tissue was found in 3_1 and 3_2. Clusters 4_1, 4_2, 4_3, 4_4 and 5 represent genes highly expressed in the filial tissue during storage-phase. Results of the two completely independent sets of experiments (see Material and Methods) are shown in red and blue (for further explanations see legend of Fig. 10). Generally, experiment 1 and 2 are in nearly perfect accordance. However, 14 out of 337 genes (about 4%) depicted remarkable changed expression profiles between experiment 1 and 2, specifically the expression profiles of cluster 6_2 (7 genes) specific for the later development of the maternal tissues vary greatly between experiment 1 and 2, and the same is true to a lower extent for the maternal- as well as the filial-specific expression profiles of cluster 6_3 (7 genes). In cluster 6_3, the difference between experiment 1 and 2 is essentially caused by 4 out of the 7 cluster members, coding for different types of heat shock proteins. In cluster 6_2, only one out of the 7 members encodes a stress protein (HY05N18, heat shock cognate 80) whereas the annotated sequences of three others (HY04K18, HY05J01, HW02J07) hint to the regulation of cell wall

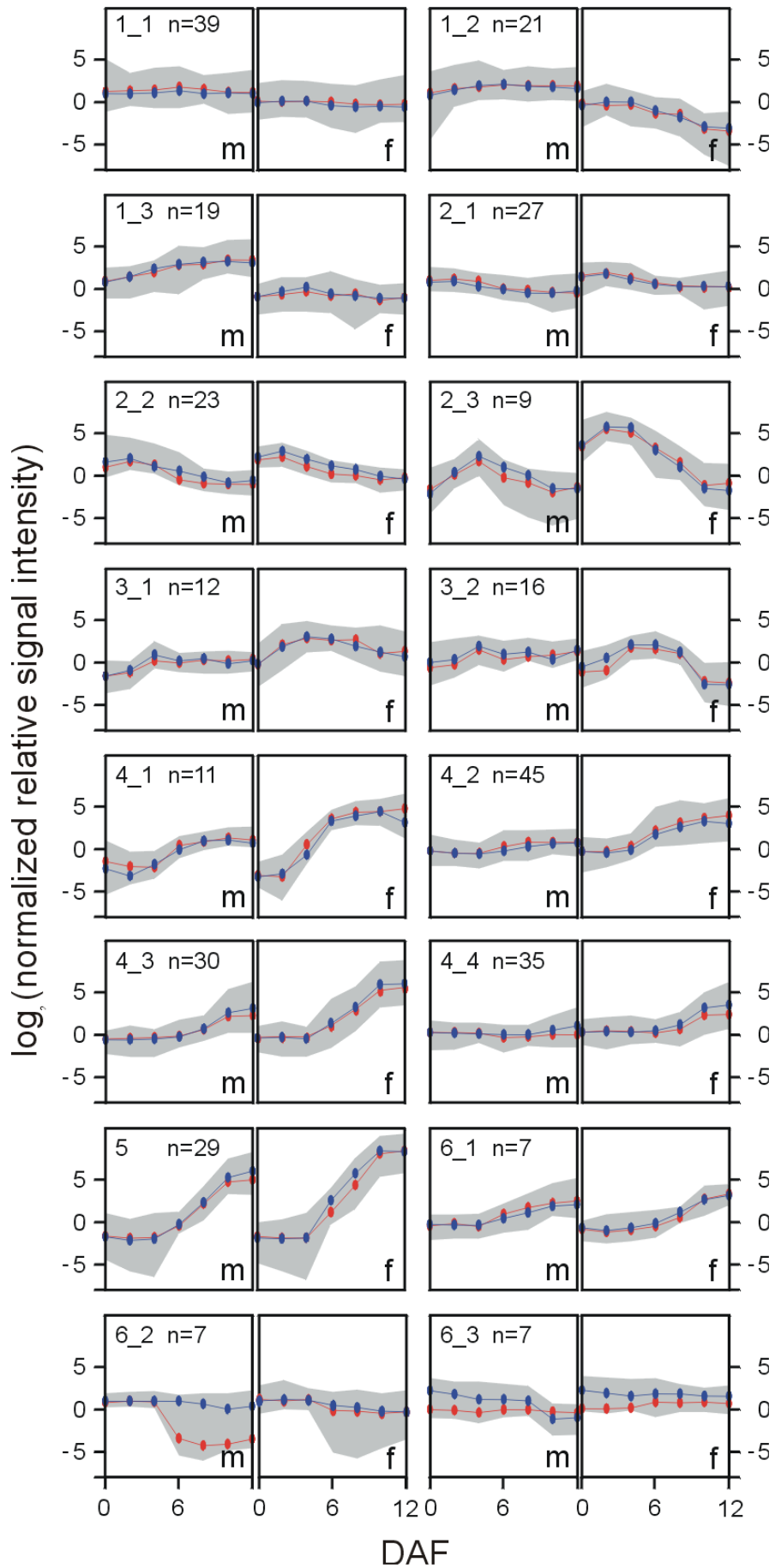


Fig.10 Tissue and development-specific expression profiles identified by k-mean cluster analysis

The 16 clusters represent 337 EST clones showing distinct expression profiles. They are grouped by numbers (top of every cluster). The numbers indicate: First number, clusters with similar profiles grouping together; second number, member number within the cluster; n, number of genes belonging to a specific cluster. The expression clusters specific for the maternal (m) or the filial fraction (f) are placed side-by-side. Every experiment necessary to generate this figure was repeated at least twice. The lines shown in red and blue in every single cluster demonstrate the median Log₂ value of experiment 1 and 2, respectively. The red and blue dots are calculated by using the median Log₂ value of the normalized expression intensity of every gene being member of the respective cluster at one of the defined time points (between 0 and 12 DAF). The areas shadowed in gray symbolize the space between the most outlying members of the respective cluster. The y-axis scaling represent Log₂ values of normalized signal intensities.

biosynthesis. The most outstanding candidate (HY09K06) has homology to a gene encoding an agamous-like mads box protein from *A. thaliana*. The up regulation of expression of stress genes only in experiment 1 (blue) speaks for changes in the environmental conditions during caryopses development noticed by the plants, although the plants were grown in phytochambers with identical environmental conditions.

2.2.3 Identification of functional classes of genes expressed specifically in pericarp tissue during caryopses development

A distinct set of 79 genes is specifically expressed to a higher level in the maternal pericarp tissue with comparison to filial one (Fig. 10; cluster 1_1, 1_2 and 1_3). The major class of genes found to be up regulated specifically in the pericarp (45%, Fig. 11, Table 1) exhibits no significant homology to data bank entries and is therefore of special interest. The major groups of identified genes are related to storage product synthesis namely carbohydrate metabolism (group 1), lipid metabolism (group 2) and degradation process represented by proteases (group 12). As expected, carbohydrate metabolic genes are highly expressed during 0-4 DAF in pericarp (Table 7; see Fig. 15 sugar to starch pathway). These findings underline the importance of the pericarp as a transient storage tissue. The k-mean cluster 1_1 represents genes with higher expression in pericarp tissue during early development (0-4 DAF). The pericarp-specific clusters 1_2 and 1_3 are characterized by a peak of expression, especially during the later stages of pericarp degeneration (8 to 12 DAF). No significant expressions of these transcripts were detected in the filial fraction (Fig. 10). We have chosen the pericarp-specific clusters 1_2 and 1_3 to visualize quantitative differences in gene expression in red and green colour as introduced by the Eisen *et al.*, 1998 (Fig. 12). Genes enclosed in the cluster groups 1_2 and 1_3 represent mainly classes of genes related to degradation processes such as proteases (cysteine proteinase 1, vacuolar processing enzyme, serine

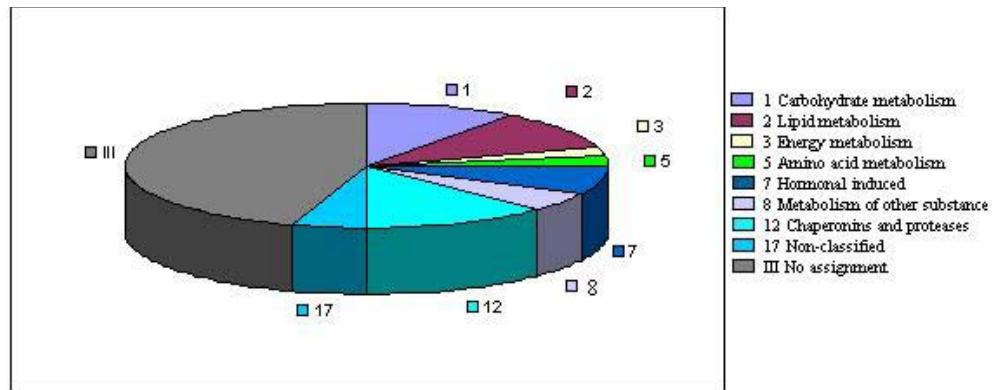


Fig. 11 Groups of genes specifically expressed in the maternal tissue (0-12 DAF)

Name identification of the functional classes is presented on the right hand side.

e_00_1
e_00_2
e_02_1
e_04_1
e_02_2
e_04_2
e_06_1
e_08_1
e_06_2
e_08_2
e_10_1
e_12_1
e_10_2
e_12_2
p_00_1
p_00_2
p_02_1
p_02_2
p_04_1
p_04_2
p_06_1
p_06_2
p_08_1
p_08_2
p_10_1
p_12_1
p_10_2
p_12_2

	cysteine proteinase 1 (maize)
	cysteine proteinase 1 (maize)
	NSH (excinuclease abc subunit, salmonella)
	estradiol 17 beta-dehydrogenase 4 (rat)
	NSH (hormone sensitive lipase, human)
	glutathione s-transferase 1 (wheat)
	0.0000
	serine carboxypeptidase (barley)
	lipxygenase 1 (barley)
	gibberellin-regulated protein 3 (arabidopsis)
	catalase isozyme 2 (barley)
	NSH (endo-1,4-beta-glucanase 4, bacillus)
	aspartic proteinase (barley)
	argonaute protein (arabidopsis)
	NSH (branched-chain amino acid aminotransferase, methanococcus)
	NSH (ribonucleoprotein, fruit fly)
	cobalamin-independent methionine synthase isozyme
	nonspecific lipid-transfer protein 5 (rice)
	fructokinase (potato)
	nonspecific lipid-transfer protein 4.1 (barley)
	NSH (zinc finger protein 40 transcription factor alphaa-crybp1, mouse)
	NSH (hypothetical 48.5 kda protein, caenorhabditis elegans)
	NSH (trimethylamine oxidase, escherichia coli)
	NSH (hypothetical 137.2 kda protein, fission yeast)
	brassinosteroid-regulated protein (soybean)
	probable nadp-dependent oxidoreductase p1 (arabidopsis)
	NSH (legumin b, garden pea)
	tonoplast intrinsic protein (common tobacco)
	NSH (insulin receptor substrate-2, human)
	NSH (keratin, ultra high-sulfur matrix protein human)
	vacuolar processing enzyme (sweet orange)
	cell wall invertase
	NSH (mucoropepsin precursor, rhizomucor)
	NSH (chaperone protein dnak, myxococcus)
	NSH (anter-specific proline-rich protein, arabidopsis)
	nonspecific lipid-transfer protein 4 (rice)

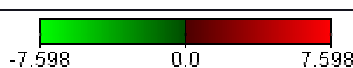


Fig. 12 Upregulation of gene expression (cluster 1_2 and 1_3) in the maternal fraction demonstrated by the Eisen method.

Genes expressed to high (red) or low intensity (green) were selected from the clusters 1_2 and 1_3. The bright-red, red, green and bright-green colour (scale represented on the bottom of the figure) were calculated by using the Log2 value of the normalized expression intensity of every gene being member of the respective cluster at one of the defined time points (between 0 and 12 DAF). Independent repetition of the complete experimental series done to generate this figure was represented by 1 and 2 (experiment 1 and 2). Expression intensities specific for the maternal pericarp and the filial embryo sac fraction containing endosperm and embryo were labelled by “p” and “e”, respectively. For instance, p_02_1 (see top of the figure) means: expression intensity of the respective genes of that column estimated for the maternal pericarp fraction of developing caryopses at 2 (02) DAF within the first (1) series of experiments. NSH-represents non significant homology clones, whose BLAST scores are fairly low.

Table 7 Members of cluster 1_1, 1_2 and 1_3 showing higher expression in pericarp tissue

Cluster Id	EST-id	putative function	assignment	EST cluster
Regulatory genes				
1_1	HY05H16	DNAj protein homolog 2 (leek)	potential	
1_1	HY02D05	DNAj protein homolog (atriplex)	secure	cl-134 ct-198
1_1	HY02F10	60s ribosomal protein l40 (rice)	secure	cl-153 ct-218
1_1	HY01E17	histidyl-trna synthetase (pyrococcus)	potential	
1_1	HY07I05	actin depolymerizing factor (trumpet lily)	potential	cl-735 ct-866
proteases				
1_1	HY05M15	ubiquitin-conjugating enzyme (tomato)	secure	cl-58 ct-626
1_1	HY09E10	cathepsin b-like cysteine proteinase precursor (blood fluke)	secure	cl-55 ct-98
1_2	HK03G06, HK03G06	cysteine proteinase 1 (maize)	secure	
1_2	HY07K19, HW01G04	cysteine proteinase 1 (maize)	secure	cl-75 ct-881
1_2	HY05P07	vacuolar processing enzyme (sweet orange)	potential	cl-1871 ct-23
1_3	HK04D21	serine carboxypeptidase (barley)	potential	
1_3	HY10O06	aspartic proteinase (barley)	secure	cl-966 ct-113
carbohydrate metabolism				
1_1	HY01A03	β -amylase (wheat)	secure	cl-1 ct-1
1_1	HY03H04	β-amylase (wheat)	secure	cl-1 ct-1
1_1	HY07C03	glucan endo-1,3-beta-glucosidase (barley)	secure	cl-1775 ct-1934
1_1	HK04H22	glucokinase (escherichia coli)	secure	cl-1626 ct-1781
1_2	HET1	hexose transporter 1	potential	
1_2	CWINV	cell wall invertase	potential	
1_3	HY05O10	fructokinase (potato)	secure	cl-512 c-t63
lipid metabolism				
1_1	HY03C16	acyl-coa-binding protein (fritillaria)	secure	cl-28 ct-368
1_2	HY02E15	lipoxygenase 1 (barley)	secure	cl-123 ct-184
1_2	HY07L03	nonspecific lipid-transfer protein 4 (rice)	secure	cl-752 ct-883
1_3	HY10O23	nonspecific lipid-transfer protein 5 (rice)	potential	cl-554 ct-674
1_3	HK04H17	nonspecific lipid-transfer protein 4.1 (barley)	secure	cl-1658 ct-1816
inositol phosphate metabolism				
1_1	HY08E09	myo-inositol-1-phosphate synthase (spirodela)	secure	cl-164 ct-1796
1_1	HY05F22	myo-inositol-1-phosphate synthase (spirodela)	secure	cl-29 ct-65
hormonal regulated genes				
1_2	HY05P23	estradiol 17 beta-dehydrogenase 4 (rat)	potential	cl-69 ct-734
1_3	HY09I02	gibberellin-regulated protein 3 (arabidopsis)	potential	cl-891 ct-127
1_2	HK03J06	brassinosteroid-regulated protein (soybean)	secure	cl-1124 ct-1264
energy production				
1_1	HY01A07	peptidyl-prolyl cis-trans isomerase (maize)	secure	cl-3 ct-3
1_1	HY04M20	peptidyl-prolyl cis-trans isomerase (maize)	secure	cl-3 ct-3
1_1	HY07G15	peptidyl-prolyl cis-trans isomerase, chloroplast precursor (broad bean)	secure	
1_1	HY09J04	ATP synthase beta chain, mitochondrial (maize)	secure	cl-894 ct-13

1_1	HY03N13	cytochrome p450 71b2 (arabidopsis)	potential	cl-1821 ct-198
		chloroplast metabolism (energy metabolism)		
1_2	HY05B22, HY05B22	probable NADP-dependent oxidoreductase p1 (arabidopsis)	potential	cl-56 ct-68
		antioxidative enzymes		
1_2	HY01C15	glutathione s-transferase 1 (wheat)	potential	cl-2 ct-5
1_3	HY08D04	catalase isozyme 2 (barley)	secure	cl-279 ct-367
		methionine metabolism (amino acid metabolism)		
1_3	HY05K19	cobalamin-independent methionine synthase isozyme	secure	cl-148 ct-212
1_1		other proteins		
1_1	HY06P18	caj1 protein (baker's yeast)	potential	cl-69 ct-819
1_1	HY05E15	dihydroflavonol-4-reductase (arabidopsis)	potential	
1_1	HY03E16	sorbitol dehydrogenase (rat)	potential	cl-254 ct-342
1_1	HW01N21	dehydrin cor410 (wheat)	secure	cl-1897 ct-256
		non-classified		
1_2	HY08I05	tonoplast intrinsic protein (common tobacco)	secure	cl-829 ct-964
1_3	HY09N04	argonaute protein (arabidopsis)	secure	cl-8 ct-934
		non-significant homology		
1_1	HK04B02	dihydrolypoamide dehydrogenase, mitochondrial precursor (garden pea)	none	
1_1	HY05N14	myosin ic heavy chain (amoeba)	none	
1_1	HY10M15	potassium channel protein 1 (fruit fly)	none	cl-39 ct-79
1_1	HY05D22	hypothetical 59.6 kda protein (baker's yeast)	none	
1_1	HY06P19	b2 protein (carrot)	none	cl-1844 ct-23
1_1	HY05G05	calcium-binding mitochondrial protein (fruit fly)	none	
1_1	HY06G03	blue copper protein precursor (garden pea)	none	cl-641 ct-768
1_1	HY07P23	no blast hit	none	cl-781 ct-915
1_1	HY02H12	zinc finger protein 90 (mouse)	none	cl-18 ct-248
1_1	HY06E13	d-ribose-binding protein precursor (bacillus)	none	cl-63 ct-757
1_1	HY09N11	s-adenosylmethionine (haemophilus)	none	cl-95 ct-141
1_1	HY08A18	heat shock factor protein 3 (chicken)	none	
1_1	HY07O10	DNA-directed rna polymerase beta' chain (pseudomesenteroides)	none	cl-772 ct-96
1_1	HY05H20	large tegument protein (herpesvirus type 1)	none	
1_2	HY02D04	legumin b (garden pea)	none	cl-133 ct-196
1_2	HY03B06	insulin receptor substrate-2 (human)	none	cl-269 ct-357
1_2	HY10J06	keratin, ultra high-sulfur matrix protein (human)	none	cl-269 ct-357
1_2	HY03G16, HY03G16	excinuclease abc subunit (salmonella)	none	cl-3 ct-389
1_2	HY03J19	hormone sensitive lipase (human)	none	cl-327 ct-432
1_2	HY03D09	mucoropepsin precursor (rhizomucor)	none	cl-285 ct-374
1_3	HK05C07	trimethylamine oxidase (escherichia coli)	none	
1_3	HK01E14	chaperone protein dnak (myxococcus)	none	cl-424 ct-536
1_3	HY06M01	hypothetical 137.2 kda protein (fission yeast)	none	cl-674 ct-83
1_3	HY08B02	anter-specific proline-rich protein (arabidopsis)	none	cl-785 ct-919
1_3	HK03G15	zinc finger protein 40 (transcription factor alpha-crybp1) (mouse)	none	
1_3	HY04P23	hypothetical 48.5 kda protein (caenorhabditis elegans)	none	cl-477 ct-591
1_3	HY08J12	branched-chain amino acid aminotransferase (methanococcus)	none	cl-668 c-t797
1_3	HY08P04	endo-1,4-beta-glucanase 4 (bacillus)	none	
1_3	HY05D10	ribonucleoprotein (fruit fly)	none	cl-564 ct-684

Cluster numbers given at the left-hand side of the table originate from Figure 10. The letters HY, HW and HK within the EST-id designate clones originating from the caryopses, root and etiolated seedling specific cDNA library, respectively. The putative function of the respective genes was identified by BLASTX2 searches. Assignment was done based on annotation as described in Material and Methods. Sequences having the same cluster id (cl) but different contig numbers (ct) building up within one and the same cluster a separate family of genes having higher homology to each other than to other members of the cluster. For expression pattern and signal intensity values see Fig. 11.

carboxypeptidase, aspartic proteinase), lipid transfer proteins (nonspecific lipid transfer protein 4, 4.1 and 5) and genes connected with hormonal regulation (gibberellin-regulated protein3, bassinosteroid-regulated protein, estradiol dehydrogenase).

2.2.4 Identification of functional classes of genes expressed in the filial fraction during pre-storage and storage phase of developing caryopses

Clusters 2, 3, 4 and 5 represent 237 genes with higher expression levels in the filial tissue fraction compared to maternal pericarp fraction. The functional classes of genes expressed specifically in filial tissue fraction during pre-storage and storage phase of the caryopsis development are depicted in Fig. 13. The spectrum of genes preferentially detected by the probe generated from the filial fraction (Fig. 13) is significantly different from that described for the maternal tissues (Fig. 11). Genes with no data base hits are less common (21 %). Genes involved in carbohydrate, amino acid and energy metabolism play a bigger role whereas lipid metabolism genes are not evident at all. Worth to mention is the group of inhibitor genes having protection functions against degradation of starch and storage proteins during seed maturation (see below). These genes are expressed in later development also in the maternal fraction, but to a significantly lower level.

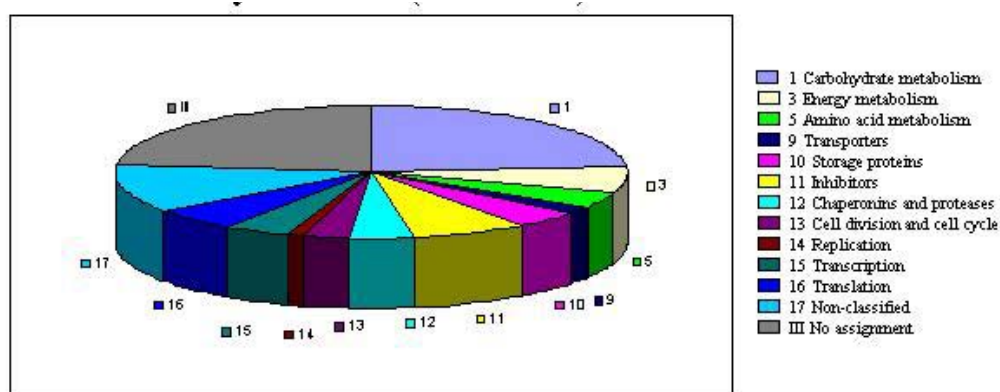


Fig. 13 Groups of genes specifically expressed in filial tissues (0 to 12 DAF)

The name of functional classes was presented on the right hand side.

Table 8 Members of cluster 2_1, 2_2 and 2_3 showing higher expression in the filial tissue during the pre-storage phase (For further explanations see legend of Table 7)

Cluster Id	EST-id	putative function	assignment	EST cluster
regulatory genes				
2_1	HY03A15	DNA replication licensing factor mcm3 (maize)	secure	cl-26 ct-348
2_1	HY02N14	meiotic recombination protein dmc1 (trumpet lily)	secure	
2_1	HY07L02	DNAj protein homolog anj1 (atriplex)	secure	cl-134 ct-197
2_1	HY01N04	zinc finger protein cth2 (baker's yeast)	potential	
2_1	HY02A19	elongation factor 2 (sugar beet)	secure	cl-381 ct-489
2_1	HY08L22	elongation factor 1-alpha (wheat)	secure	cl-5 ct-22
2_1	HY08O22	histone H2a. (parsley)	secure	cl-116 ct-176
2_1	HY07J01	histone H2a (parsley)	secure	cl-116 ct-176
2_2	HY02B14	histone H2a.1 (wheat).	secure	cl-118 ct-178
2_2	HY08A16	histone H2a.1 (wheat).	secure	cl-567ct-688
2_2	HY02K17	histone H2a.2.2 (wheat).	secure	cl-213 ct-285
2_2	HY04A04	histone H3. (wheat)	secure	cl-223 ct-39
2_2	HY02B11	histone H4.(wheat)	secure	cl-5 ct-24
2_2	HY05H10	tubulin β -1 chain (wheat)	secure	cl-55 ct-623
2_2	HY05C21	cell division control protein nda4 (fission yeast)	potential	
2_3	HY07E21	replication factor C 38 kD, subunit (human)	potential	cl-1488 ct-1638
carbohydrate genes				
2_1	HY03C18	hexokinase 2 (potato)	potential	
2_1	HY02J07	6-phosphofruktokinase (castor bean)	potential	cl-11 ct-4
2_1	HY08G16	fructose-bisphosphate aldolase 1, chloroplast (garden pea)	secure	cl-6 ct-13
2_1	HY02G23	endoglucanase precursor (kidney bean)	potential	
2_2	HW02F11	vacuolar invertase 1 (maize)	potential	cl-172 ct-1212
2_2	HW01H17	cell wall invertase (garden pea)	secure	
2_2	HY02J11	beta-1,3- endoglucanase (barley)	secure	cl-1775 ct-1934
glycolysis genes				
2_2	HY03D17	pyruvate kinase, cytosolic isozyme (common tobacco)	secure	cl-773 ct-97
2_2	HY04B15	alcohol dehydrogenase 1 (pearl millet)	secure	cl-1831 ct-199
amino acid metabolism genes				
2_2	HW01L14	peroxidase p7 (turnip)	secure	
2_3	HY10H08	cationic peroxidase 1 precursor (peanut)	potential	
2_2	HY02E22	alanine aminotransferase 2 (proso millet)	secure	
photosynthetic genes				
2_1	HY02F14	magnesium-chelatase subunit (common tobacco)	secure	cl-1763 ct-1922
stress genes				
2_1	HY04D19	heat shock cognate 70 kD protein 1 (arbidopsis)	secure	cl-24 ct-59
2_1	HY01D06	heat shock cognate 70 kD protein (petunia)	secure	
2_1	HY05F13	heat shock cognate 70 kD protein 1 (arabidopsis)	secure	cl-24 ct-58
others				
2_1	HY01F06	protein At2g41620 (arabidopsis)	potential	
2_1	HY01C19	ring finger protein 12 (human)	potential	cl-171 ct-1869
2_1	HW08O24	auxin-repressed 12.5 kD protein (strawberry)	potential	
2_1	HY10G22	hypothetical 38.2 kD protein (escherichia coli)	secure	
2_1	HY04F10	phnb protein (escherichia coli)	secure	
2_2	HY01M16	acidic proline-rich protein prp25 precursor (rat)	potential	cl-547 ct-667
2_2	HY06H10	ref(2)p protein (fruit fly)	potential	
2_2	HY05I22	ferritin 1 precursor (maize)	secure	cl-497 ct-612
2_2	HY04O22	ubiquitin carboxyl-terminal hydrolase 5 (mouse)	potential	
2_3	HY03I14	mabinlin ii precursor (mabinlang)	potential	cl-251 ct-339
2_3	HY07E10	nonspecific lipid-transfer protein, aleuron- specific (barley)	potential	cl-716 ct-847
no putative function				
2_1	HY04G02	anthocyanin regulatory r-s protein (maize)	none	cl-419 ct-529
2_1	HY07I11	14-3-3 protein homolog (neospora)	none	
2_1	HW06F11	retinoblastoma-like protein 1 (human)	none	cl-14 ct-1549
2_1	HY08M07	valyl-tRNA synthetase (neisseria)	none	

2_1	HY05O16	probable metabolite transport protein csbc (bacillus)	none	cl-65 ct-19
2_1	HY06C15	dTDP-glucose 4,6-dehydratase (neisseria)	none	cl-621 ct-747
2_2	HY07P04	hypothetical protein kiaa0136 (human)	none	cl-775 ct-99
2_2	HY03L17	olfactory receptor-like protein (dog)	none	
2_2	HY04F08	hypothetical 145.8 kda protein (fission yeast)	none	
2_2	HY04K01	exodeoxyribonuclease v alpha chain (haemophilus)	none	
2_2	HY03H19	lysozyme precursor (silk moth)	none	cl-311 ct-413
2_3	HY07C10	von willebrand factor precursor (dog)	none	cl-72 ct-831
2_3	HY09L21	nuclear transition protein 2 (pig)	none	cl-665 ct-794
2_3	HY09L18	NOF1 protein (human)	none	
2_3	HY04C02	hypothetical pe-pgrs family protein rv3508 (mycobacterium)	none	
2_3	HY07K16	2-oxoglutarate synthase subunit kora (archaeoglobus)	none	cl-749 ct-88

Time-scale dependent modulation of gene expression belonging to various classes was observed in the developing filial tissue of barley (Fig. 11). Three distinct phases of development could be designated based on the difference in the expression profile viz., pre-storage, intermediate and initial-storage phases. The pre-storage phase (0-4 DAF) is characterized by a peak of expression (cf. clusters 2_1, 2_2 and 2_3) especially in the filial fraction and no significant expression of storage-specific transcripts (cf. clusters 4_1 – 4_4 and 5, respectively) were detected. More than 25% of the member genes in cluster group 2 are involved in processes necessary to regulate cell division and elongation processes in the cellularizing endosperm and embryo tissues. Examples from cluster 2_1 and 2_2 are: cell division control protein NDA4, meiotic recombination factor DMC1, replication factor C, DNA replication licensing factor mcm3, histones H2a, H2a1, H2a2, H3 and H4 and elongation factor 1- α . Cluster 2_3 contains mostly candidates for which no secure function could be annotated (for further information see Table 8). The pre-storage phase of both, maternal and filial fraction is characterized by a high hexose concentrations mediated by high activity of vacuolar as well as cell wall-bound invertases (Weschke *et al.*, 2002). As expected, those genes are highly expressed together with hexokinases (see carbohydrate genes, Table 7). Hexokinases are necessary to phosphorylate the hexoses resulting from invertase activity. Additionally, some glycolysis genes as well as genes of the amino acid metabolism are expressed.

Table 9. ESTs included in cluster 3_2 showing upregulation of expression in the intermediate phase of development in filial tissues. (For further explanations see legend of Table 7)

Cluster Id	EST-id	putative function	assignment	EST cluster
regulatory genes				
3_2	HY03H10	developmentally regulated GTP-binding protein 1 (african clawed frog)	potential	cl-36 ct-396
carbon fixation				
3_2	HY09O01	phosphoribulokinase (wheat)	secure	cl-97 ct-143
3_2	HY07K23	ribulose biphosphate carboxylase small chain (wheat)	secure	cl-487 ct-62
3_2	HY06P01	ribulose biphosphate carboxylase large chain (wheat)	secure	cl-119 ct-179
3_2	HY02B17	ribulose biphosphate carboxylase large chain (wheat)	secure	cl-119 ct-18
3_2	HY07N21	plastocyanin precursor (barley)	secure	cl-769 ct-92
3_2	HY02C13	chlorophyll a-b binding protein 3c precursor (tomato)	secure	cl-37 ct-76
3_2	HY05I05	oxygen-evolving enhancer protein 2, chloroplast precursor (wheat)	secure	cl-387 ct-496
3_2	HY05D21	oxygen-evolving enhancer protein 1, chloroplast precursor (common tobacco)	secure	cl-565 ct685
3_2	HY02P17	photosystem ii 22 kD protein (tomato)	secure	
pentose phosphate cycle				
3_2	HY08K09	glucose-6-phosphate 1-dehydrogenase, cytoplasmic isoform (potato)	secure	cl-837 ct-972
oxidative phosphorylation				
3_2	HY02P15	ATP synthase 6 kda subunit, mitochondrial (potato)	secure	
others				
3_2	HY05A19	O66929 aquifex aeolicus. uridylylate kinase (ec 2.7.4.-) (uk) (uridine monophosphate kinase) (UMP kinase). 10/2000	potential	
no functional classification				
3_2	HY04D16	putative amino-acid permease (fission yeast)	none	
3_2	HK04P15	hypothetical 50.6 kda protein in the 5'region of gyra and gyrb (haloferax)	none	cl-569 ct-693
3_2	HY07M23	exo-poly- α -D-galacturonosidase precursor (erwinia)	none	

Up regulation of gene expression in the intermediate phase was found in only one (3_2) out of the 16 clusters shown in Fig. 10. A characteristic increase in gene expression of cluster 3_2 is visible in the filial part, a rather weak peak only 4 DAF was found for the maternal fraction. Surprisingly, 9 out of 16 genes showing up regulation in this intermediate developmental phase code for proteins associated to photosynthetic reactions (cf. Table 9). Two further candidates characterised by secure annotation, HY08K09 and HY02P15, hint to energy flow via the pentose phosphate cycle (glucose-6-phosphate 1-dehydrogenase) and ATP production, respectively. Somewhat outstanding appears the amino acid permease, HY04D16, classified as being non-secure in the annotation process, but having clear transporter characteristics (12 membrane-spanning domains) which was shown by analysis of the full-length sequence (M. Miranda, personal communications). The up regulation of genes involved in photosynthesis between 4 to 8 DAF (Fig. 14) is an interesting and unexpected observation giving some evidence for the caryopsis-own photosynthetic activity in a specific developmental phase. This could further be explained to some extent by the green tissue contamination existing during tissue separation (see section of tissue separation for details). Young developing

caryopses contain a layer of chloroplast-containing cells surrounding the developing embryo sac (i.e., from 4DAF onwards the chloroplast-containing cell layers stick to the embryo sac fraction whereas before the green cell layers were found to be connected to the parenchyma cells of the pericarp).

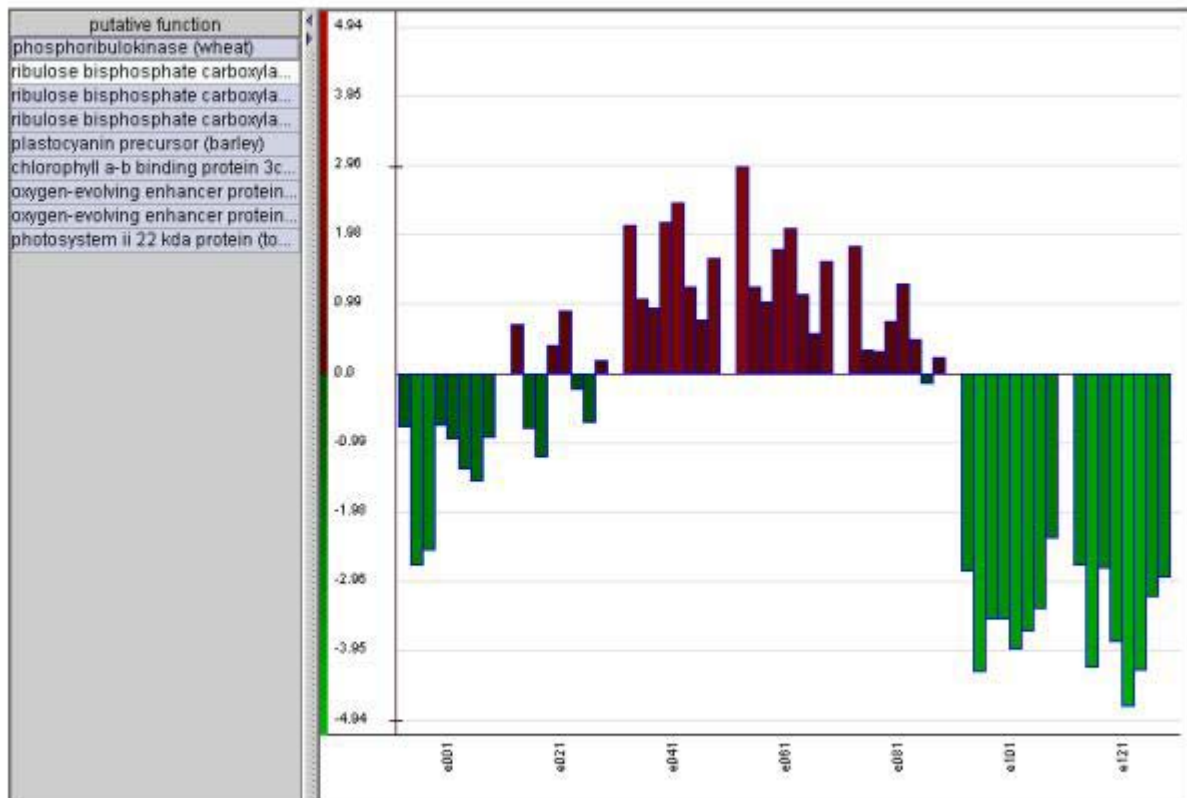


Fig. 14 Expression of photosynthetic genes in the filial fraction of the caryopsis during 4 to 8 DAF

Expression intensities of every genes represented in columns were given in log values. The labels, for instance e021 (see bottom of the figure) means: expression intensity of the genes estimated for filial embryo sac fraction (e) of developing caryopsis at 2 (02) days after flowering within the first (1) series of experiments.

During the storage phase (10 - 12 DAF) genes grouped in cluster 4_1, 4_3 and 5 (Fig. 11) are dramatically up regulated in the filial tissue. Cluster group 4 represents mainly genes whose products control the accumulation of starch (i.e. genes encoding sucrose synthase 1, sucrose synthase 2, ADP-glucose pyrophosphorylase large subunit, ADP-glucose pyrophosphorylase small subunit, UDP-glucose 6-dehydrogenase, hexokinase 1 and hexokinase 3; for further candidates see Table 10), fructose and mannose metabolism (6-phosphofructokinase α and β subunits), glycolysis (glyceraldehyde 3-phosphate dehydrogenase, the cytosolic isoforms of

pyruvate kinase and phosphoglycerate kinase), amino acid metabolism (cytosolic isoforms of aspartate aminotransferase and glutamine synthetase, cysteine synthase, glutamate-1-semialdehyde aminotransferase, early nodulin) and energy production (pyrophosphate-energized vacuolar membrane proton pump, ATPase8, inorganic pyrophosphatase, β -2 subunit of 5'-AMP-activated protein kinase). Remarkably, cluster 4_1 is highly specific for sucrose synthase 2, which is well separated from sucrose synthase 1 represented in cluster 4_2 (Fig. 11 and Table 10). Together with 9 cDNA fragments completely homologous to sucrose synthase 2 from barley, this cluster contains only two cDNA fragments different from sucrose synthase 2. Transcripts encoded by these genes show the most prominent up regulation within the cluster group 4_1 two days before the onset of transcription of storage protein genes. For these fragments, no data base hit could be found (cf. Table 10). Together with a glutenin subunit, cluster 5 contains genes coding for hordein b1, b3 and γ -hordein 3, i.e., some of the most important barley storage protein genes. Additionally, inhibitors of α -amylase and trypsin are up regulated (cf. Table 11), preventing starch and storage proteins degradation. Other storage protein genes, especially the high molecular weight subunit of glutenin as well as genes encoding α -amylase and proteinase inhibitors are found in the cluster group 4 (cf. Table 11).

Table 10. ESTs included in cluster 4_1, 4_2, 4_3 and 4_4 showing up regulation of expression in the storage phase of the filial tissues. (For further explanations see legend of Table 7)

Cluster Id	EST-id	putative function	assignment	EST cluster
regulatory genes				
4_2	HY08F11	histone H1 (tomato)	potential	cl- 31 ct-67
4_2	HY09D22	transcriptional activator HAP5 (baker's yeast)	potential	
4_4	HY02B12	60s ribosomal protein (turnip)	potential	cl-139 ct-23
4_4	HY06I07	elongation factor 2 (sugar beet)	secure	cl-174 ct-1863
4_4	HY06K20	eukaryotic initiation factor 4a (rice)	secure	
4_4	HY01L10	DNA-binding protein hexbp (leishmania)	secure	cl-74 ct-126
starch metabolism				
4_2	HY10D02	sucrose synthase 1 (barley)	secure	
4_2	HY09D18	sucrose synthase 1 (barley)	secure	
2_2	HY01F08	sucrose synthase 1 (barley)	secure	
4_2	HY10G10, HY07L04	sucrose synthase 1 (barley)	secure	cl-33 ct-69
4_2	HY01H24, HY05O13, HY01H24,	sucrose synthase 1 (barley)	secure	cl-47 ct-87
4_2	HY07F09, HY07F09, HY10F20,	sucrose synthase 1 (barley)	secure	cl-47 ct-87
4_2	HW08D05, HY03P12	sucrose synthase 1 (barley)	secure	cl-47 ct-87
4_2	HY08H21, HY04L06	sucrose synthase 2 (barley)	secure	cl-128 ct-191
4_2	HY04I11, HY04I11	sucrose synthase 2 (rice)	secure	cl-437 ct-55
4_1	HY09L14, HY09N16, HY07C09,	sucrose synthase 2 (barley)	secure	cl-128 ct-191
4_1	HY06C06, HY09N15, HY07H01	sucrose synthase 2 (barley)	secure	cl-128 ct-191
4_1	HY10D14, HY04D17, HY03J05	sucrose synthase 2 (barley)	secure	cl-322 ct-427cn511
4_2	HY01D18, HY04D04	ADP-glucose pyrophosphorylase large subunit1 (barley)	secure	cl-27 ct-62
4_3, 4_3	HY10G16, HY10G16	ADP-glucose pyrophosphorylase small subunit1 (wheat)	secure	cl-59 ct-12

4_3	HY08N11	ADP-glucose pyrophosphorylase small subunit (barley)	potential	
4_3	HK03F04	ADP-glucose pyrophosphorylase small subunit (barley)	secure	cl-319 ct-424
4_4	HY03B24	UDP-glucose 6-dehydrogenase (soybean)	secure	cl-1795 ct-1954
4_4	HY08N17	hexokinase 1 (spinach)	secure	cl-1539 ct-1692
4_4	HY08N17	hexokinase 1 (spinach)	secure	cl-1539 ct-1692
4_4	HY05M20	(1->3)-beta-glucanase (wheat)	potential	cl-59 ct-627
kinases				
4_2	HY01A21	serine/threonine-protein kinase ask1 (arabidopsis)	secure	cl-6 ct-25
4_3	HY06C05	shaggy-related protein kinase ntk-1 (common tobacco)	secure	cl-466 ct-579
fructose and mannose metabolism				
4_2	HY07D12	6-phosphofructokinase (potato)	secure	cl-542 ct-661
4_3	HY08O12	6-phosphofructokinase (castor bean)	secure	cl-11 ct-41
4_4	HW06P12	6-phosphofructokinase β subunit (castor bean)	secure	
4_4	HW03P06	6-phosphofructokinase β subunit (castor bean)	secure	cl-1738 ct-1897
glycolysis				
4_3	HY03A22	glyceraldehyde 3-phosphate dehydrogenase (yeast)	potential	cl-265 ct-353
4_4	HW02G03	pyruvate kinase, cytosolic isozyme (common tobacco)	secure	
4_4	HY06C21	phosphoglycerate kinase, cytosolic (wheat)	secure	cl-45 ct-85
galactose metabolism				
4_2	HY03H07	α -galactosidase (coffee)	secure	cl-35 ct-395
glyoxylate and carboxylate metabolism				
4_3	HY06L21	aconitate hydratase, cytoplasmic (pumpkin)	secure	cl-672 ct-81
purine metabolism				
4_3	HY03E22	bifunctional purine biosynthesis protein (inosinase)	potential	
lignin biosynthesis				
4_3	HY06G20	cinnamyl-alcohol dehydrogenase (perennial ryegrass)	secure	cl-1769 ct-1928
methane metabolism				
4_2	HY09L19	mitochondrial formate dehydrogenase precursor (potato)	secure	cl-373 ct-481
thiamine metabolism				
4_4	HY02J16	thiazole biosynthetic enzyme 1-2, chloroplast precursor (maize)	secure	cl-21 ct-27
amino acid metabolism				
4_2	HY06L03, HY02N15	aspartate aminotransferase, cytoplasmic (rice)	secure	cl-239 ct-326
4_2	HY04K11	glutamine synthetase cytosolic isozyme 2 (grape)	secure	cl-1848 ct-27
4_4	HY06L08	cysteine synthase (wheat)	secure	cl-669 ct-798
4_4	HY07D13	glutamate-1-semialdehyde aminotransferase (barley)	secure	
4_4	HY01K03	early nodulin 93 (soybean)	potential	cl-64 ct-18
energy production				
4_2	HY06D04	pyrophosphate-energized vacuolar membrane proton pump (barley)	secure	cl-624 ct-75
4_2	HY09E19	ATPase 8, plasma membrane-type (arabidopsis)	secure	cl-789 ct-923
4_2	HY05F08	inorganic pyrophosphatase, vacuolar (mung bean)	secure	cl-624 ct-75
4_2	HY09K05	protein disulfide isomerase (barley)	secure	cl-23 ct-274
4_4	HY02J22	protein disulfide isomerase, endosperm protein (barley)	secure	cl-23 ct-274
4_3	HY05G12, HY05G12, HY05G12	5'-AMP-activated protein kinase, β -2 subunit (human)	potential	
proteases				
4_2	HY04J24	aspartic proteinase oryzasin 1 (rice)	secure	cl-443 ct-556
4_3	HY03C19	serine carboxypeptidase iii precursor (barley)	potential	cl-281 ct-369
4_4	HY02B16, HY02B16	serine carboxypeptidase i precursor (barley)	secure	
4_3	HY06J08	proteasome subunit α -type 5 (rice)	secure	cl-661 ct-79
inhibitor genes				
4_1	HY06E14	P82659 helianthus annuus (common sunflower). flower-specific gamma-thionin precursor (defensin sd2). 10/2000	potential	cl-631 ct-758
4_2	HY03I05	gamma-thionin homolog (petunia)	potential	cl-315 ct-417
4_2	HY05L03	α -amylase/trypsin inhibitor cmd (barley)	secure	cl-58 ct-11
4_3	HY06J10	α -amylase/subtilisin inhibitor precursor (barley)	secure	
4_4	HY07A19	α -amylase inhibitor bdai-i (barley)	secure	cl-25 ct-6
transporter genes				
4_2	HY03H23, HY03H23	potassium uptake protein (escherichia coli)	potential	
4_4	HY01D12	putative protein transport protein (arabidopsis)	potential	cl-26 ct-61
storage proteins				

4_3	HY01J16	glutenin, high molecular weight subunit (wheat)	secure	cl-63 ct-17
4_4	HY01K05	glutenin, high molecular weight subunit (wheat)	secure	cl-63 ct-17
stress genes				
4_2	HK03A01	heat shock protein 83 (japanese morning glory)	potential	cl-719 ct-85
4_2	HY04M11	anter-specific proline-rich protein (arabidopsis)	potential	cl-34 ct-447
4_2	HY10B17	L-ascorbate peroxidase, cytosolic (garden pea)	secure	cl-921 ct-157
4_2	HY09D05	glutathione peroxidase homolog (sweet orange)	secure	cl-874 ct-11
other proteins				
4_3	HY02B21	sex determination protein tasselseed 2 (maize)	potential	cl-121 ct-182
4_3	HY05C12	lin-10 protein (caenorhabditis elegans)	potential	
4_3	HY05G19	mitochondrial uncoupling protein 2 (rat)	potential	
4_3	HY07H03	ring finger protein 12 (mouse)	potential	cl-1489 ct-1639
4_3	HY08D17	centroradialis protein (garden snapdragon)	potential	cl-764 ct-897
4_3	HY03E04	selenium-binding protein 2 (mouse)	secure	cl-177 ct-1866
4_4	HY10K10	hypothetical protein kiaa0017 (human)	potential	
4_4	HY01L24	dynamain (fruit fly)	potential	cl-79 ct-132
no putative function				
4_2	HY09P15	P33363 escherichia coli. periplasmic β -glucosidase precursor (ec 3.2.1.21) (gentiobiase) (cellobiase) (β -D-glucoside glucohydrolase). 10/2000	none	
4_2	HY04O11	P22200 solanum tuberosum (potato). pyruvate kinase, cytosolic isozyme (ec 2.7.1.40). 2/1995	none	cl-467 ct-58
4_2	HY04P01	P52499 candida albicans (yeast). RCC1 protein. 10/2000	none	cl-471 ct-585
4_2	HY06B24	P10674 drosophila melanogaster (fruit fly). fasciclin i precursor (fas i) (fcn). 2/1996	none	
4_2	HW03113	P03071 polyomavirus bk (bkv). large t antigen. 7/1999	none	
4_2	HY09G09	P53807 homo sapiens (human). phosphatidylinositol-4-phosphate 5-kinase type iii (ec 2.7.1.68) (1-phosphatidylinositol-4-phosphate kinase) (pip5kiii) (ptdins(4)p-5- kinase c isoform) (diphosphoinositide kinase). 10/2000	none	
4_1	HY04N22	no blast hit	none	
4_1	HY05J17	wiskott-aldrich syndrome protein interacting protein (human)	0,0000none	
4_3	HY10K02	retinoblastoma binding protein 1 (human)	none	
4_3	HY03G04		none	
4_3	HY03F20		0,0000none	
4_3	HY03E05	P49717 mus musculus (mouse). dna replication licensing factor mcm4 (mouse)	none	
4_3	HY03C04	t-brain-1 protein (mouse)	none	
4_3	HY06E07	rubber elongation factor protein (para rubber tree)	none	
4_3	HY07M21	zinc finger protein (human)	none	cl-763 ct-896
4_3	HY06N23	D-lactate dehydrogenase (yeast)	none	
4_4	HY01O19	α -amylase/subtilisin inhibitor (rasi) (rice)	none	cl-1 ct-155
4_4	HY02J10	homeobox protein hox-a4 (human)	none	
4_4	HY09G09	diphosphoinositide kinase (human)	none	
4_4	HY06K19	hypothetical 46.2 kda protein (baker's yeast)	none	
4_4	HY01O11	npc derived proline rich protein 1 (mouse)	none	cl-96 ct-151
4_4	HY04A17	casein kinase i homolog hhp2 (fission yeast)	none	cl-382 ct-491
4_4	HY05K20	single-strand binding protein (brucella)	none	cl-52 ct-618
4_4	HY02B09	glycophorin-binding protein precursor (plasmodium)	none	cl-1321 ct-1468
4_4	HY03J24	neural wiskott-aldrich syndrome protein (bovine)	none	

Table 11 Members of cluster 5 showing high expression especially in the storage phase of the filial tissues. (For further explanations see legend of table 7)

Cluster-id	EST-id	putative function	assignment	EST cluster
regulatory genes				
5	HY04P15	tubulin β -3 chain (garden pea)	secure	cl-141 ct-25
5	HY06M23	DNA excision repair protein haywire (fruit fly)	potential	cl-645 ct-773
5	HY05K12	nuclear polyadenylated rna-binding protein (baker's yeast)	potential	
5	HY06E05	myb-related protein (moss)	potential	
5	HY08M21	glycyl-tRNA synthetase (arabidopsis)	secure	
inhibitors				
5	HY09N22	trypsin inhibitor cme precursor (barley)	secure	cl-259 ct-347
5	HY02P19	α -amylase inhibitor bmai-1 (barley)	secure	cl-196 ct-265
5	HY06K18	α -amylase/trypsin inhibitor cmb (barley)	secure	cl-314 ct-416
5	HY08P07	α -amylase inhibitor bdai-i (barley)	secure	cl-25 ct-6
5	HY03M02	α -hordothionin (purothionin ii) (barley)	secure	cl-122 ct-183
5	HY04J03	trypsin/factor xiia inhibitor precursor (maize)	potential	cl-439 ct-552
storage protein				
5	HY06G01	b1-hordein (barley)	potential	cl-468 ct-581
5	HY06A05	b3-hordein (barley)	potential	cl-468 ct-582
5	HY07A07	b3-hordein (barley)	secure	cl-468 ct-581
5	HY06E20	γ -hordein 3 (barley)	secure	cl-632 ct-759
5	HY10K04	glutenin, high molecular weight subunit (wheat)	secure	cl-63 ct-17
energy production				
5	HY06M18	inorganic pyrophosphatase (yeast)	potential	cl-637 ct-764
5	HY05G12	5'-amp-activated protein kinase, β -2 subunit (human)	potential	
5	HY05G12	5'-amp-activated protein kinase, β -2 subunit (human)	potential	
5	HY02L08	plasma membrane ATPase 4 (leadwort-leaved tobacco)	secure	cl-789 ct-923
no putative functional classification				
5	HY01D10	ornithine decarboxylase antizyme, long isoform (zebrafish)	none	cl-25 ct-6
5	HY03N12	gamma-interferon inducible thiol reductase precursor (human)	none	cl-353 ct-461
5	HY04M15	periodic tryptophan protein 1 homolog (human)	none	
5	HY08A03	glutenin, high molecular weight subunit (wheat)	none	cl-65 ct-11
5	HY04F23	adenovirus type 2 late 100 kda protein (human)	none	
5	HY04F23	adenovirus type 2 late 100 kda protein (human)	none	
5	HY02H10	prolamin pprol 17(rice)	none	cl-179 ct-247
5	HY04G19	large proline-rich protein bat2 (human)	none	
5	HY08I07	puroindoline-b precursor (wheat)	none	cl-83 ct-965

2.2.5 Carbohydrate metabolism during seed development

2.2.5.1 Expression patterns of genes encoding enzymes of the sucrose-to-starch biosynthetic pathway in maternal and filial tissues

In sink organs like seeds, sucrose is the main pre-requisites for accumulation processes and additionally, source for energy production. Therefore, two pathways were selected for detailed analysis: the sucrose to starch biosynthetic pathway and the sucrose to pyruvate glycolytic pathway (see Fig. 15 and 16). Expression data of all cDNA clones with homology to genes encoding enzymes of the starch and glycolytic pathway were selected and analysed with respect to differences in expression between the two tissues (maternal and filial) during

the pre-storage (0-4 DAF) and storage phase (6-12 DAF) of caryopsis development. The two pathways have in common sucrose cleavage by either invertases or sucrose synthases and phosphorylation of the resulting hexoses to hexose-6-phosphates by different sub-types of hexokinases. Therefore, the mRNA expression profiles of the enzymes included in this first common part of sucrose metabolism are shown only in one (Fig. 15) of the two figures.

The sucrose-to-starch pathway is dominated by two events: sucrose catabolism and conversion of hexoses into starch. The results obtained indicate that during the pre-storage phase (0-4 DAF) the genes involved in starch synthesis are confined to pericarp tissue (cf. Fig. 15). The invertase pathway of sucrose breakdown is predominantly activated in pericarp during 0-4 DAF, which is evidenced by high expression levels of different invertase isoforms (cell wall invertase 1 and vacuolar invertase 1). As shown in a recent paper (Weschke *et al.*, 2002), activity of cell wall-bound and especially vacuolar invertase is high in the early pericarp development. In correspondence to that, high mRNA levels of both enzymes were found in expression analysis. The early peak of expression of the sucrose synthase isoform 3 (SUS3) in early pericarp is remarkable; its function needs to be characterized. The early stage specific expression profiles of 3 different hexokinases (FK1, HK1, HK2) are seen both in maternal and filial tissues between 0-4 DAF. Higher level of expression of fructokinase 2 seems to be specific for pericarp tissue. Genes involved in starch biosynthesis starting with hexose phosphates (PGM to SS2 in Fig. 15, left-hand panel) seem to be co-regulated, leading to the characteristic starch accumulation pattern in early pericarp (cf. Fig. 8 in Weschke *et al.*, 2000). During this period, expression of β -amylase was also observed in the pericarp tissue, which could effect the mobilization of starch into the growing filial tissue (data not shown).

During 0-4 DAF, the filial fraction also encodes enzymes of the invertase mediated sucrose catabolism. Expression of VCINV is rather low and restricted to 4 DAF. The same is true for the pericarp-specific CWINV2, whereas the CWINV1 is higher expressed in the filial tissue during the ongoing storage phase (10-12 DAF). The specific expression profile of the glucokinase transcript is strongly down regulated during later development of the filial tissues, but shows a nearly continuous expression in the pericarp. Remarkably, the up regulation of HK3 expression in later developmental stages of the filial fraction correlates

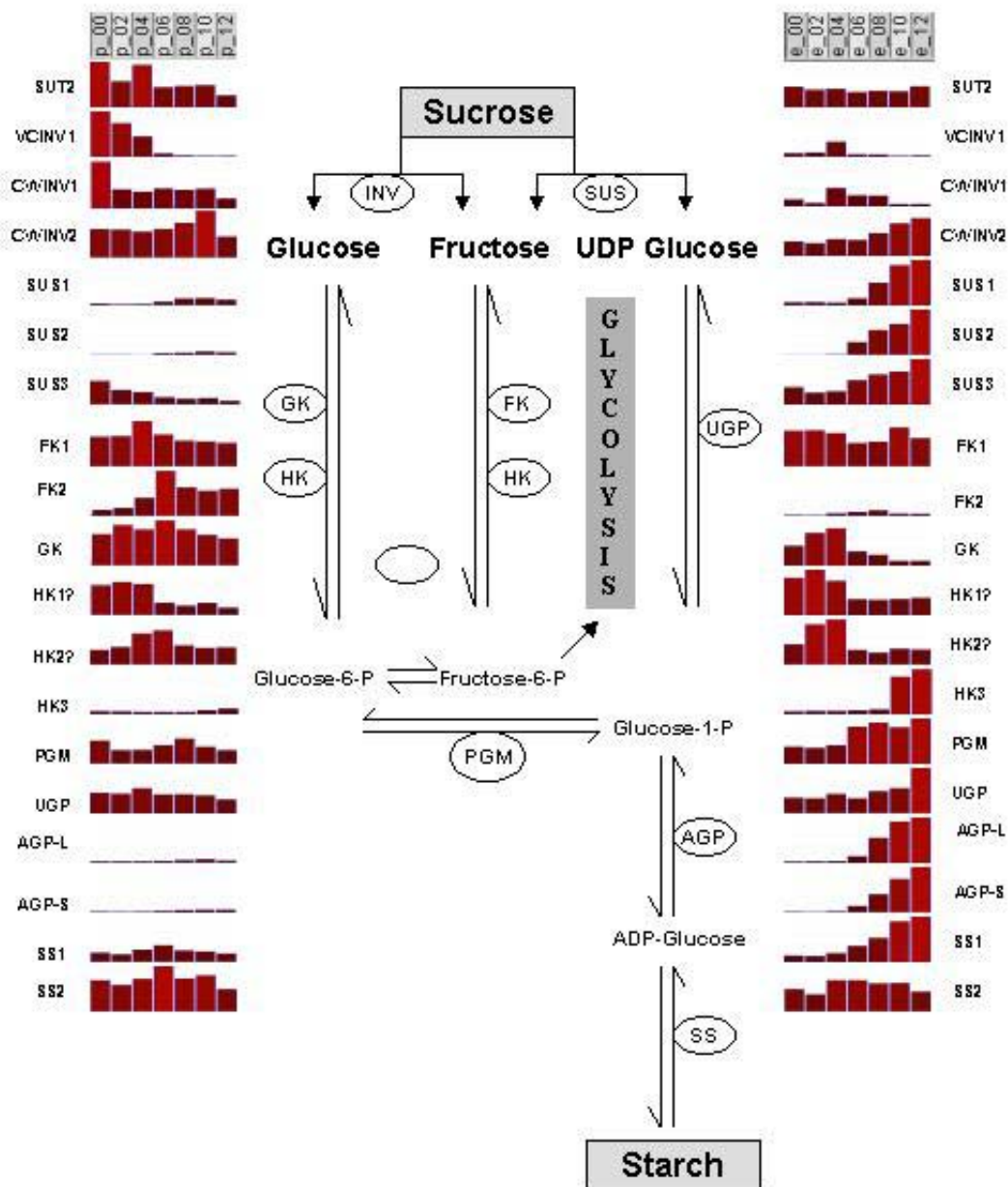


Fig. 15 Schematic representation of the sucrose-starch pathway and mRNA level of the respective enzymes as determined by expression analysis in both maternal pericarp (p) and filial tissue containing endosperm and embryo (e)

For instance p_02 (see top of the Figure) means: expression intensity of the respective gene for the maternal pericarp fraction (p) of developing caryopses at 2 (02) DAF. The intensities of mRNA expression obtained after the normalization procedure are given in red bars. Question mark indicates low score (below 60) of BLAST result.

INV, invertase;	PGK, phosphoglucomutase;
SUS, sucrose synthase;	UGP, UDP-glucose pyrophosphorylase
SUT, sucrose transporter;	<i>AGP-L</i> , large subunit of ADP-
STP, hexose transporter;	glucose pyrophosphorylase
VCINV, vacuolar invertase;	AGP-S, small subunit of ADP-
CWINV, cell wall-bound invertase;	glucose pyrophosphorylase
FK, fructokinase;	SS, starch synthase
GK, glucokinase;	
HK, hexokinase;	

with the expression pattern of CWINV1 in the same tissue (cf. Fig. 15). The reversible cleavage of sucrose to fructose and UDP-glucose is mediated by 3 different isoforms of sucrose synthase (SUS 1-3). All three isoforms show a high transcript level during the storage phase of the filial fraction (Fig. 15). Typically, all transcripts of starch biosynthetic pathway such as PGM, UGP and the large and the small subunit of AGP and the granule bound starch synthase SS1, are up regulated in the later development of the filial fraction indicating the ongoing accumulation of starch in the starchy endosperm. To the contrary, the transcript levels of all those genes were found to be very low in the maternal fraction between 10 and 12 DAF. Among the starch synthase family, SS1 expression seems to be relatively specific for the filial fraction in later developmental stages whereas SS2 is expressed to a comparable level in the filial as well as the maternal tissues (Fig. 15).

2.2.5.2 Expression patterns of genes encoding enzymes of the glycolysis pathway in maternal and filial tissues

Hexoses generated by sucrose cleavage can enter the glycolytic pathway depicted in Fig. 16. Gene expression of HK, GK and FK isoforms feeding the hexose-6-phosphate pools are up regulated in both, maternal and filial fraction during early development. In maternal tissue, the co-regulated expression of genes GPD1, PGK, BPGM, EL1, EL2, PK1 and PK2 involved in the conversion of hexose-6-phosphates into pyruvate is noticed along with hexokinases. In the filial fraction, the genes involved in the conversion of hexose-6-phosphates into 3-phospho-glycerate, i.e. FBA and the GPD1 as well as GPD2 are down regulated during early development nearly blocking the initial part of the glycolytic pathway and up regulated later when starch is accumulated in the cells of the starchy endosperm (Fig. 16). Generally, transcript levels of those glycolysis enzymes metabolizing the hexose-6-phosphates to 3-

phosphoglycerate and further on to pyruvate seem to be up regulated in the storage phase of the filial tissues. Only one enzyme, PK2, may be regulated in the opposite direction. The glycolytic pathway seems to be up regulated during accumulation of starch in the endosperm cells.

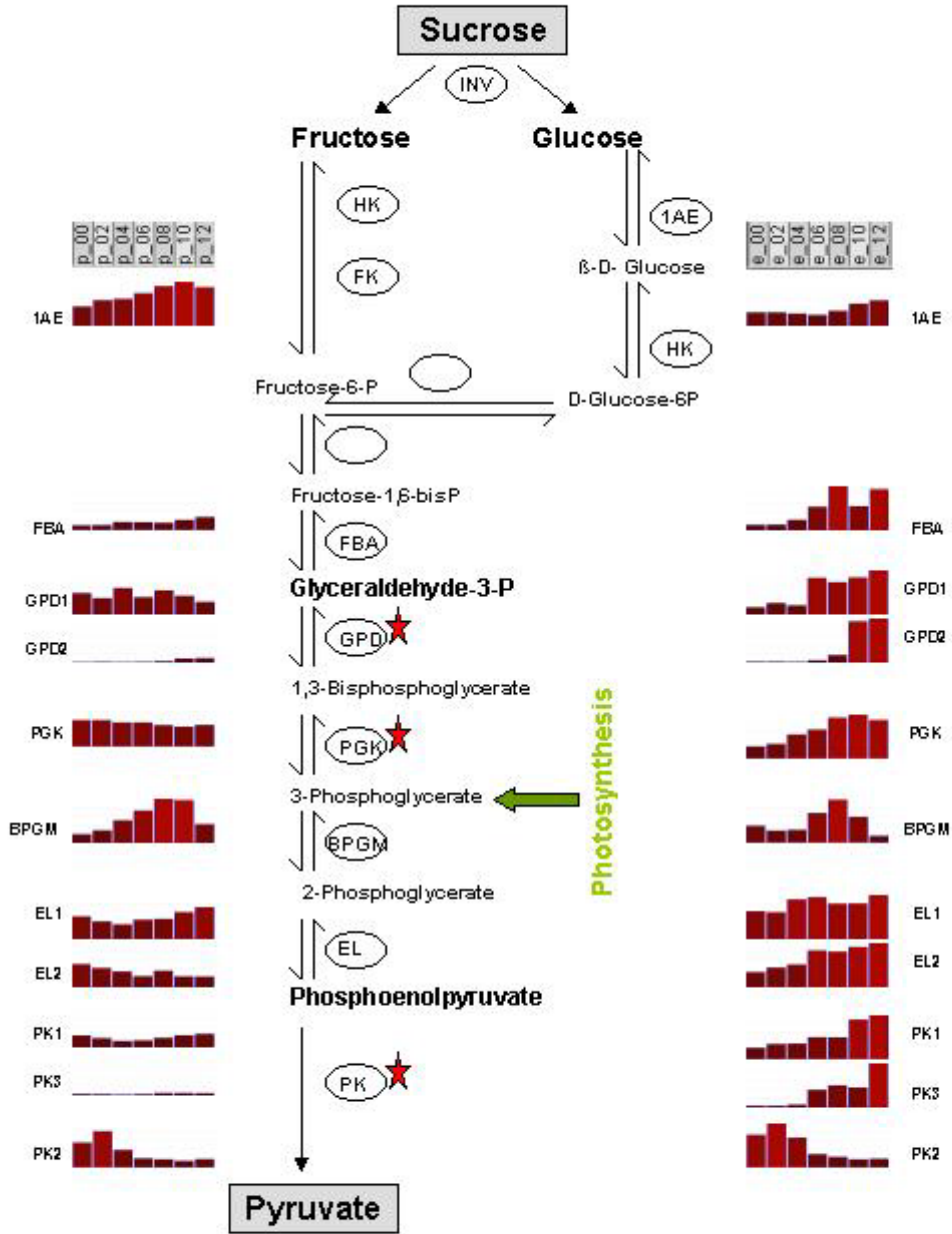


Fig. 16 Schematic representation of the glycolysis pathway and mRNA level of the respective enzymes as determined by expression analysis in both the maternal fraction containing mainly pericarp (p) and filial tissues containing endosperm and embryo (e)

The intensities of mRNA expression obtained after the normalization procedure are given in red bars.

AE, aldolase epimerase;	GPD, glyceraldehydes-3-phosphate dehydrogenase;
HK, hexokinase;	PGK, phosphoglycerate kinase;
FK, fructokinase;	BPGM, bis-phosphoglycerate mutase;
FBA, fructose 1,6 bis-phosphatase;	EL, enolase;
	PK, phosphoenolpyruvate kinase

2.3 DISCUSSION

In the present study, an attempt has been made to understand the gene expression pattern during the early phase of caryopses development in barley by using array hybridization technology. This technique proved to be a powerful approach in the present study (i) to look into the interaction of maternal and filial tissues by expression profiling, (ii) to identify a large number of genes co-regulated during specific phases of barley caryopses development and (iii) to understand the network of gene expression responsible for the regulation of various biochemical pathways during pre-storage and ongoing storage-phase of embryo sac development.

The “functional genomic” analysis of barley seed metabolism has been initiated to gain knowledge about complex phenomenon of seed metabolism by transcript profiling of barley caryopses ESTs derived from either 5’ or 3’ end sequences. One of the major achievements of this study is the identification of a large number of genes that are expressed either in pericarp or embryo sac tissues during caryopses development. Based on the recently annotated data, approximately 40% of the total unique clones selected for array preparation belongs to the unknown category with respect to their function. Description of the expression patterns of such unknown genes, confined either to pericarp or embryo sac tissues during caryopses development, produces valuable information and might help to characterise them further. As an example, the highest hybridization signal found in embryo sac tissue was found for clone HY09L21, which did not exhibit significant homology to any gene of known function. The histological localization of HY09L21 by *in situ* hybridization revealed expression exclusively in the cells of the maternal nucellar projection (Sreenivasulu *et al.*, 2002). The massive expression of the gene in the tissue specific for unloading of assimilates destined to the embryo suggests an important function in this process. On the other hand, spatial localisation strictly within the maternal part of the maternal-filial boundary and massive expression at a defined developmental stage (4 DAF, complete cellularization of the starchy endosperm, see

Weschke *et al.*, 2002) hint to a possible function in signal transduction from the maternal to the filial part of the caryopsis.

2.3.1 Pericarp specific expression during the development of barley caryopses (0-12 DAF)

In the early stage of grain development the pericarp tissue transports assimilates and nutrients to the growing embryo sac tissues and also stores starch transiently (Weschke *et al.*, 2000). This view is supported by the expression profiles, which revealed significant signals for some mRNAs assigned to carbohydrate metabolism in pericarp tissue (see Table 7: HY01A03, HY05O10, HW02F11, HY07C03, HK04H22, HET1 and CWINV). The detailed account on the pattern of expression is discussed in the later section 2.3.3. The second larger class of genes expressed specifically in the pericarp tissue during its later development includes proteases, such as cathepsin b-like cysteine proteinase, cysteine proteinase 1, aspartic proteinase, serine carboxypeptidase, vacuolar processing enzyme and ubiquitin-conjugating enzyme (Table 7). Xu and Chye (1999), demonstrated the expression of cysteine proteinase associated with programmed cell death during several developmental events such as leaf senescence, fruit senescence, xylogenesis, nucellar cell degeneration and anther senescence in eggplant. Hence, the expression of cysteine proteinase 1 and cathepsin b-like cysteine proteinase could be associated to programmed cell death or senescence of the pericarp tissue. It is known that pericarp starts degeneration with the onset of storage activity in endosperm tissue (6 DAF onwards). During the same phase, expression of lipid metabolism genes has been observed. Lipoxygenase 1 expression was found to be specific for degenerating pericarp tissue, it is believed that it could be related to the senescence of pericarp tissue. Additionally, a pericarp-specific expression of the family of non-specific lipid transfer protein was registered (Table 7: HY07L03, HY10O23 and HK04H17). In cereals, non-specific lipid transfer proteins are found in seeds and are reported to be involved in different physiological events including formation of cutin. Furthermore, it is believed to be involved in stress and pathogen response (Lindorff-Larsen and Winther 2001). Although it is known from earlier studies that these proteins could transport lipid compounds *in vitro*, the *in vivo* function of the different types of lipid transfer proteins expressed specifically during degeneration of pericarp tissue towards later stages of seed development is unclear. Expression of hormonal regulated genes could also be found specifically in pericarp tissue (Table 7: HY05P23, HY09I02, HK03J06) but the function of their products is not clear. In addition, we noticed an interesting

observation that approximately 40% of genes found to be expressed specifically in pericarp tissue are unknown (Table 7). This finding is of high importance for further characterization of putative functions of the maternal tissue.

The cDNA with the highest hybridization signal in the maternal tissues (see Table 1 and 7: HY05K19) represents a methionine synthase / methyl transferase (EC 2.1.1.14) with 87-89% homology to genes from *Solanum tuberosum*, *Mesembryanthemum crystallinum*, *Arabidopsis thaliana* and *Catharanthus roseus*. The enzyme catalyses the formation of methionine by the transfer of a methyl group from 5-methyltetrahydrofolate to homocysteine. This is the last step in the cobalamin-independent *de novo* biosynthesis of L-methionine, and also serves to regenerate the methyl group of S-adenosylmethionine used for methylation reactions (Eichel *et al.*, 1995). The high expression of methyl transferase mRNA in pericarp indicates either a site of massive methylation reactions and/or the tissue produces high amounts of methionine. *In situ* hybridization localized the major sites of expression to the outer part of the pericarp especially in the micropylar region and also in endospermal transfer cells (Sreenivasulu *et al.*, 2002). Eckermann *et al.* (2000), detected this enzyme by immunohistochemistry in cotyledons of *C. roseus* seedlings in the upper epidermis and suggested its involvement mainly in methylation reactions. Since massive storage protein synthesis could not be observed in pericarp tissue, the expression of methyl transferase could have a primary function in methylation processes. In animal reproductive biology, methyl transferase has been identified to play a role in maintaining the methylation status of imprinted genes. Adams *et al.* (2000), recently investigated the global role of methylation in imprinting effects on seed development in *Arabidopsis* by crossing methyltransferase 1 antisense transgenic plants with wild type plants. Their results show that DNA methylation is an important part of the parent-of-origin imprinting. In plants, post-fertilization methylation reactions and its role in seed development has not been investigated so far. The massive expression of the methyl transferase gene in pericarp tissue opens up channels to look into the probable functional role of the maternal tissue in post-fertilization methylation reactions in barley seed development.

2.3.2 A gene expression map of the filial tissue during caryopsis development (0-12 DAF)

The development of endosperm and embryo starts with double fertilization and subsequently differentiation processes are initiated. Genes expressed in the syncytial and cellularizing endosperm encodes products involved in DNA replication, protein synthesis and cell division.

Additionally, tubulin genes involved in late cell expansion processes; genes having a role in early events of cell wall synthesis and lignification are expressed (Table 8). This set of genes is mainly represented by cluster 2_1, 2_2 and 2_3, and their highest expression could be observed during 0-4 DAF (Fig. 10). The up regulation of these classes of genes can be correlated with the cellular events such as syncytium formation, cell wall initiation and cellularization as evidenced in histological documentation (Weschke *et al.*, 2002). During the pre-storage phase (0-4 DAF) of the filial tissue, high hexose concentrations were evident (Weschke *et al.*, 2000, 2002) and exactly in that stage cell division occurs. Based on the temporal and spatial gene expression patterns, it has been shown in *Vicia faba* that high hexose concentration leads to cell division and higher concentration of sucrose enhances starch biosynthesis (Weber *et al.*, 1998). Looking into the correlation patterns of high hexose concentration measured in early embryo sac development (Weschke *et al.*, 2000) and higher expression of regulatory genes a similar conclusion can be drawn. i.e. hexoses might be associated with cell division activity in barley as well. Increased sucrose levels trigger the biosynthesis of starch and storage proteins in the endosperm. Sugar responsiveness of the key enzymes in starch and storage protein synthesis has been shown in developing seeds (Weber *et al.*, 2000) and potato tubers (Kosßmann *et al.*, 1991). Genes encoding storage proteins such as sporamin in sweet potatoes (Hattori *et al.*, 1990) and protease inhibitors (Müller-Röber *et al.*, 1990) have been reported to be sugar-responsive. During the initial storage phase, the expression of genes connected with sugar to starch pathway is found to be up regulated in embryo sac tissue. Genes up regulated heavily in the filial tissue of barley caryopses during the onset of storage phase are involved in starch (Table-3; sucrose synthase, ADP glucose pyrophosphorylase large and small subunit, starch synthase 2) and storage proteins (Table-4; hordein family) biosynthesis, possibly positively correlated to higher sucrose concentration. These classes of genes are mainly represented in cluster 4_1, 4_2, 4_3 and 4_4 and 5, expressed specifically during 6-12 DAF (Fig. 10). It is important to note that as a part of sucrose responsive gene expression we observed the class of genes related to amylase inhibitors and protease inhibitors in the filial tissue during storage phase, which could be expected to prevent storage product degradation.

2.3.3 Interaction of maternal and filial tissues with reference to starch storage function

Comparison of gene expression profiles of maternal and filial tissue development during pre-storage and initial storage phase revealed characteristic patterns. In order to get a more complete picture of the regulatory mechanism of sucrose metabolism, the expression profiles of the sucrose-to-starch and sucrose-to-pyruvate pathway were compared in maternal and filial tissues during caryopses development. In the pre-storage phase, the photosynthate is discharged into the pericarp tissue, where part of the sucrose is catabolised by invertases to yield hexoses. The gene expression of vacuolar invertase and cell wall-bound invertase 1 is highly up regulated in the pericarp tissue between 0-4 DAF (Fig. 15). Invertases are involved in the cleavage of sucrose into the hexoses fructose and glucose. In addition, a pericarp-specific isoform of sucrose synthase 3 (SUS3) is expressed. The activity of sucrose synthases result in the cleavage of sucrose into fructose and UDP-glucose, additional sucrose catabolism pathway has been found. Because of the presence of higher levels of transcripts of fructokinase1, glucokinase, hexokinase1, hexokinase 2 (Fig. 16), fructose and glucose phosphorylation should be expected, and the resulting hexose phosphates can either be metabolised further through glycolysis or used for starch production in pericarp. Fructokinase may play a specific role in this process in sink tissues as suggested by Schaffer and Petreikov (1997) and could also function as a sugar sensor (Pego and Smeekens, 2000). The transcripts encoding enzymes of the starch biosynthetic process (UDP-glucose pyrophosphorylase, cytosolic and chloroplastic isoforms of phosphoglucomutase, ADP-glucose pyrophosphorylase large and small subunits and granule bound starch synthase) are co-regulated in pericarp between 0-4 DAF. As mentioned before (Weschke *et al.*, 2000), pericarp-specific starch accumulation is only transitory. Mobilization of transitory starch is possibly catalysed by β -amylase, whose transcript is almost exclusively found in tissues of the maternal fraction (Table 1: HY01A03). The genes responsible for the glycolysis pathway are up regulated in parallel with transient starch accumulation in the pericarp tissue during early stages of development.

During 0-4 DAF, the hexoses are found in filial tissue because of expression of cell wall-bound invertase 1 in the first cell rows of the cellularizing endosperm and expression of HvSTP1 transporting the hexoses produced in the apoplastic space between maternal and filial tissues against a concentration gradient into the filial endosperm (Weschke *et al.*, 2002). These hexoses can be phosphorylated by fructokinase 1, glucokinase, hexokinase 1 and

hexokinase 2 as evidenced by the abundance of the respective mRNAs. Though, up regulation of phosphorylating kinases was observed in the filial tissue, the transcripts of FBA, GPD and PGK are down regulated producing a remarkable gap in the transcripts encoding enzymes of glycolysis pathway. Starting with the first stable intermediate of the Calvin cycle (3-phosphoglycerate), increasing expression of the glycolysis enzymes, especially EL1 and PK3, was registered (cf. Fig. 16). From that, it can be speculated that the caryopsis-own photosynthesis has a remarkable influence on the production of energy necessary for the growing filial tissue.

In contrast to the maternal tissue, in the filial part of the caryopsis genes involved in the starch biosynthetic pathway are transcribed predominately between 6-12 DAF. In the beginning of that phase, sucrose concentration increases dramatically. The increase of sucrose concentration triggers the expression of genes involved in starch biosynthesis. We noticed increased expression of two sucrose cleavage enzymes, mainly sucrose synthase but also invertase to a lower extent. Sucrose synthase (SUS1 and 2 are specific for the filial tissue) converts sucrose to fructose and UDP-glucose, which is converted by UDP-glucose pyrophosphorylase to glucose-1-phosphate, which enters the starch biosynthetic pathway. Alternatively, the cleavage products could be used in cell wall biosynthesis or energy production. In addition, up regulation of the CWINV2 transcript is observed, possibly the resulted activity breaks down sucrose to glucose and fructose. During starch accumulation, co-regulation of CWINV2 and HK3 was found in the filial tissue. This opens up two possibilities. (1) Possibly, activity of CWINV2 and HK3 may open up an invertase-dependent way of starch accumulation (the glucose generated by the activity of CWINV2 may be phosphorylated into glucose-6-phosphate by hexokinase 3, which is isomerised to glucose-1-phosphate by phosphoglucomutase and subsequently enters starch synthesis) or (2) activity of CWINV2 and HK3 may be specific for the growing embryo tissue (it is important to note that filial fraction contains both endosperm and embryo). To distinguish between one or the other possibility, localisation of the transcripts and measurements of invertase activity in one and the other tissue is necessary. During storage phase, the up regulation of transcripts coding for enzymes such as ADP glucose pyrophosphorylase large and small subunit as well as starch synthase 2 was noticed (Fig. 15). The starch biosynthetic pathway transcript profiles up regulated during the pre-storage (0-4 DAF) in the pericarp and the initial storage phase (6-12 DAF) in the filial tissues positively correlate with starch measurements and starch localisation early in pericarp (3-6 DAF) and during initial storage phase in endosperm tissue (Weschke *et*

al., 2000; 2002). While a major portion of the resultant hexoses is spent to synthesise starch, a part is also diverted to glycolysis, which is reflected in our expression analysis. It is interesting to note that transcripts of the glycolytic pathway (Fig. 16) are up regulated at a time when there is increased accumulation of starch in the endosperm cells in order to generate reducing power / energy needed to synthesise starch more rapidly.

2.4 SUMMARY

Based on the transcript profiling data of 1400 macroarray, our study provides a unique global examination of gene expression patterns for maternal and filial tissue fractions at specific developmental stages such as pre-storage and ongoing storage phase of caryopsis development. The observed tissue specific/developmental stage specific expression patterns reflect the existence of metabolic networks. Genes strongly expressed in maternal pericarp tissue are related to lipid metabolism, proteases and large number of unknown genes. In the filial tissue during pre-storage phase (0-4 DAF) most up regulated genes are related to cell division and elongation. During the storage phase (6-12 DAF), most mRNAs up regulated in the filial tissue fraction encode genes of the sugar to starch pathway, glycolysis, energy production and storage proteins. The most noteworthy is that significant subset of genes shows no significant homology to any sequences in the current databases showing maternal and filial tissue specific expression. The present transcript-profiling map demands further physiological and metabolic data to deepen knowledge of caryopses development in barley. In order to gain the deeper understanding of the complexity of seed metabolism and its control in barley we focused analysis of gene expression patterns in *seg8* seed mutant by transcript and metabolite based profiling (see Chapter 3).

CHAPTER 3

Seg8 mutant analysis during seed development

3.1 INTRODUCTION

Developing caryopses of cereals accumulate starch in the endosperm as the major carbon and energy resource, and several mutants defective in starch accumulation have been isolated (Miller and Chourey, 1992; Cheng *et al.*, 1996; Tyynelä *et al.*, 1995; Harrison *et al.*, 1998; Maitz *et al.*, 2000). The majority of the described mutants are either defective in early stages of cell division and morphogenesis or fail to accumulate storage compounds such as starch during maturation. In the past, research has been focused on genetic and molecular physiological aspects of carbohydrate metabolism in miniature, shrunken and brittle mutants of maize. Miller and Chourey (1992) demonstrated that the miniature-1 seed mutation is connected to cell wall-bound invertase, and Cheng *et al.* (1996) identified miniature1 seed loci encoding isoforms of cell wall-bound invertase 2 in maize. *Shrunken* (*sh*) mutants are affecting sucrose synthase (Chourey and Nelson, 1976; Doehlert and Kuo, 1990; Tobias *et al.*, 1992) and *shrunken2* and *brittle2* affect the small and large subunit of ADP glucose pyrophosphorylase, respectively (Hannah and Nelson, 1976; Bhave *et al.*, 1990; Tobias *et al.*, 1992). Waxy mutants on the other hand lack granule bound starch synthase and amylose (McDonald *et al.*, 1991). Similar studies are scarce in barley.

Normal seed development in barley is significantly dependent on the maternal tissue. Sucrose and other nutrients are unloaded first into the maternal pericarp tissue through the vascular bundles, are further symplastically transported via the nucellar projection cells and finally released into the endosperm cavity. Despite the importance of the maternal tissues to supply sucrose and other nutrients to the developing filial tissues (endosperm and embryo), little is known about the maternal-filial interaction. The analysis of gene expression networks as well as generated molecular-physiology data from developing grains of shrunken endosperm mutants in barley during seed development will provide new knowledge about the role and the importance of maternal tissues.

In barley the shrunken endosperm mutants *xenia* (*sex*), non-*xenia* (*seg*) and the high lysine (*lys*) mutants appear to alter carbohydrate metabolism in the endosperm. Endosperm differentiation in *sex* mutants has been described by Bosnes *et al.* (1992). Further, a recessive shrunken endosperm mutant called *shx* has been isolated as spontaneous mutation. Schulman and Ahokas (1990) reported that the *shx* mutant has only 25% of the starch content found in grains of the wild type cv Bomi. To analyse the block of starch synthesis, enzyme activities of ADP glucose pyrophosphorylase and soluble starch synthase were measured and found to be reduced by about 20%. Northern blot analysis has shown that the transcript for ADP glucose pyrophosphorylase (small subunit) is less abundant in the mutant (Tyynelä *et al.*, 1995). Although several other enzymes involved in starch synthesis are affected, the authors suggested that the soluble starch synthase might be the primary site of mutation in *shx*. Among *seg* mutants, eight different shrunken endosperm mutants (*seg1-8*) have been identified and designated as maternal effect mutants (Jarvi and Eslick, 1975; Ramage and Crandall, 1981). The *seg* mutants may become useful to study maternal-filial interaction during endosperm development. Felker *et al.* (1985) described them based on the anatomy of immature grains. Based on histological descriptions, the shrunken endosperm mutants were classified into two groups: the chalazal necrosis mutants (*seg1*, *seg3*, *seg6* and *seg7*) and the abnormal endosperm mutants (*seg2*, *seg4*, *seg5* and *seg8*). In the first category, death of the maternal chalaza and nucellar projection tissue during early seed development cuts off the supply of assimilates and causes the shrunken endosperm phenotype, while in the second one the maternal tissue develops normally and abnormality occurs in the endosperm tissue itself. Felker *et al.* (1985) speculate that the lack of factor(s) in the cytoplasm of the central cell causes the phenotype in the second category. Furthermore, they suggested the mutants as powerful source to study maternal effects on endosperm development.

Seg8 is one of the eight mono-factorial recessive shrunken endosperm mutants in barley that do not express *xenia*, *i.e.* the source of pollen does not affect the embryo or endosperm phenotype. Ramage and Crandall (1981) originally identified and characterised the *seg8* mutant from a field stock of the cultivar 'Klages'. *Seg8* seeds exhibit shrunken endosperm and weigh about 21% of the seeds produced by normal plants. When the seeds from mutants were sown in the green house, the resulting plants were normal having seven pairs of chromosomes. Pollen mother cell meiosis as well as pollen and ovule fertility were normal too. Moreover the researchers did not observe any change in the mutant due to variation in

environmental conditions and they have not encountered difficulties in establishing the stands of the mutant. The *seg8* mutant has been crossed with other shrunken mutants *seg1* to *seg7*, and in all crosses the F1 plants always produced plump seeds. F2 plants were grown from all of the allele crosses and all segregated in an approximately 9 plump seeded : 7 shrunken seeded ratio indicating that *seg8* is a distinct non-allelic *seg* mutant. Ramage (1983) reported that *seg8* is located on chromosome 1 (7H). Djarot and Peterson (1991) studied seed development in the *seg8* mutant. The anatomical description therein indicates that the mutant phenotype, *i.e.* the shrunken endosperm appeared at 4 DAF, and some biochemical estimates revealed that the mutant had lower starch content and higher sucrose concentration than the wild type. Though studies have addressed barley seed mutants at morphological, anatomical and biochemical levels, molecular physiological and genetic studies are lacking. Hence an attempt in this direction has been made in the present study to study expression profiling by macroarray analysis to look into the seed development of barley *seg8* mutant. A *seg8* mutation was used which had been transferred to the genetic background of “Bowman” (kindly provided by Prof. D. Frankowiak, NDSU, USA).

The results of expression profiling of the *seg8* mutant compared to wild type ‘Bowman’ are presented on both whole caryopses level and in the dissected maternal and filial fraction of developing caryopses during pre-storage and the ongoing storage-phase (0-14 DAF). Furthermore, an attempt was made to compare transcript and metabolite profiling data of the *seg8* mutant and the Bowman wild type.

3.2 RESULTS

3.2.1 Fresh weight of developing caryopses of *seg8* and wild type

The fresh weight of developing *seg8* mutant and Bowman wild type caryopses was measured (Fig. 17). The fresh weight of *seg8* and Bowman grains were similar until 8 DAF. From 10 DAF onwards Bowman grains were significantly heavier (Fig. 17A). A similar pattern is seen in the data for the filial part of the caryopses (embryo and endosperm) with a decrease in fresh weight content in the mutant as compared to wild type beginning 10 DAF (Fig. 17B). Fresh weight did not vary in the maternal pericarp fraction between mutant and wild type during caryopses development until 16 DAF. On the other hand the filial tissue fraction of mutant showed a drastic reduction in fresh weight from 10 DAF onwards (Fig. 17B). This seems to be due to accumulation of higher amounts of starch in the embryo sac fraction of the wild type caryopses. Further, we calculated fresh weight ratio of pericarp and embryo sac fractions of developing caryopses of mutant and wild type were measured, the prominent differences were observed from 12 DAF onwards (Fig. 17C).

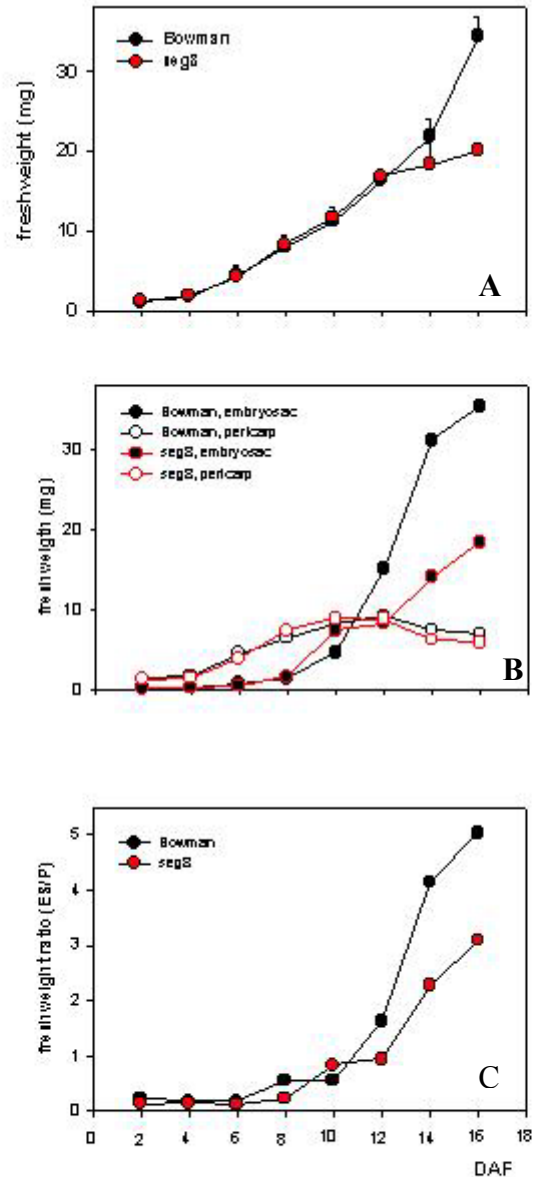


Fig. 17

After separation of maternal (pericarp) from the filial part (embryo sac), fresh weight of both fractions was estimated and the fresh weight ratio was calculated. On X-axis the developmental scale 2-14 DAF (Days After Flowering) is given in every two day intervals.

3.2.2 Starch content in caryopses of *seg8* and wild type

During development starch content of *seg8* and wild type seeds was measured in two-day intervals. During 2 to 6 DAF of pre-storage phase the starch content remains similar in both *seg8* and wild type seeds. From 10 DAF onwards, the starch content in *seg8* seeds was significantly lower in mutant than in wild type (Fig. 18). During 12 to 14 DAF the starch accumulates to only 40% of wild type, resulting in reduced grain weight.

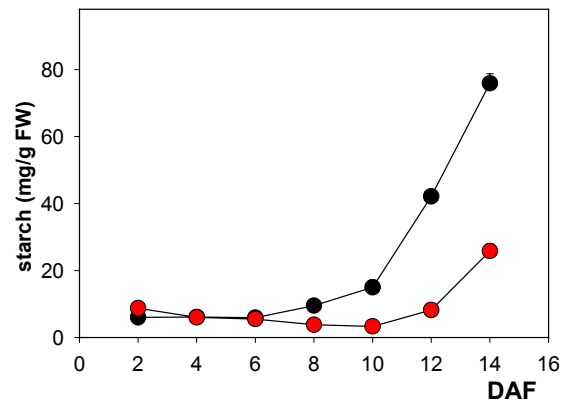
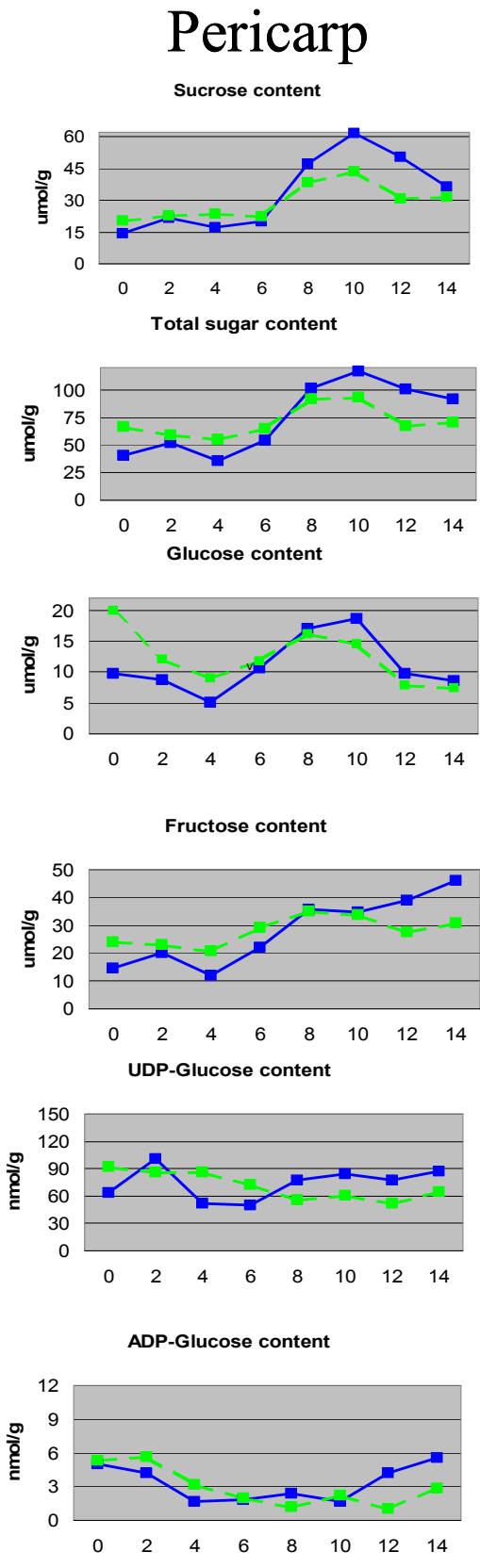


Fig. 18

Red colour filled circles- *seg8*
Black colour filled circles- Bowman
For further legend see Fig. 17

3.2.3 Characteristic changes in sugar and metabolite concentrations in *seg8* and Bowman during pre-storage and storage phase in pericarp and embryo sac fractions

Sugar and metabolite profiles of carbohydrate metabolism were determined in maternal pericarp and filial embryo sac fractions of *seg8* and Bowman (Fig. 19). Total sugar content and glucose content are comparatively lower in *seg8* mutant pericarp during 0-4 DAF and sugar and key metabolites such as UDP-glucose and ADP-glucose concentration increased in the mutant pericarp during later stages (12-14 DAF). Strikingly, but not surprisingly, sugar levels (glucose and fructose) and the metabolite ADP-glucose decreased in the embryo sac fraction of the mutant during the onset of storage process in comparison to wild type (Fig. 19). A further interesting observation is the increase of sucrose content and UDP-glucose in the mutant during initial storage phase (8-12 DAF).



■ Seg8
■ Wild type

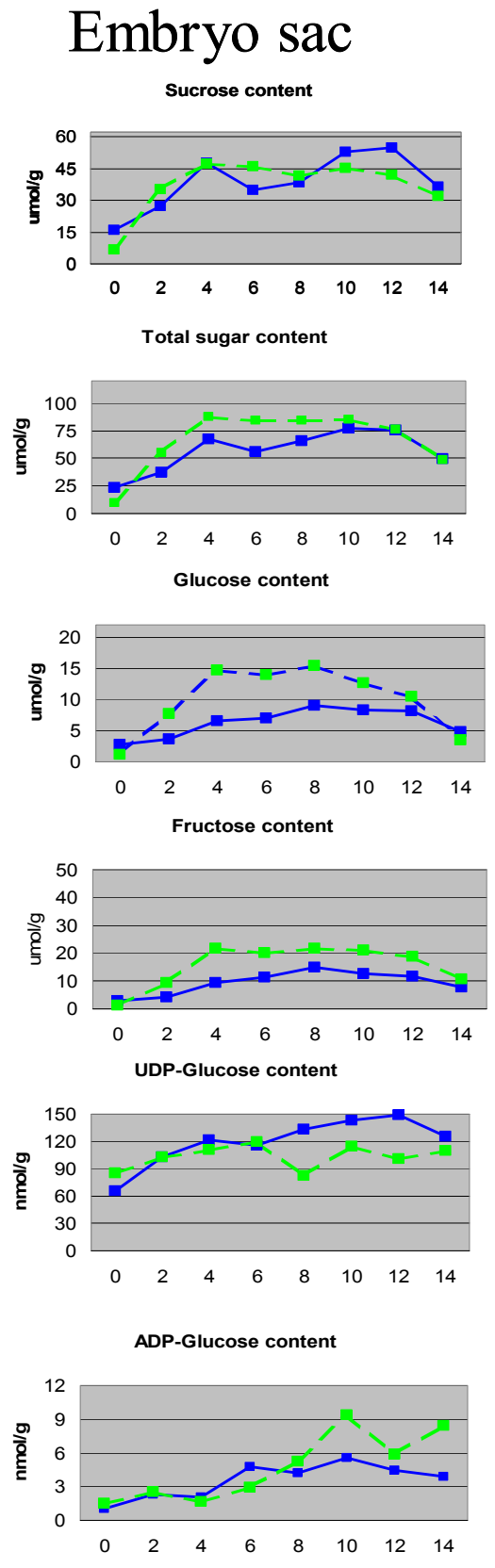


Fig. 19 Sugar and metabolite concentrations determined in maternal and filial fraction of *seg8* and wild type of developing caryopses (0-14 DAF) in two day intervals, scaled on X-axis) and measurement values represented on Y-axis.

3.2.4 Anatomy and starch distribution pattern in developing grains of *seg8* mutant and wild type

The *seg8* seeds show normal development of the pericarp tissue during caryopses development. However, the shrunken endosperm phenotype was noticed during the onset of starch accumulation. The endosperm develops as two separate lobes with the abnormal nucellar projection touching the dorsal crease of the caryopses. The starch distribution pattern was studied in developing grains of *seg8* mutant and wild type during onset of starch accumulation (8-12 DAF) by iodine staining (Fig. 20 A,B,C). Contrary to the wild type accumulating first starch grains in the wings of the starchy endosperm (20 G), starch accumulation in the mutant endosperm starts in the regions adjacent to the maternal-filial boundary during 8 DAF (20 A,D). The starch accumulation is drastically reduced in the two lobes of the endosperm mutant (20 E,F) in comparison to a well-filled starchy endosperm of wild type during 10 and 12 DAF (Fig. 20 I). Quantitative measurements of starch content (Fig. 19) carried out in developing caryopses of *seg8* and wild type developing caryopses confirmed the result visualised by Iodine staining.

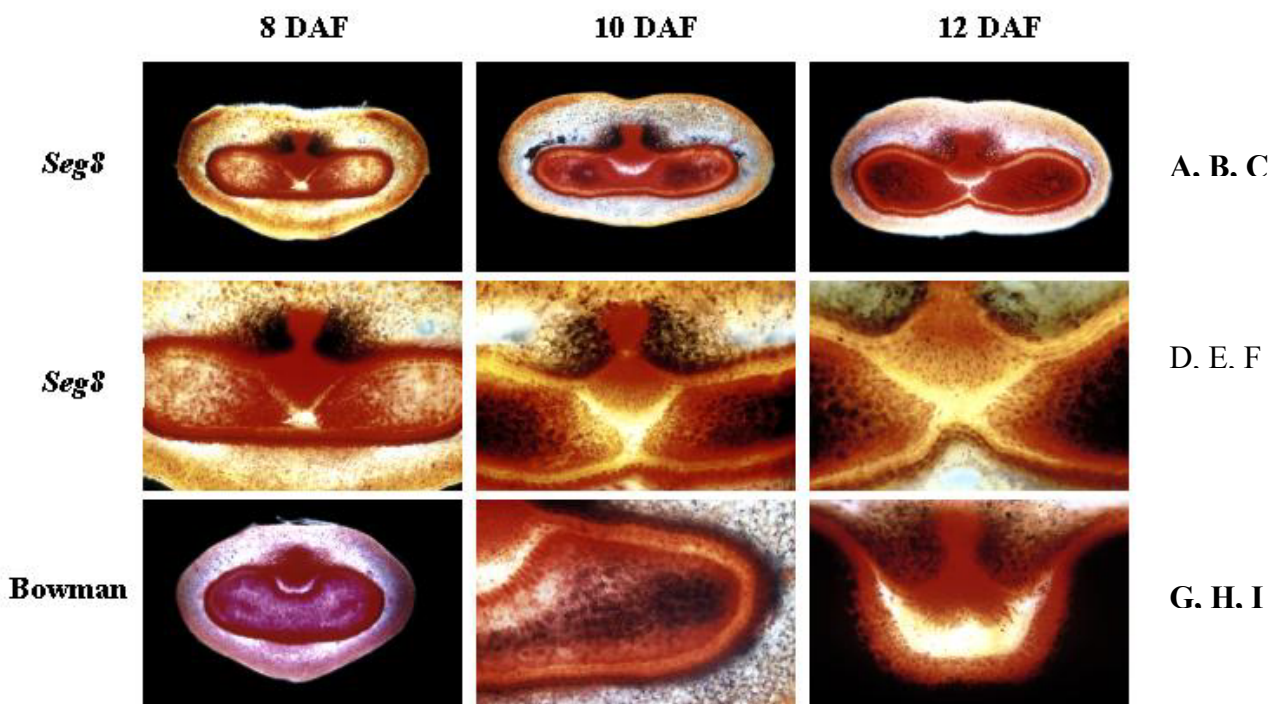


Fig. 20

Starch distribution pattern of *seg8* caryopses shown in median-transversal sections (8-12 DAF) by Iodine staining. Dark field images, scale 1mm. Images provided by Dr . R. Panitz

3.2.5 Characteristic changes of gene expression in developing caryopses of *seg8* and Bowman

To monitor difference in gene expression patterns between mutant and wild type by DNA macroarray analysis, we prepared ^{33}P -labelled cDNA probes from pooled whole caryopses (2-14 DAF) and hybridised them to the 1412 macroarray. The experiments were repeated at least twice with independent plant material. In expression analysis, 48 genes were found to be down-regulated in the mutant as compared to wild type by at least by two-fold or more (Fig. 21). The reproducibility of data generated by the two independent materials is shown in scatter-plot representation.

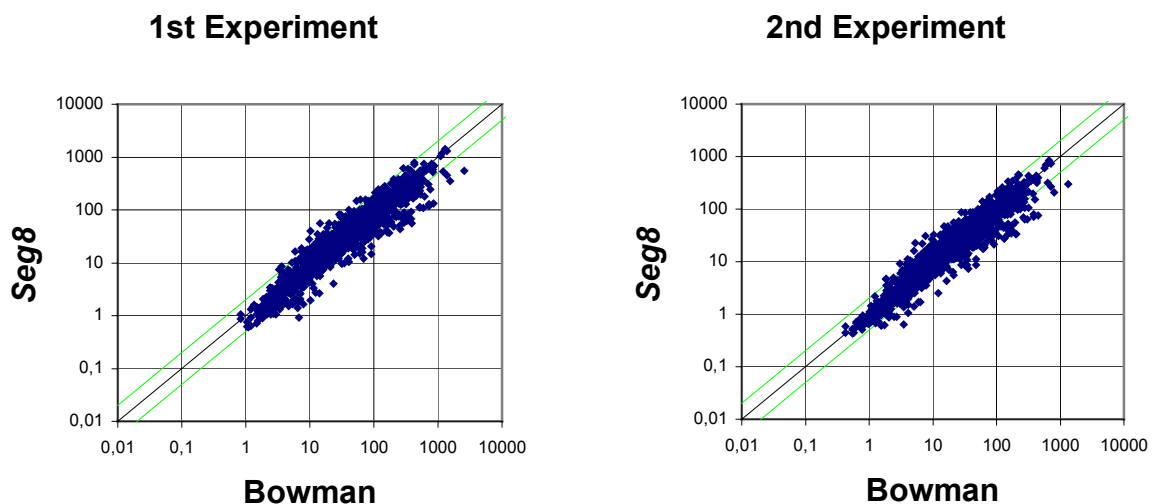


Fig. 21

Comparison of the normalized signal intensities obtained from two independent experiments (experiment 1 and 2). Two different arrays were hybridised with the labelled cDNA from *seg8* and, after successful stripping, with Bowman developing caryopses (pooled probe 2-14 DAF). Experiments were repeated with independent probe preparation from plant material and hybridization to independently spotted arrays. Signals outside the green lines differ by more than a factor of two between mutant and wild type.

Examination of the EST clones showed that differences in expression between *seg8* and Bowman caryopses (pooled 2-14 DAF) belong to the starch biosynthetic pathway. As shown in Table 12, 25 ESTs belonging to the starch biosynthetic pathway displayed at least two-fold or more differential expression. Among them 10 clones represent unique candidates (alpha-amylase tetrameric inhibitor, alpha-amylase/trypsin inhibitor, alpha-amylase/subtilisin inhibitor, alpha-hordothionin precursor, sucrose synthase1, sucrose synthase2, ADP-glucose

pyrophosphorylase small subunit, UDP-glucose pyrophosphorylase and UDP-glucose-6-dehydrogenase). Those transcripts were expressed at a lower level in the mutants as compared to wild type. The other classes of genes down-regulated in the mutant represent amino acid metabolism (aspartate aminotransferase, glycyl-tRna synthetase), oxidative phosphorylation mainly involved with energy production (H⁽⁺⁾-transporting ATPase, inorganic pyrophosphatase, 5'-amp-activated protein kinase, beta-1 subunit), stress related and hypothetical proteins (data not shown).

Table 12: ESTs belongs to the sugar to starch pathway are preferentially down regulated in developing caryopses of *seg8* mutant

EST-ID	EC nr	Putative gene identity	1st experiment			2nd experiment			2ndexperiment_rehybridized		
			Signal intensity		Ratio	Signal intensity		Ratio	Signal intensity		Ratio
			Bowmann	Seg8	Bow/Seg8	Bowmann	Seg8	Bow/Seg8	Bowmann	Seg8	Bow/Seg8
Carbohydrate metabolism											
HY06K18	0	alpha-amylase tetrameric inhibitor	397,75	33,97	11,71	324,54	62,63	5,2	59,28	21,23	2,8
HY06J10	0	alpha-amylase/subtilisin inhibitor	53,95	10,99	4,91	66,18	18,68	3,5	21,48	5,77	3,7
HY09N22	0	alpha amylase/trypsin inhibitor BTI-CME3	653,26	151,75	4,30	764,48	245,32	3,1	144,94	65,15	2,2
HY03M02	0	alpha-hordothionin precursor	2995,67	301,52	9,94	2570,44	543,94	4,7	566,32	99,47	5,7
HY09N15	2.4.1.13	sucrose synthase 2	283,68	33,29	8,52	390,27	55,06	7,1	50,81	14,21	3,6
HY04H11	2.4.1.13	sucrose synthase 2	411,00	49,47	8,31	60,41	14,90	4,1	7,46	1,34	5,6
HY07C09	2.4.1.13	sucrose synthase 2	495,55	81,01	6,12	731,06	128,86	5,7	147,27	33,23	4,4
HY09L14	2.4.1.13	sucrose synthase 2	556,67	106,29	5,24	531,92	196,64	2,7	213,93	24,35	8,8
HY06C06	2.4.1.13	sucrose synthase 2	109,77	21,17	5,18	174,95	37,08	4,7	26,30	8,22	3,2
HY09N16	2.4.1.13	sucrose synthase 2	171,25	41,28	4,15	11,48	3,31	3,5	0,72	0,51	1,4
HY04L06	2.4.1.13	sucrose synthase 2	37,43	12,06	3,10	61,68	18,42	3,3	10,37	3,77	2,8
HY08H21	2.4.1.13	sucrose synthase 2	123,40	41,41	2,98	165,11	73,01	2,3	41,99	8,76	4,8
HY09D18	2.4.1.13	sucrose synthase 1	153,50	33,84	4,54	382,39	67,90	5,6	73,65	32,48	2,3
HW08D05	2.4.1.13	sucrose synthase 1	2,69	0,62	4,31	94,75	34,21	2,8	34,49	8,08	4,3
HY03P12	2.4.1.13	sucrose synthase 1	46,06	11,30	4,08	91,35	20,54	4,4	9,57	5,67	1,7
HW08D05	2.4.1.13	sucrose synthase 1	78,89	20,08	3,93	94,75	34,21	2,8	34,49	8,08	4,3
HY05O13	2.4.1.13	sucrose synthase 1	131,46	33,65	3,91	294,56	56,67	5,2	61,63	28,70	2,1
HY10D02	2.4.1.13	sucrose synthase 1	79,00	21,72	3,64	126,53	37,26	3,4	22,98	9,32	2,5
HY10G10	2.4.1.13	sucrose synthase 1	111,07	32,29	3,44	150,29	54,95	2,7	47,22	17,05	2,8
HY07L04	2.4.1.13	sucrose synthase 1	55,57	18,57	2,99	81,63	27,92	2,9	19,97	6,52	3,1
HY08O12	2.7.1.90	6-phosphofructokinase (pyrophosphate)	19,06	2,54	7,51	23,52	3,99	5,9	6,33	1,33	4,8
HY10G16	2.7.7.27	ADP-glucose pyrophosphorylase, small chain	228,50	49,07	4,66	133,65	77,89	2,8	55,59	15,70	3,5
HY08N11	2.7.7.27	ADP-glucose pyrophosphorylase, small chain	77,09	24,24	3,18	161,39	38,17	4,2	30,87	7,36	4,2
HY03B24	1.1.1.22	UDP-glucose-6-dehydrogenase	109,91	31,56	3,48	48,36	53,00	1,1	17,81	4,07	4,4
HY01E15	2.7.7.9	UDP-glucose pyrophosphorylase	321,57	106,89	3,01	142,46	185,18	1,3	52,31	9,51	5,5

ESTs that are preferentially down regulated in the *seg8* mutant are defined as those giving Bowman/*seg8* signal intensity ratios larger than 2 and absolute signal intensities greater than 5 au in three array experiments. Normalized signal intensities for Bowman and *seg8* pooled caryopses probes (2-14 DAF), as well as the corresponding Bowman/*seg8* ratios are listed for three experiments involving two independent probe syntheses and a 2nd experiment probe rehybridized onto a new membrane. The BlastX2 search against the protein database SwissProt provides secure functions for all EST clones represented in the Table.

3.2.6 Different expression profiles of genes encoding enzymes of the sugar-to-starch pathway monitored in maternal and filial fractions of developing *seg8* mutant and Bowman wild type grains

As shown before (cf. 3.2.3.), starch filling phase of *seg8* grains is characterised by higher levels of total sugar as well as hexoses and sucrose in the maternal tissues, as compared to the wild type “Bowman”. In the filial tissue fraction, both the total sugar content and hexose levels of the mutant caryopses are lower. These findings, together with the remarkably lower starch content of the embryo sac fraction (cf. Fig. 20 and 18) hint to *seg 8*-specific disturbances in the starch accumulation process. To identify differences in gene expression possibly causing the diminished starch content of the mutant grain, expression profiles of genes encoding enzymes of the sucrose-to-starch pathway were identified on the cDNA array and compared between *seg 8* and Bowman (see Fig. 22). In the maternal tissues, no remarkable differences in the abundance of the respective mRNAs were observed. However, this is true only from 2 DAF onwards. In the moment of pollination (0 DAF), mRNAs of sucrose synthase (SUS) 1 and 2, CWINV1, hexokinases 1cyt and 2 as well as fructokinase and UGP glucose pyrophosphorylase are clearly down regulated in the *seg8* maternal fraction. In the early development of the filial fraction, down regulation of the hexose-producing enzymes as well as two hexokinases (GK, Hkcyt1) was registered, too. During the ongoing filling phase of the starchy endosperm, SUS1 and 2 as well as the small and the large subunit of AGP glucose pyrophosphorylase and the granule bound starch synthase (SS1), i.e. the key enzymes of the starch biosynthetic pathway, are down regulated on mRNA level in the filial fraction of *seg8* caryopses.

Fig. 22

Expression data of EST clones with homology to genes coding sugar to starch pathway were selected. The expression intensities were normalized by setting the highest intensity measured either in mutant or wild type to 100% in maternal and filial tissue fraction depicted at the left-hand (maternal) or the right hand-side (filial fraction) of the figure 22. The intensities of mRNA expression obtained after the normalization procedure are plotted on the Y-axis. On the X-axis the developmental time scale 0-14 DAF (Days After Flowering) is given in two day intervals. AGP-L, large subunit of ADP-glucose pyrophosphorylase; AGP-S, small subunit of ADP-glucose pyrophosphorylase; CWINV, cell wall-bound invertase; FK, fructokinase, GK, glucokinase; Hkcyt, hexokinase cytosolic; HKchl, hexokinase chloroplatic; PGM, phosphoglucomutase; SUS, sucrose synthase; SS, starch synthase; UGP, UDP-glucose pyrophosphorylase; VCINV, vacuolar invertase.

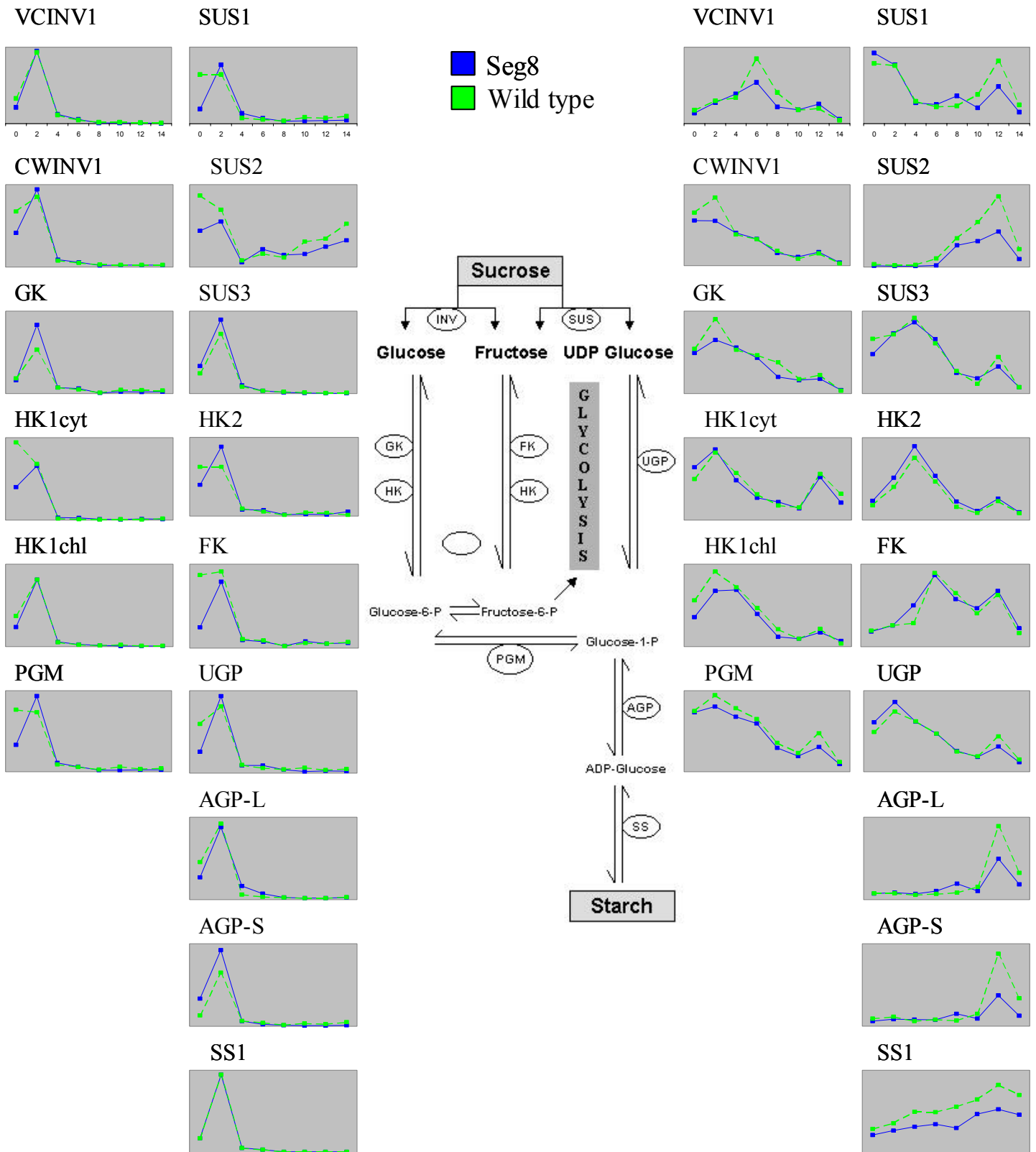


Fig. 22 For legend please see page number 76

3.2.7. mRNA expression of some transporter genes is drastically reduced in the filial fraction of developing *seg 8* grains

On the 1412 cDNA macro array filter, 12 cDNA fragments are spotted encoding putative transport proteins. Among them, three showed clear differences in their mRNA expression during the analyzed developmental period (0-14 DAF). As shown in Fig. 24, especially the potassium transporter expression is strongly influenced. In early development of the filial fraction, this transporter has a higher expression level in the mutant than in the wild type, whereas later in development expression decreases strongly in the mutant fraction, but increases to relatively high levels in the wild type. The ABC transporter, on the other hand, shows a general reduction of its mRNA expression level in the mutant filial fraction as compared to the wild type. Contrary to these two transporters that should be localised within the plasmamembrane of the starchy endosperm transfer cells, the ATP/ADP transporter is integrated in plastid membranes. Nevertheless, its expression is drastically reduced in the mutant, too (cf. Fig. 23).

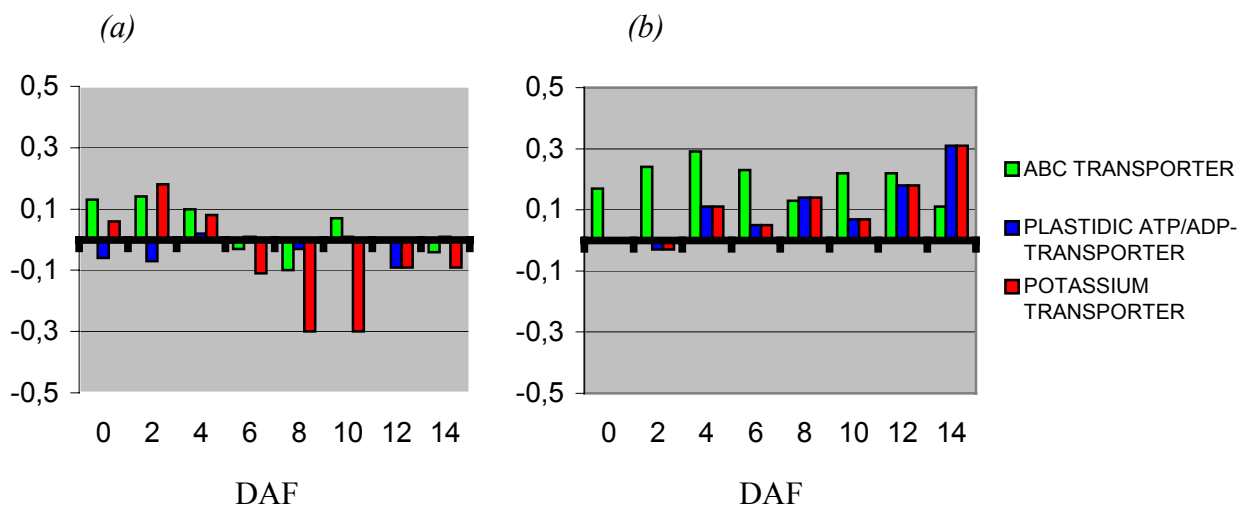


Fig. 23

Expression profiles of transporter genes in filial fraction of mutant (a) and wild type (b) during early and mid caryopses development. Putative function of the selected cDNA is provided on the right-hand side. The normalized signal intensity values are presented in Log 2 scale on the Y-axis. On the X-axis the developmental time scale 0-14 DAF (Days After Flowering) is given.

3.3 DISCUSSION

3.3.1 The *seg8* genomic environment integrated in “Bowman” displays the same features described for the original mutant identified in “Klages”.

As reported by Felker et al. 1985, the main characteristic of mutant *seg8* is development of the starchy endosperm in two lobes clearly separated from each other by the non-occurrence of endosperm cells in front of the grains maternal-filial boundary. Based on iodine staining of median-transversal sections of developing *seg8* caryopses, this finding was reproduced for grains expressing *seg8* in the “Bowman” background (see Fig. 20). Further on, as shown in Fig. 18, our analyses confirm the lower starch content measured by Djarod and Peterson (1991) in developing *seg8*/Klages grains. However, the overall reduction of the sucrose concentration estimated by Djarod and Peterson in the original mutant has been observed for the *seg8*/Bowman caryopses only during the ongoing starch accumulation period (10-12 DAF), and the total sugar content as well as hexoses levels are higher or lower in the maternal or filial part of the mutant grain, respectively, as compared to the wild type. Nevertheless, the reduction of starch content shown in Fig. 18 is exclusively due to the filial tissues as shown by the reduction of fresh weight only in the embryo sac fraction of *seg8* grains. This finding underlines the description of the mutant as maternally influenced but phenotypically expressed in the starchy endosperm.

3.3.2 Low mRNA expression of genes encoding key enzymes in the starch biosynthesis pathway may cause the reduced starch content of the mutant grain.

As shown in Fig. 18, starch content is drastically reduced in *seg8* grains. Starch biosynthesis in barley grains starts with increasing sucrose levels of the filial tissues (Weschke *et al.*, 2000), and more general, with increasing sucrose/hexoses ratios in the storage organs of the seed (Weber and Wobus, 1999). A steep sucrose gradient, build up in the cell rows adjacent to the transfer tissues of developing *Vicia faba* seeds, regulates the activity of the sucrose utilising enzymes, for instance sucrose synthase (SUS) (Borisjuk *et al.*, 2002a). In a reversible reaction, SUS cleaves sucrose to fructose and UDP glucose. A general reduction in the mRNA expression of different isoforms of this enzyme as shown in the filial fraction of the *seg8* grain (cf. Fig. 22) may reduce the amount of active enzymes molecules and, therefore, sucrose cleavage, leaving back the higher sucrose content measured in the mutant’s starchy endosperm (cf. Fig. 19). However, fructose as well as UDP glucose levels are higher in the filial fraction of *seg8* grains. Possibly, this finding can be explained by the reduced expression

of the two AGP glucose pyrophosphorylase subunits. If this lower expression is indicative for a general reduction of the enzyme activity, lower amounts of glucose-1-phosphate will be utilised to ADP glucose (compare the lower ADP glucose level in the *seg8* endosperm, Fig. 19) which may influence in turn the equilibrium between glucose-1-phosphate and UDP glucose resulting in the higher UDP glucose level measured. The low ADP glucose content together with the reduced amount of starch synthase (SS) (cf. Fig. 22) is indicative for the low starch content measured in *seg8* grains.

3.3.3 High sucrose levels in the maternal and filial fraction during storage phase hint to a delay in sugar utilisation and reduced starch accumulation in the mutant's endosperm.

The ongoing starch accumulation in the filial tissues causes higher sucrose demand of the filial endosperm, which will be supplied by maternal tissues. The sucrose imported via the vascular bundles into the maternal tissue will be supplied to the filial endosperm through the maternal-filial boundary. The establishment of sucrose gradients in the maternal tissues and in the maternal-filial boundary is nearly independent from disturbances in the development of the filial part in the pea *E2748* mutant (Borisjuk *et al.*, 2002b). In *seg8* mutant the drastic reduction of starch content is sensed in filial tissues. To accumulate lower amounts of starch in mutant, lower amounts of sucrose are expected. However, the maternal as well as filial tissues of mutant accumulate comparatively higher sucrose levels. Since there is a reduced expression in key enzymes of starch biosynthesis (sucrose synthase, ADP-glucose pyrophosphorylase and starch synthase) higher sucrose concentration must be expected, which is noticed in the *seg8* maternal pericarp as well filial fraction shown in Fig. 19. Important explanatory clues may come from a detailed study of the distribution of sucrose in wild type and *seg8* mutant and the possible detection of a sucrose concentration gradient between maternal and filial tissues.

On the other hand, detailed histological analyses comparing the structure of the maternal-filial boundary between *seg8* and Bowman have clearly shown an abnormal development of both, nucellar projection and endospermal transfer cells in *seg8* grains (S. Gubatz, personal communication). As shown in Fig. 23, mRNA expression of some of the genes encoding transporter proteins such as the potassium transporter, the ABC transporter and the plastidic ATP/ADP transporter is down regulated in the filial fraction of *seg8*, which could be correlated to abnormal development of endospermal transfer cells. Since a significant difference in mRNA levels of sucrose transporter between mutant and wild type was not

found and, more over, due to presence of higher concentration of sucrose in filial tissues of mutant, we prefer the interpretation that possibly the abnormal structure of the transfer tissues negatively influences the sucrose gradient in *seg8* grains.

3.3.4 A defect in starch accumulation can be expected for the developing gynoeceium.

The style tissue, dominating the female gynoeceium immediately before pollination, accumulates a lot of storage compounds, especially starch. At 0 DAF, sugar and UDP glucose content as well as the mRNA level of major enzymes of the sucrose-to-starch pathway are down regulated in the maternal fraction of *seg8* grains (cf. Figs. 19, 22). Similar to the down regulation of starch biosynthetic transcripts observed in starchy endosperm of the mutant during storage phase, the decreased levels of transcripts of starch-biosynthetic pathway is noticed during 0 DAF in maternal tissue. Despite the fact, that only the last moment in the development of the female gynoeceium (0 DAF) was analysed, a slight decrease in starch accumulation of the maternal tissue (0 DAF) can be concluded. Thus, possibly not only the filial parts of the seed but also the maternal tissues prior to anthesis are influenced by decrease in starch accumulation. We speculate that the *seg8* mutant may have a defect in starch accumulation in all tissues of the seed before as well as after pollination.

3.4 SUMMARY

The *seg8* mutant with impaired starch accumulation provides an ideal and unique experimental system to analyze the gene expression networks in relation to the sugar-to-starch pathway and to carry out metabolite profiling. Expression analysis results provide an eclectic overview of gene expression networks in the starch metabolism and sucrose/hexose distribution pattern in maternal and filial tissues during early and mid caryopsis development between mutant and wild type. Although, the *seg8* mutant has been described as maternal mutant, the analysis revealed that the mutant phenotype “shrunk endosperm” and disturbances at the maternal-filial boundary determine the observed seed phenotype. Although we see defects in transfer cells, sucrose flow into endosperm cells seems to be not the major limiting factor of lower starch accumulation because of higher sucrose levels and lower levels of glucose, fructose and starch content. Thus, a deficiency in maternal tissues causing a limitation in the supply of sucrose to the endosperm can be ruled out and the failure of hexose utilization appears to be the resulting cause for the low content of starch in *seg8* seeds. In addition, it is also clear that transcripts of key enzymes in starch biosynthesis are affected mainly in the filial fraction of the mutant during the storage phase and in pericarp during early stages of grain development (0 DAF).

CHAPTER 4

Expression analysis of foxtail millet genotypes differing in salt tolerance

4.1 INTRODUCTION

Environmental conditions have been shown to affect both plant growth and development and their productivity. Plants face threat both from biotic, which includes pathogen, pests and insects, and abiotic stresses, which includes factors like salinity, osmotic imbalance, temperature extremes etc. In agricultural systems, the abiotic stresses, salinity, low temperature and drought in particular are responsible for most of the reduction that differentiates yield potential from harvestable yield (Boyer, 1982). Though enormous amount of money is being spent world wide to tackle these problems, these are still challenges to those who are involved in crop production. The cultivable land available is constantly shrinking because of human encroachment and the available lands are also being spoiled to the greater extent by accumulation of salts in high concentration especially in arid and semi-arid regions. As soil salinity is one of the important constraints, better understanding of the mechanisms that enable plants to adapt to salt stress is necessary for exploiting saline soils/water.

Salt stress can lead to changes in development, growth and productivity and severe stress may threaten survival. Salt stress results in alterations in plant metabolism including reduced water potential, ion imbalance and toxicity (Cramer *et al.*, 1994; Bohnert and Jensen, 1996). High salinity causes both hyper osmotic and hyper ionic stress effects and the consequence of these can be lethal (Hasegawa *et al.*, 2000). Most commonly, the stress is caused by high Na⁺ and Cl⁻ concentrations in the soil solution and an altered water status most likely brings about initial growth reduction, membrane disorganization, generation of reactive oxygen species, metabolic toxicity, inhibition of photosynthesis and altered nutrient acquisition. Under these circumstances, the need to develop plants, which could withstand stress, retaining an

acceptable level of productivity, is of utmost importance. During the course of evolution different plants have developed adaptive characters against these stress factors. There are various mechanisms reported in the literature by which plants protect themselves from these stresses, including accumulation of osmoprotectants, presence of ion carriers, ion compartmentation, transporters and symporters, water channels, chaperones, superoxide radical scavenging systems and signaling molecules. All these phenomenon's have been well reviewed by several authors in different species of halophytes and glycophytes (Bohnert *et al.*, 2001; Cushman and Bohnert, 2000).

Salt tolerance is a complex trait involving responses to cellular osmotic and ionic stresses, as well as secondary stress effects. Many studies have examined the multitude effects of salt stress, and importance of protecting the plant from reactive oxygen species (ROS) seems to be one of the important components of the complex tolerance trait. The high salt concentrations normally impair the cellular electron transport within the different sub cellular compartments and lead to the generation of reactive oxygen species such as singlet oxygen, superoxide, hydrogen peroxide and hydroxyl radicals. Excess of ROS triggers phytotoxic reactions such as lipid peroxidation, protein degradation and DNA mutation. The primary source of ROS is superoxide radicals, which are generated in the sub cellular compartments such as mitochondria, chloroplast and cytoplasm via a number of metabolic pathways during oxidative stress conditions (Noctor and Foyer, 1998). The degree of peroxidative damage of cells is controlled by the potency of the antioxidative peroxidase enzyme system. Though the responses are stress specific, it is believed that some of them overlap. As reported in a number of studies, environmental stresses such as salt, drought and cold stress lead to increased free radical formation (Singha and Choudhuri, 1990; Smirnoff, 1993) and lipid peroxidation (Del Río *et al.*, 1991; Leprince *et al.*, 2000). At the physiological level, the multitude of effects of salt stress such as ion toxicity and water deficit impair photosynthesis, which results in production of reactive oxygen species.

The degree of oxidative cellular damage in plants exposed to salt stress is controlled by the antioxidative systems. A correlation between the antioxidant capacity and NaCl tolerance has been demonstrated in a number of crops such as pea (Hernández *et al.*, 2000), cotton (Gossett *et al.*, 1994) and foxtail millet (Sreenivasulu *et al.*, 2000). To overcome salt-mediated oxidative stress, plants detoxify ROS by up-regulating antioxidative enzymes like superoxide dismutase (SOD; EC 1.15.1.1), ascorbate peroxidase (APX; EC 1.11.1.11), glutathione

peroxidase (PHGPX; E.C. 1.11.1.9), glutathione cycle enzymes and produce low molecular mass antioxidants like flavonones, anthocyanines, α -tocopherol, ascorbate, glutathione and polyphenolic compounds. Bueno *et al.* (1998), showed the up regulation of antioxidants, superoxide dismutase and ascorbate peroxidase in response to salt stress at the transcriptional and translational level. Also implicated are the protective roles played by the accumulation of specific metabolites that seem to act in more than one function; for instance preventing radical formation, acting as low molecular weight chaperones contributing to redox control and functioning as compatible solutes by decreasing the osmotic potential. A main protective role is attributed to SOD in catalyzing the dismutation of superoxide anions to dioxygen and hydrogen peroxide (H_2O_2). In order to quench the generated H_2O_2 , plants evolved H_2O_2 scavenging antioxidative enzymes such as peroxidases and catalases (Halliwell and Gutteridge, 1989; Sen-Gupta *et al.*, 1993). Plant peroxidases utilize different substrates such as guaiacol, ascorbate and glutathione to scavenge intracellular H_2O_2 . Based on substrate specificity, peroxidases are classified into guaiacol peroxidase (POX; EC 1.11.1.7), ascorbate peroxidase and glutathione peroxidase. The H_2O_2 generated in glyoxysomes and peroxisomes by the process of β -oxidation is detoxified to H_2O mainly by catalase (CAT; E.C 1.11.16), while in other sub cellular compartments H_2O_2 is converted to H_2O by ascorbate peroxidase and glutathione peroxidase.

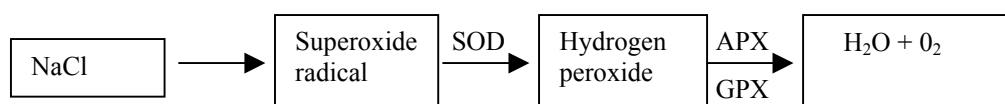


Fig. 24

A proposed model for pathways leading to the induction of reactive oxygen species (superoxide radical, hydrogen peroxide and hydroperoxides) during NaCl treatment and the role of the protective antioxidative enzymes superoxide dismutase (SOD), ascorbate peroxidase (APX) and phospho glutathione peroxidase (PHGPX) in scavenging superoxide, hydrogen peroxide and hydroperoxide radicals respectively.

Glutathione peroxidases are a family of multiple isozymes, which catalyze the reduction of H₂O₂, organic hydroperoxides and lipid hydroperoxides using GSH as a reducing agent (Ursini *et al.*, 1995) and thus help to protect the cells against oxidative damage (Flohé and Günzler, 1984). In animals, glutathione peroxidases have been studied extensively and various forms of GPX have been identified, which includes cytosolic GPX, plasma membrane GPX, gastrointestinal GPX and phospholipid hydroperoxide glutathione peroxidase (PHGPX). Even though all four groups reveal similarity in their primary structure, PHGPX differs from the other three by being a monomer and having ability to interact with peroxidised lipids and complex lipids, which are integrated in bio-membranes. Therefore the PHGPX reaction has been considered the main line of enzymatic defense against oxidative bio-membrane destruction in animals (Ursini *et al.*, 1995). Some reports showed the presence of PHGPX cDNAs for instance in *Citrus sinensis* (Holland *et al.*, 1993), *Nicotiana sylvestris* (Criqui *et al.*, 1992), *Spinacia oleracea* (Sugimoto *et al.*, 1997a), *Arabidopsis thaliana* (Sugimoto *et al.*, 1997b), *Lycopersicon esculentum* (Depège *et al.*, 1998), *Hordeum vulgare* (Churin *et al.*, 1999) and *Oryza sativa* (Li *et al.*, 2000). Further, PHGPX mRNA levels have been shown to increase in tissues of several plant species undergoing stress such as salinity (Gueta-Dahan *et al.*, 1997), heavy metals (Sugimoto *et al.*, 1997), herbicide resistance (Cummins *et al.*, 1999), mechanical stimulation (Depège *et al.*, 1998; Depège *et al.*, 2000) and infection by viral or bacterial pathogens (Levine *et al.*, 1994).

Although a wide range of significant physiological mechanisms and genetic adaptations to salinity stress has been observed, the underlying mechanisms of salt-tolerance in plants are still poorly understood. The best possible approach to explore tolerance mechanisms is to compare the components involved in stress response in tolerant as compared to sensitive plants. In foxtail millet (*Setaria italica* L.) salt sensitive and tolerant lines have been identified (Sreenivasulu *et al.*, 1999; 2000). Foxtail millet is an important food crop in India, China and Japan. Increasing salinisation of agricultural land causes toxic effects, primarily at the seedling level in plant development. Hence, improved understanding of acute adaptive and general protective mechanisms conferring enhanced salt tolerance in seedlings becomes an important issue in stress physiology to ensure further growth and yield of crop plants. An attempt has been made to study the biochemical difference between these lines in terms of the ROS scavenging system. The differential response of the system might pave the way for the better understanding of the phenomenon of salinity resistance and might in turn lead to the development of elite lines which could withstand increased salinity levels.

Present day technologies have opened ways to understand the biological principles also at the molecular/cellular level. For example newer tools are now available which allows to address the complexity of stress responses at a larger scale through genome wide expression profiling. Kawasaki *et al.* (2001), used DNA microarrays to monitor transcript abundance and expression patterns in two lines of rice differing in their response to salinity. The results indicate a progression of regulated functions such that different categories of transcripts show regulation at different developmental time scales. A difference between the two lines existed with respect to the onset of the initial response. Desikan *et al.* (2001), have undertaken a large-scale analysis of *Arabidopsis* transcriptome during oxidative stress. Using cDNA microarray technology, they identified 175 non-redundant ESTs that are regulated by hydrogen peroxide. Further, they could demonstrate that other stresses such as wilting, UV radiation and elicitor challenge also induce the expression of many of these genes. Progress is now anticipated through comparative genomic studies of an evolutionarily diverse set of model organisms. As described before, foxtail millet has the advantage to have salt tolerant and sensitive lines, and comparison of these lines for gene expression studies during high salinity stress by cDNA array analysis should be a very useful experimental tool. The discovery of novel genes, determination of their expression patterns in response to stress, and an improved understanding of their roles in stress adaptation will provide the basis of effective engineering strategies leading to greater stress tolerance.

The objectives of the following work have been

- i) Using barley macroarrays as a tool to analyze related heterologous probes (foxtail millet) by gene expression studies,
- ii) to study the performance of salt sensitive and tolerant lines of foxtail millet under salinity stress,
- iii) to look into gene expression patterns of these two lines under high saline conditions by cDNA array analysis and
- iv) to study the ROS scavenging system during salinity stress in seedlings of foxtail millet.

4.2 RESULTS

4.2.1 Growth attributes

The impact of salinity on the growth and development of crop plants has been demonstrated (Boyer, 1982). To gain knowledge about the impact of salinity on the growth and development of foxtail millet seedlings, seeds of both the tolerant (Prasad) and the sensitive (Lepakshi) variety were germinated on Hoagland medium supplemented with 0, 150, 200, 250 and 300 mM NaCl. After 5 days, seedlings were harvested and growth rates were determined by measuring the shoot and root lengths. As shown in Fig. 25, increasing NaCl concentration inhibited gradually the growth rate of both cultivars. The growth of the salt-sensitive cultivar was extensively inhibited at salt concentrations lower than 200 mM NaCl. In contrast, the salt-tolerant cultivar still developed shoots up to 250 mM NaCl, but growth was almost completely inhibited at 300 mM NaCl. The percentage of relative growth inhibition of the shoots upon increasing NaCl concentrations is indicated in the insert of Fig. 25.

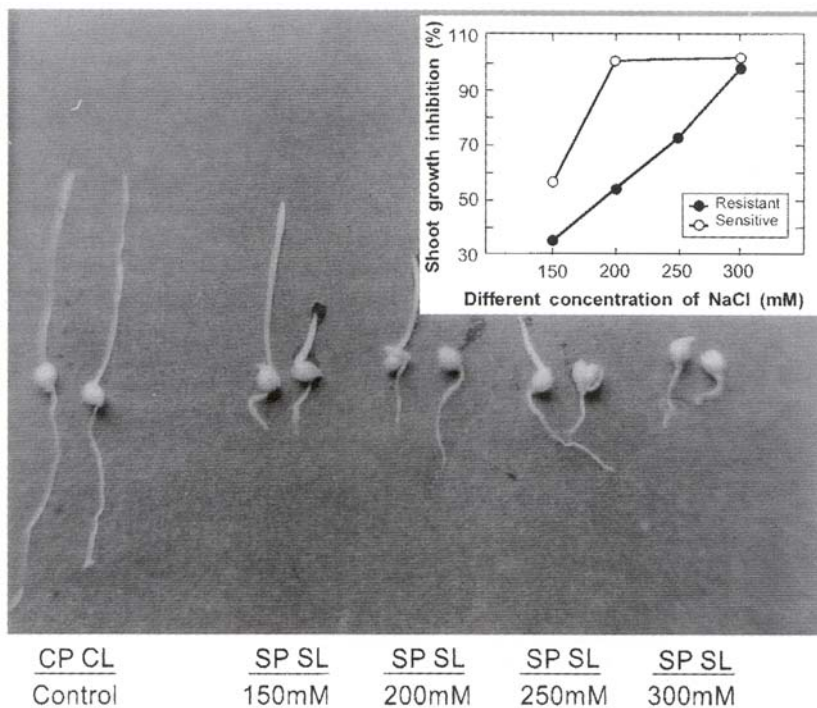


Fig. 25 Differences in root and shoot length of 5-day old seedlings of a salt-tolerant (P – Prasad) and a salt-sensitive (L – Lepakshi) foxtail millet cultivar grown under control conditions (CP – control Prasad; CL – control Lepakshi) and at different NaCl concentrations (SP – salt-treated Prasad; SL – salt-treated Lepakshi). Percentages of relative shoot growth inhibition are shown in the insert. Seedlings were grown at 25°C in Hoagland medium without NaCl (control) and with different NaCl concentrations (150, 200, 250 and 300 mM)

4.2.2 Sodium content measurements

To understand the accumulation of endogenous Na⁺ in the cultivars studied, the Na⁺ concentration was determined in tolerant and sensitive seedlings after five days of treatment with different concentration of NaCl. As shown in Fig. 26, seedlings of the two foxtail millet cultivars exhibited

a remarkable difference in the accumulation of endogenous Na^+ concentration upon increasing NaCl concentration in the medium, which is indicative of the differences of both cultivars in the adaptive response to salinity. In the salt-sensitive cultivar, Na^+ accumulated progressively with increasing amounts of exogenous salt. In the tolerant cultivar, the endogenous Na^+ content remains pretty low up to 150 mM NaCl treatment and increased only at 200 mM NaCl.

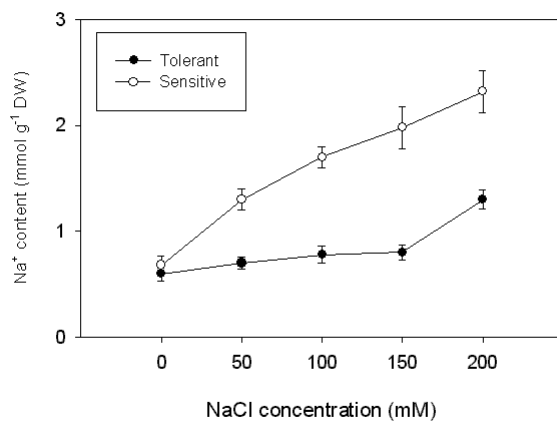


Fig. 26 Na^+ accumulation in 5-day-old seedlings of the tolerant and sensitive foxtail millet cultivar grown at different NaCl concentrations. The presented data are the average of 3 independent sets of experiments. DW - dry weight.

4.2.3 Effect of salinity on electrolyte leakage

The extent of membrane damage by salinity stress was assessed by an indirect measurement of solute leakage in tolerant and sensitive seedlings. The electrolyte leakage was subsequently measured after growing the seedlings in Hoagland medium with (different concentrations) and without (control) NaCl. The estimated ion leakage of seedlings correlates with increasing NaCl concentrations. While the sensitive cultivar showed the highest electrolyte leakage after incubation with 150 mM NaCl, the salt-tolerant cultivar displayed a 1/3 lower leakage at this NaCl concentration (Fig. 27). Results show a lower impairment of membrane permeability in the cells of the tolerant seedlings in comparison to the sensitive one.

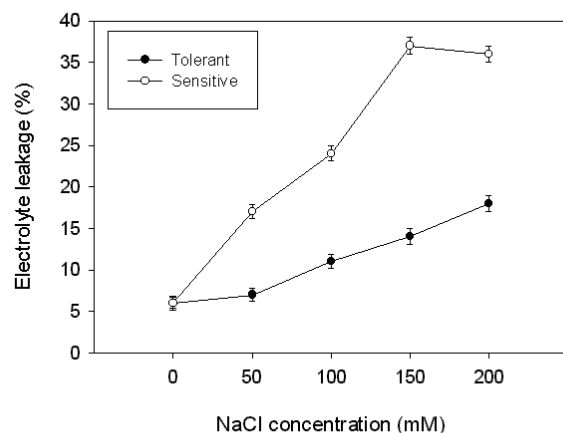


Fig. 27 Electrolyte leakage rate measured in cells of 5-day-old seedlings of the tolerant and sensitive foxtail millet cultivars grown at different salt concentrations. The presented data are the average of 3 independent sets of experiments.

4.2.4 Effect of salinity on malonaldehyde content (MDA)

The extent of membrane damage was assessed by measuring the MDA content of five-day old seedlings of the tolerant and sensitive cultivar grown on different NaCl concentrations and without NaCl (control). In both cultivars, increased salt concentration caused a significant increase in the MDA level. However, MDA accumulation was higher in the salt-susceptible one (Fig. 28). Up to 100 mM NaCl, no significant difference was found in the MDA level of the two cultivars. At higher NaCl concentrations, the amount of MDA remains nearly constant in the tolerant cultivar (around 20 μmol at 100 mM and 28 μmol at 250 mM NaCl), but increases to more than double the amount (around 55 μmol) in seedlings of the sensitive cultivar exposed to 250 mM NaCl.

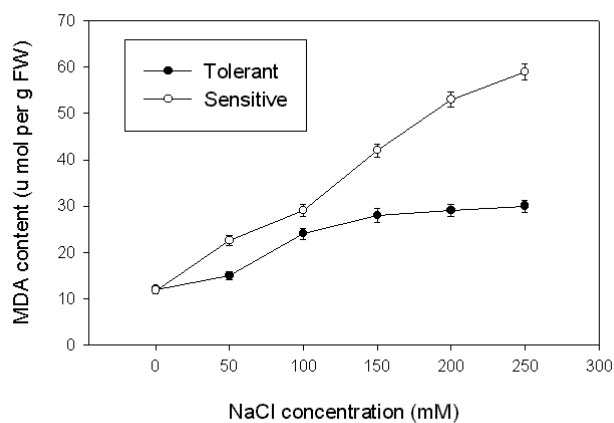


Fig. 28 Variation in the MDA content of salt-tolerant and salt-sensitive seedlings of foxtail millet grown under different concentrations of NaCl. The presented data are the average of 3 independent sets of experiments.

4.2.5 High-throughput expression analysis of salt stress responsive genes

In the present study macroarray containing 711 barley cDNA fragments described in Chapter 1 was used to study salt stress responses. It includes 58 stress responsive genes. To monitor NaCl-stress induced gene expression, mRNA samples from five-day-old tolerant and sensitive foxtail millet seedlings grown upon 250mM NaCl and without salt treatment (control) were isolated and reverse transcribed into first-strand cDNA probes. Four different ^{33}P -labelled second-strand cDNAs, two generated from tolerant (salt-treated, control) and two from sensitive seedlings (salt-treated, control) were hybridized to the barley cDNA array. The complete hybridization procedure was repeated using independently grown seedlings as material for probe preparation. The global expression changes among all the expressed sequence tags (ESTs) on the macroarray were compared between tolerant and sensitive cultivars during high NaCl treatment and control conditions. From these expression analyses, 16 non-redundant ESTs were found to be up regulated 2-fold and higher in the salt treated tolerant cultivar with respect to control, whereas in the salt-

sensitive cultivar these transcripts were not up regulated to a significant extent (see Table 13). In order to determine whether the transcripts up regulated in the salt-tolerant cultivar belong to a particular class of genes, we associated expression data with the functional classification. The functional classification of ESTs was described in annotation section of Chapter 1. The ESTs up regulated in the salt-tolerant cultivar represent mainly hydrogen peroxide scavenging enzymes and additionally, hypothetical and unknown genes. Some transcripts such as heat shock proteins are generally down regulated in both lines.

Table 13 cDNA clones that are preferentially expressed in salt-treated tolerant seedlings

EST-id	Putative function	Exp1	Exp1	Exp1	Exp1	Exp1	Exp1	Exp2	Exp2	Exp2	Exp2	Exp2	Exp2
		ct	tt	ratio	cs	ts	ratio	ct	tt	ratio	cs	ts	ratio
	hydrogen peroxide scavenging												
HY09D05	glutathione peroxidase homolog	20,00	44,23	2,21	30,36	22,68	1,31	18,9	39,0	2,1	19,0	29,0	1,5
HY10B17	l-ascorbate peroxidase, cytosolic	75,98	164,28	2,18	61,21	57,06	1,07	54,0	111,9	2,1	110,0	80,9	1,4
HY03C01	catalase	18,00	37,66	2,09	17,52	20,54	1,17	21,0	45,0	2,1	24,9	33,7	1,4
	fuctose metabolism												
HY06N11	fructose-bisphosphate aldolase, cytosolic	8,26	17,54	2,12	5,29	12,81	2,42	9,2	18,0	2,0	8,0	14,0	1,8
	purine metabolism												
HY03K17	phosphoribosylformylglycinamide	21,00	42,75	2,03	12,98	28,11	2,16	18,0	36,4	2,0	25,2	36,2	1,4
	lysine biosynthesis												
HY03O15	dihydrodipicolinate synthase 2	26,04	52,76	2,02	19,61	21,59	1,10	32,1	66,5	2,1	25,2	33,1	1,3
	energy production												
HY01A07	peptidyl-prolyl cis-trans isomerase	9,00	23,21	2,58	3,59	16,79	4,68	14,0	32,1	2,3	12,0	25,4	2,1
HY05K13	peptidyl-prolyl cis-trans isomerase	7,77	18,00	2,30	4,28	10,39	2,43	6,6	17,0	2,6	8,1	15,3	1,9
	protease inhibitor												
HY05L03	alpha-amylase/trypsin inhibitor cmd	110,00	229,81	2,09	118,00	149,48	1,27	108,7	218,3	2,0	119,3	133,0	1,1
	non-classified												
HY10M15	open rectifier potassium channel protein	291,98	1136,2	3,89	404,49	703,07	1,74	321,0	816,9	2,5	341,8	680,3	2,0
HK04B02	dihydrolipoamide dehydrogenase	27,00	55,84	2,06	24,51	22,68	1,08	15,2	29,8	2,0	7,2	9,3	1,3
HY06G06	open rectifier potassium channel protein	30,18	61,25	2,03	28,96	39,74	1,37	29,9	65,5	2,2	48,0	49,6	1,0
HY02G05	carboxyvinyl-carboxyphosphonate	26,00	52,69	2,02	22,47	29,03	1,29	23,6	49,0	2,1	32,0	34,5	1,1
HW01M06	amphiregulin precursor, human	13,28	26,04	2,00	8,75	16,55	1,89	14,9	29,2	2,0	12,6	18,6	1,5
HY09N04	argonaute protein	36,00	72,00	2,00	19,59	45,17	2,31	36,8	74,7	2,0	43,5	61,0	1,4
HY09O22	npc derived proline rich protein 1, mouse	71,00	142,00	2,00	64,19	72,42	1,13	63,3	124,5	2,0	50,9	62,2	1,2

Clones that are preferentially expressed in salt-treated tolerant cultivar are defined as those that give ratios of control: NaCl-treatment signal intensity larger than 2 with higher signal intensity values and absolute signal intensities greater than 5 au in the two independent array experiments. Putative function of secured annotated clones is given. ct – control tolerant; tt - treated tolerant (250 mM NaCl); cs –control sensitive; ts – treated sensitive (250 mM NaCl).

4.2.6 Hydrogen peroxide scavenging enzymes

Concerted attempts have been made to understand the expression of salt-mediated oxidative stress-induced hydrogen peroxide scavenging genes such as phospholipid hydroperoxide glutathione peroxidase (PHGPX), ascorbate peroxidase (APX) and catalase I (CATI). It was shown before that APX transcript and protein levels are up regulated under salt-treatment (200 mM) only in the tolerant cultivar (Sreenivasulu *et al.*, 2000). Using the cDNA array analysis we confirmed the observed changes in transcript levels of APX. As shown in Table 13, the PHGPX transcript level increased 2-fold in the tolerant cultivar under high concentrations of NaCl (250 mM), whereas no remarkable difference was found in the PHGPX expression level of salt-treated sensitive seedlings. We have evaluated the validity of the PHGPX-specific array results by using a fragment of the millet PHGPX gene as probe in northern blot analysis. The membrane was hybridized with a PHGPX-specific fragment 316 bp in length amplified from millet RNA by RT-PCR (see below). As shown in Fig. 29, the level of the PHGPX transcript is induced to higher levels in the tolerant cultivar during salt treatment, whereas in salt-sensitive cultivar PHGPX mRNA was expressed to the lower levels. Comparing the results of the two methods, i.e. cDNA array analysis and Northern blotting, nearly the same profile of PHGPX-mRNA expression was found.

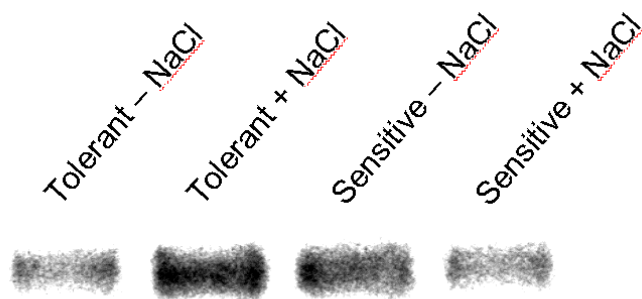


Fig. 29 Northern blot analysis of PHGPX mRNA accumulation following salt treatment (250 mM NaCl) in the tolerant foxtail millet cultivar as compared to the salt-sensitive cultivar. Total RNA was prepared from control and salt-treated seedlings, approximately 15 µg total RNA was loaded per lane, electrophoresed, blotted and hybridized with ³²P-labelled SiGPX (*Setaria italica* PHGPX) probe.

4.2.7 Isolation and identification of a cDNA coding for a PHGPX from millet

To isolate PHGPX cDNA from millet, conserved domains of known PHGPX sequences from different species including barley sequences (Churin *et al.*, 1999) together with the barley PHGPX EST/cDNA spotted on our cDNA macroarray were used to design degenerated primers for RT-PCR. Total RNA was isolated from seedlings of the salt-tolerant and the salt-sensitive cultivar grown upon 250 mM NaCl. The RNA probes were used as template for RT-PCR. Bands were amplified only from that RNA sample extracted from tolerant seedlings (data not shown). After

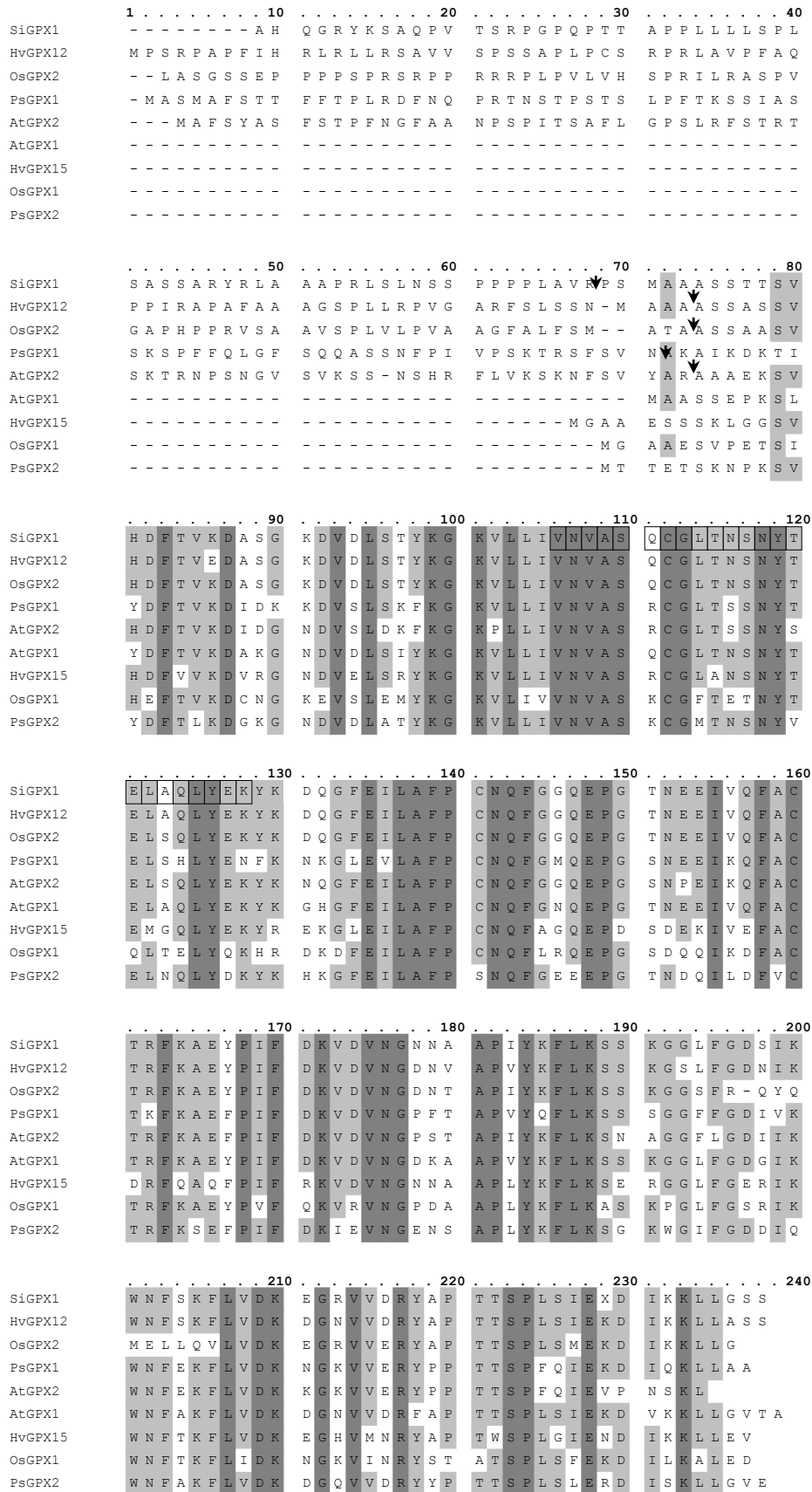


Fig. 30 Amino acid sequence alignment of cDNA clone isolated from *Setaria italica* PHGPX (SiGPX) with PHGPX sequences from other species. Database searches were carried out using the BLAST program and sequence alignment was performed with OMEGA 2.1 program. Amino acid sequences of PHGPX are aligned as follows: *Setaria italica* (SiGPX1); *Horedium vulgare* (HvGPX12-Acc Nr CAB 59893; HvGPX15-ACC Nr CAB 59894); *Oryza sativa* (OsGPX2-Acc Nr

BF430853; OsGPX1- Acc Nr CAC 17628); *Pisum sativum* (PsGPX1- Acc Nr CAA04142: BF430853; OsGPX1-Acc Mr CAC 17628); *Pisum sativum* (PsGPX1- Acc Nr CAA04142: PsGPX2); *Arabidopsis thaliana* (AtGPX2- Acc Nr CAB 40757: AtGPX1- Acc Nr AAC 09173). Residues common to all 9 proteins are shown by dark gray shading, whereas those shared by 6 to 9 proteins are shadowed by light gray colour. The putative transmembrane domains are predicted by the TMHMM program. Arrow head indicates the predicted chloroplast cleavage site. The boxed region represents the peptide sequence identified from purified protein.

cloning of the RT-PCR fragments, sequence analyses showed that the fragments obtained with two different combinations of primers (see Material and Methods) represent the same PHGPX gene. The RT-PCR amplified millet cDNA fragment (316 bp in length) shared 85% and 95% homology with the PHGPX EST from barley at the nucleotide and amino acid level, respectively. This cDNA fragment was used to screen a cDNA library prepared by Dr. Winfriede Weschke from salt-treated (200 mM) tolerant foxtail millet seedlings at high stringency (65°C). Sequence analysis of seven independent positive clones of different length revealed that all represent the same PHGPX gene. The longest cDNA was chosen and designated as millet PHGPX1. The alignment of the amino acid sequence of millet PHGPX1 to recently published putative plant and mammalian PHGPX proteins is shown in Fig. 30. Although a very high degree of homology was found to the plastid targeting sequence of barley PHGPX12, an additional in-frame ATG located in the 5' region of PHGPX12 could not be identified in the 5' region of the millet gene (compare Fig. 30). On the other hand, a second glutathione peroxidase found in barley HvGPX15 has not been detected in millet. Up to now, it is unclear whether the millet PHGPX1 cDNA contains the complete 5' transcribed region of the corresponding gene. Starting with the ATG identified up to now (see Fig. 30), the predicted millet PHGPX1 protein has 237 amino acids and a molecular mass of 25.7 kD.

4.2.8 Identification of a PHGPX gene family in millet

To analyze the genomic organization of millet PHGPX1, genomic DNA from seedlings of the tolerant and sensitive cultivar was isolated, digested by different restriction enzymes and subjected to Southern blot analysis using the ³²P-labelled 316 bp RT-PCR fragment as a probe. Because none of the enzymes used to cut the genomic DNA has a restriction site within this fragment, different fragments visible to nearly the same high intensity within one lane of the Southern blot should represent different genomic loci of highly homologous genes. Therefore, at least two nearly identical PHGPX genes can be expected within the millet genome (see Fig. 31). Furthermore, Southern blotting revealed no differences between the two varieties in the major bands whereas a polymorphism is visible in minor bands (identified by Fig. 31).

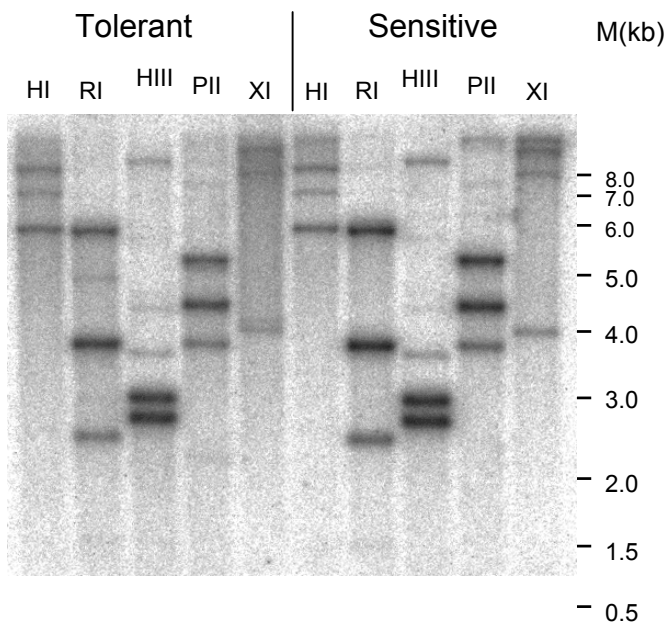


Fig. 31 Southern blot analysis of *Setaria italica* PHGPX gene. Genomic DNA (10 μ g) from foxtail millet seedlings of the tolerant and sensitive genotypes were digested with restriction endonucleases (HI-Bam HI ; RI-Eco RI ; HIII-HindIII ; PII-PVUII ; XI-XhoI) Digested DNA was subjected to electrophoresis and hybridized with the 32 P-labelled SiGPX cDNA probe. Fragment length of the standard DNA marker (M; 1 Kb ladder, BRL) are indicated in kilo bases (kb) on the right hand side.

4.2.9 Salt-specific induction of the PHGPX protein (25 kD)

Proteins were extracted from tolerant seedlings exposed to NaCl (24 hours, 250 mM NaCl), drought (24 hours, 20% polyethylene glycol 8000), higher temperature (45⁰C, 5 hours) and cold (4⁰C, 5 hours) and separated on a 12-15% SDS-PAGE gradient gel. The protein patterns obtained after silver staining of the gradient gel indicate that a 25 kD protein is specifically induced by NaCl stress. Only a slight increase in concentration of this protein was registered under temperature stress (Fig. 32).

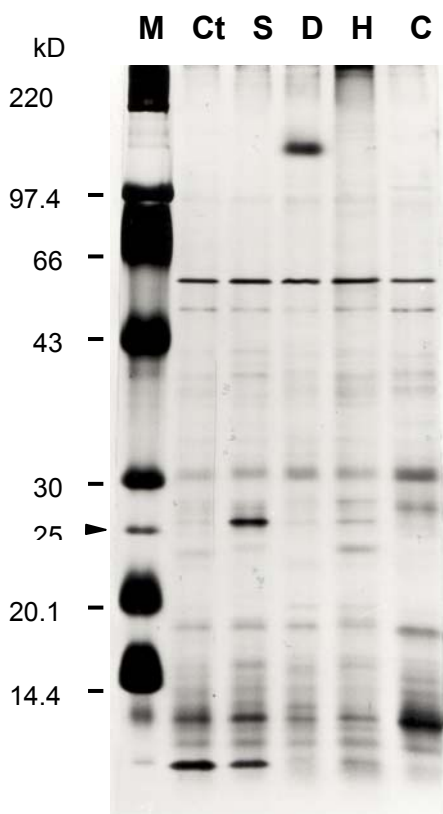


Fig. 32 Protein patterns of 5-day-old tolerant seedling samples grown under control (Ct) conditions and different types of stress such as 150 mM NaCl (S), drought (D), high temperature (H) and cold (C) depicted on a 12-15% gradient acrylamide gel. Positions of the marker (M) proteins (220, 97.4, 43, 30, 20.1 and 14.4 kilo Daltons, kD) were represented on the left hand side of gel. The arrowhead marks the position of the of 25 kD protein induced under salt treatment.

4.2.10 Purification of the salt-induced 25 kD PHGPX protein

The 25 kD protein specifically induced under salt treatment in seedlings of the tolerant cultivar was detected in the soluble fraction. The protein extract was subjected to DEAE ion-exchange chromatography. Fractions number 12-18 eluted at 0.6 M NaCl exhibited a clear protein peak and high peroxidase activity (Fig. 33a). The fractions were pooled, lyophilized and subjected to two-dimensional (2D) gel analysis. The DEAE-sepharose pooled fraction contains a 25 and a 27 kD protein with apparent isoelectric point of 4.8 and 3.7, respectively (Fig. 33b). The DEAE-Sephacel fraction containing 25 and 27 kD proteins were subjected to Superose FPLC. The 25 kD and the 27 kD protein were eluted at 141 and 121 min respectively (Fig. 33c). The homogeneity of the salt-induced 25 kD purified protein is shown in the insert of Fig. 33c.

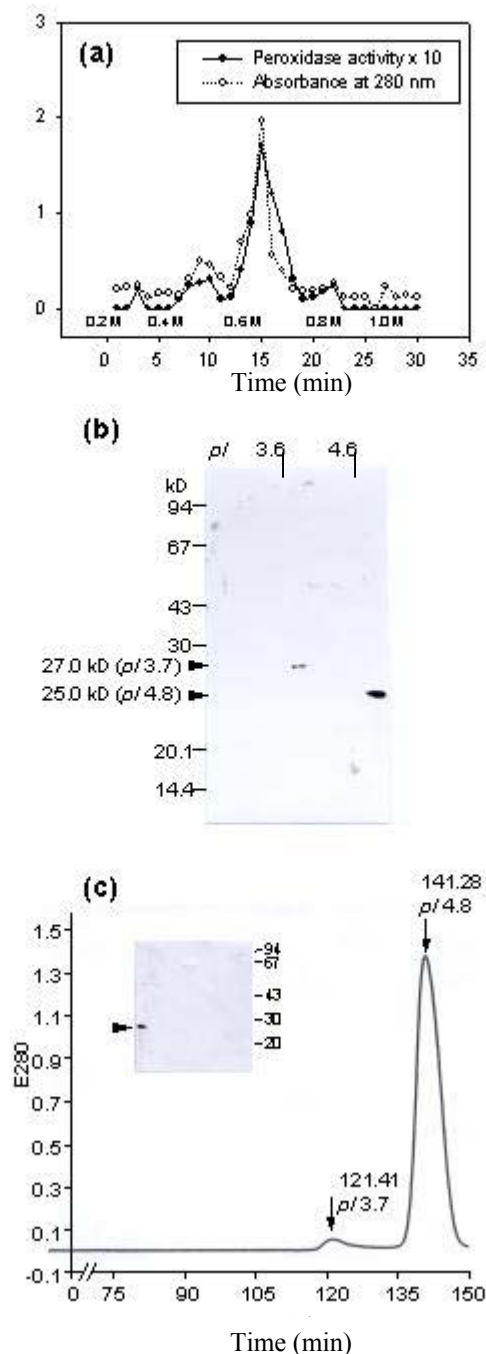


Fig. 33 Purification of the salt-induced 25 kD protein from NaCl-treated tolerant seedlings by DEAE-Sephacel and FPLC.

(a) DEAE-Sephacel column chromatography of bound protein eluted at different concentrations of NaCl (0.2, 0.4, 0.6, 0.8 and 1.0 M). The elution time-scale is given on X-axis. Peroxidase activity and absorbance values at 280 nm were scaled on Y-axis.

(b) Two-dimension gel analyses of 0.6 M eluted fraction to confirm the molecular weights of partially purified fraction of 27 kD (pI 3.7) and 25 kD (pI 4.8) proteins. The standard molecular weight marker were represented in kD on the left hand side and Standard pI markers are represented on of the gel.

(c) Superose FPLC chromatogram of purified 25 kD (pI 4.8) and 27 kD (pI 3.7) proteins represented as eluted peak at 121.41 min and 141.28 min, respectively.

4.2.11 Amino acid (AA) sequence analysis of the salt-induced 25 kD protein

The purified 25 kD protein (*pI* 4.8) was subjected to amino acid analysis of the N-terminal region. Since the N-terminal region of the protein was blocked, it was subjected to trypsin digestion. The generated peptides were isolated by reversed-phase HPLC and sequenced (by Prof. Prakash). The amino acid sequence of the major well resolved peptide (VNVASQCGLTNSNYTELAQLYEK) showed high homology to non-selenium glutathione phospholipid hydroperoxide peroxidase from plants and human as shown in Fig. 30.

4.3 DISCUSSION

4.3.1 Application of barley macroarrays to foxtail millet

It is well known that, in the grasses, conservation of gene orders (synteny) extends beyond species and even tribes (Chao *et al.*, 1988; Whitkus *et al.*, 1992; Ahn and Tanksley 1993; Peterson *et al.*, 1995). Establishment of the relationship between the genomes of different species provides researchers with the possibility of trans-genomic gene identification and isolation. Foxtail millet and other millet species for which little is known at the genomic level will benefit greatly from the EST information already available in other grasses, especially in cereals such as barley. Since several cereals are phylogenetically close to foxtail millet, we explored the ability of barley-based arrays to examine the expression patterns in foxtail millet genotypes differing in salt tolerance. Since we worked with a heterologous system (barley chips and millet probes), hybridizations were performed at 60⁰ C. Based on expression data presented in the result section (Table 13), the conclusion can be drawn that barley macroarrays are a very useful tool to analyze foxtail millet with a minor loss in sensitivity in comparison to homologous probes (data not shown). Using foxtail probes we identified specific mRNAs induced by NaCl in the tolerant cultivar to a 2-fold levels (Table 13). In only a few studies, mRNA profiles resulting from cDNA array analyses can be compared to both, protein amount and enzyme activity of the same gene. In order to validate the data generated by array experiments we selected PHGPX and APX (Sreenivasulu *et al.*, 2000) genes to conduct independent confirmation by northern blot analysis. Further we isolated the PHGPX gene from the salt-tolerant foxtail cultivar “Prasad” to follow the line mRNA abundance → protein amount → enzyme activity and to analyze whether the increase in mRNA expression seen on the macroarray filter is reflected at the level of enzyme activity. Northern analyses using a PHGPX and APX probe from foxtail millet as probe in principle confirmed the array data. The induction of the PHGPX transcript was correlated to the increased level of the PHGPX protein in the tolerant foxtail millet cultivar treated by NaCl treatment.

4.3.2 Differential response of physiological parameters to salinity stress in salt-tolerant and salt-sensitive seedlings of foxtail millet

As salinity is one of the important limiting factors in agriculture, a better understanding of the behavior or responses of plants to salinity is necessary to develop plants, which could withstand higher salinity. Therefore, an attempt has been made to understand the mechanism behind salt tolerance taking two cultivars of foxtail millet differing in their sensitivity to salinity. The analysis of endogenous Na^+ ions content showed a higher accumulation of Na^+ in the sensitive cultivar as compared to that of the tolerant one (Fig. 26). Growth of the salt tolerant foxtail millet cultivar is certainly favored by the maintenance of a constant Na^+ ion level in the plant. In this context, it is important to mention that an antiserum raised against proteins of the salt-tolerant cultivar recognized a putative Na^+/H^+ antiporter, which is highly enriched in the tolerant foxtail millet seedlings as compared to the sensitive one (Sreenivasulu *et al.*, unpublished data). Similar observations on a relationship between endogenous Na^+ concentrations and salt tolerance have been reported for different organs of rice (Yeo and Flowers, 1983; Dionisio-Sese and Tobita, 1998). Furthermore, salinity causes stronger electrolyte leakage of sensitive seedlings in comparison to the tolerant seedlings (Fig. 27). Likewise, strong differences in electrolyte leakage between tolerant and sensitive cultivars were described for 3-week-old rice seedlings grown under salinity stress (Dionisio-Sese and Tobita, 1998). Increase in MDA content in sensitive seedlings was observed at 150 mM NaCl treatment (Sreenivasulu *et al.*, 1999) whereas tolerant seedlings maintained constant MDA levels even up to 200 mM NaCl (Fig. 28). The constant value of electrolyte leakage in combination with a low content of MDA observed in the tolerant seedlings, provide some evidence for lower lipid peroxidation and less affected membrane integrity in comparison to the sensitive seedlings.

4.3.3 The possible role of hydrogen peroxide scavenging enzymes in salt-mediated oxidative stress tolerance

Results of biochemical studies showed that better growth of tolerant foxtail millet seedlings under high salt conditions is accompanied by an efficient antioxidative system as part of tolerance mechanism to cope-up salt mediated oxidative stress (Sreenivasulu *et al.*, 1999; 2000). It was noticed earlier that salt induces the up regulation of superoxide dismutase (SOD) activity mainly due to the induction of cytosolic Cu/Zn-SOD and Mn-SOD isoforms in tolerant, but not in the salt-sensitive foxtail millet cultivar, is expected to scavenge superoxides, which in turn resulted in formation of H_2O_2 (Sreenivasulu *et al.*, 2000). SOD converts relatively less toxic O_2^- radicals to the more toxic H_2O_2 . The excess H_2O_2 produced under salt stress needs to be scavenged at the

production site itself in order to achieve salt-induced oxidative tolerance during long-term salt stress (Foyer *et al.*, 1994). Plants have evolved various protecting mechanisms to adapt themselves against such menace and one such system is the presence of antioxidant enzymes such as peroxidases and catalases, which detoxify H₂O₂. During NaCl treatment the salt-tolerant foxtail millet cultivar exhibited a higher activity of the H₂O₂-detoxifying enzyme APX (Sreenivasulu *et al.*, 2000). The increase of both SOD and APX activity shown by our previous results (Sreenivasulu *et al.*, 2000) is in agreement with the induction of both activities in a salt-treated *Arabidopsis* mutant line (PS1) with salt tolerance (Tsugane *et al.*, 1999) and in salt-tolerant peas treated with NaCl (Hernandez *et al.*, 1993).

Using the EST approach, we dissected the oxidative stress effects of complex-salt tolerance trait, and identified salt-mediated-oxidative stress induced hydrogen peroxide scavenging transcripts such as PHGPX, APX and CAT1 in tolerant seedlings under high NaCl treatment (250 mM NaCl). In order to investigate the molecular mechanism of salt-mediated oxidative stress, a detailed study was initiated including molecular cloning of the PHGPX cDNA as well as characterization and purification of the protein. In the present study, data obtained from expression analysis by using barley ESTs indicates that the transcript accumulation of PHGPX was increased significantly at 250 mM NaCl treatment in the tolerant cultivar (Table 13). Our findings are consistent with other reports, for instance about induction of PHGPX during NaCl treatment in citrus (Beeor-Tzahar *et al.*, 1995) and barley (Churin *et al.*, 1999). The present results are also in agreement with results of Gueta-Dahan *et al.* (1997) with respect to higher expression of PHGPX under NaCl treatment when compared to control conditions. On the other hand, Gueta-Dahan *et al.* (1997) showed that long-term exposure of salt resulted in similar increases in the amount of PHGPX in both salt-sensitive and salt-tolerant citrus cells. As part of their recent investigations they reported that short-time NaCl treatment increased PHGPX more in salt treated sensitive seedlings of citrus cells than in salt-tolerant ones (Avsian-Kretchmer *et al.*, 1999), which is in contrast to our present findings. Recently, Hernández *et al.* (2000) showed that PHGPX mRNA level was significantly induced in the NaCl-tolerant pea variety in comparison to the NaCl-sensitive variety during long-term salt stress. This data strongly correlate with our results and suggest that induction of PHGPX is at least part of the tolerance mechanism in tolerant millet as well as salt-tolerant pea genotypes under long-term salt-stress.

In plants, PHGPX was not known until recently. In animals, PHGPX is considered as one of the key enzymes involved in scavenging hydroxyl radicals and hydrogen peroxide. Both the plant and

mammalian PHGPX enzyme contain three conserved domains: NVASQ(C/X)G, ILAFPCNQF and IKW^UNF(S/T)DFL(V/I)DK with catalytic residues X, Q and W respectively. The presence of the amino acids selenocysteine, glutamic acid and tryptophan is known as being critical for the catalytic activity in mammalian PHGPX enzyme (Chu *et al.*, 1993). The most prominent difference between plant and mammalian PHGPX is replacement of selenocysteine (present in the mammalian enzyme) by cysteine in plant PHGPX. This replacement results in a drastic decrease of the activity of the plant enzyme in comparison to the mammalian PHGPX one (Eshdat *et al.*, 1997). Similar to other plant PHGPXs, millet PHGPX contains cysteine instead of selenocysteine, suggesting that millet PHGPX is one of the non-selenium PHGPX. However, the two other amino acids, glutamic acid and tryptophan (see Fig. 30) known to be critical for the catalytic activity, are present in the millet PHGPX sequence.

Based on amino acid alignments of many plant PHGPXs, at least two protein/enzyme classes could be discerned (see Fig. 30). The longer cDNA most likely encodes an isoform targeted to the plastid and the shorter cDNA a cytosolic isoform of PHGPX. In barley, Churin *et al.*, (1999) have isolated 3 PHGPX cDNA clones, out of them two clones are up regulated under salt stress. The longer isoform would be targeted by a transit peptide to the chloroplast, whereas the isoforms lacking such transit peptide would be localized within the cytoplasm. In the predicted protein derived from the SiGPX cDNA an in-frame methionine residue was identified (position 63), which corresponds to the start codon of the cytoplasmic isoform. On the other hand, computer analyses have predicted a transit peptide located in the region upstream of this methionine residue, which shares similarity to the probable transit peptide of the barley HvGPX12. It seems that the millet cDNA 5'-region is incomplete and possibly, also possesses a plastid transit peptide. Most likely, the SiGPX is localized in plastids as recently demonstrated for a PHGPX from barley, *Arabidopsis* and pea (Mullineux *et al.*, 1998; Churin *et al.*, 1999). Interestingly, the third PHGPX isoform found in barley is down regulated under salt stress (Churin *et al.*, 1999). As expected from that finding, expression of this cDNA could not be demonstrated in the salt-treated tolerant millet cultivar, but its existence would explain the Southern analyses result, which hints to the presence of a small PHGPX gene family in the millet genome (Fig. 31).

Until now, the salt-induced PHGPX was purified from the cytosolic fractions in citrus (Ben-Hayyim *et al.*, 1993; Beor-Tzahar *et al.*, 1995) and another PHGPX isoform was purified to homogeneity from total membrane fractions of *Hansenula markii*, a yeast strain resistant against lipid hydroperoxide treatment (Tran *et al.*, 1993). In the present study, we purified the 25 kD millet salt-induced PHGPX protein (*pI* 4.8) from the soluble fraction of 5-day-old seedlings of a

tolerant foxtail millet cultivar (see Fig. 33b). Expression of the 25 kD protein was found under high salt conditions; it was not induced by other abiotic stresses (see Fig. 32). Thus, the induction of protein expression can be correlated to salinity tolerance. Furthermore, the peptide sequence of the purified 25 kD protein (*pI* 4.8) showed high similarity to mammalian PHGPX. Because a high similarity was found to several PHGPX sequences from other plant species, and further on, the isolated peptide could be assigned to the expected region of the PHGPX proteins (Fig. 30), PHGPX from *Setaria italica* (SiGPX) should have the physiological function of a glutathione peroxidase, i.e. to reduce directly peroxidized membrane lipids.

4.4 SUMMARY

On the basis of cDNA array analysis, hydrogen peroxide scavenging genes such as PHGPX, APX and CAT were found to be up regulated in the tolerant cultivar under long-term 250 mM NaCl exposure. Further on, the strong increase of PHGPX mRNA expression was the starting point for a detailed investigation of one of the most interesting antioxidant enzyme in plants. The transcript induction of PHGPX gene in salt-tolerant cultivar during NaCl treatment revealed by macroarray analysis can be juxtaposed to protein level. The induction of hydrogen peroxide scavenging genes in the salt tolerant cultivar in response to salt (250 mM NaCl) stress corroborates earlier data (Mullineux *et al.*, 1998; Churin *et al.*, 1999). The present study shows substantial differences in the cellular reactivity between the salt-tolerant and salt-sensitive foxtail millet cultivars in response to salinity stress. Upon high NaCl concentrations, seedlings of the salt-sensitive cultivar show a high internal Na⁺ concentration, resulting in symptoms of oxidative damage, which are accompanied by a decrease in PHGPX, APX and CAT gene activity. The process leads to electrolyte leakage and ultimately cell death. Growing upon the same NaCl concentration, seedlings of the tolerant cultivar show maintenance of cellular intactness and display a significantly lower Na⁺ accumulation. The increase of antioxidative enzyme activity induced in parallel at low intracellular Na⁺ concentration represents a part of the complex salt tolerance mechanism. This could explain the ability of the tolerant foxtail millet cultivar to grow at higher NaCl concentrations than the sensitive one.

5. Materials and Methods

5.1 Methodology adopted for genomic studies in barley seed development and *seg8* mutant analysis

5.1.1 PLANT MATERIAL

Plants of *Hordeum vulgare* cv Barke, cv Bowman, the two-rowed barley spring cultivars, and the mutant *seg8* in Bowman background were grown in growth chambers at 20°C/18°C under 16 h light/8 h dark cycles. The developmental stage of the caryopses were determined in the mid-region of the ear as described by Weschke *et al.* (2000) and young developing seeds were harvested at 0, 2, 4, 6, 8, 10, 12 and 14 days after flowering (DAF). The developing caryopsis includes the maternal tissues, mostly pericarp and the filial tissues i.e. endosperm and embryo. The pericarp and embryo sac fraction were isolated by manual dissection. The tissue composition of the two fractions has been described (Sreenivasulu *et al.*, 2002).

5.1.2 EST IDENTIFICATION, ANNOTATION AND METABOLIC PATHWAY ASSIGNMENT

Based on the availability of resources generated at the Plant Genome Resource Centre, Institute of Plant Genetics and Crop Plant Research (IPK), Gatersleben, 6,319 EST sequences from developing caryopses (Michalek *et al.*, 2002) were considered for annotation. Sequence similarity searches against databases were conducted with HUSAR (Heidelberg Unix Sequence Analysis Resource) using BlastX2 and BlastN2 from release 2.09 of the Blast2 (www.ncbi.nlm.nih.gov/; Altschul *et al.*, 1997). The BLASTX2 searches were performed by recent releases of the Swissprot and Gene Bank databases. By using a PERL script (IPK, Pleisner K) we extracted the top hits of BLAST score, E-value, percent identity, percent similarity and position of the alignment of both 5' and 3' end sequences. We considered score value and alignment length from top hits to annotate ESTs into secure, putative and no assignment categories by length and score values (see Section 1.2.2 for criteria of categorization). Based on the putative gene identification by BLASTX results, we extracted EC numbers of all genes in the set belonging to metabolic pathways. For all the metabolic pathway analysis, we first collected information's from the plant data set of the KEGG database (<http://www.genome.ad.jp/kegg/metabolism.html>) and based on EC number the classification of ESTs were performed and assigned to the respective pathways. To classify regulatory genes, the ESTs were categorized based on sequence homology to regulatory genes

of the KEGG database. After annotation and functional classification of developing caryopses barley ESTs, the starch biosynthetic pathway and glycolytic pathway ESTs were identified in our collection and expression data was extracted from macroarrays for all the clones belonging to the respective pathways. For an estimation of the number of unique genes represented on the array we used the results from a cluster analysis of a larger set of ESTs (Michalek et al. 2002) produced by using Stack Pack (Miller *et al.*, 1999).

5.1.3 MACROARRAY PREPARATION

5.1.3.1 Selection of cDNA clones: The cDNA clones (plasmid DNA) specific for developing barley caryopsis were obtained from the EST collection of the IPK plant genome resources centre (Michalek *et al.*, 2002). In the initial phase of this work 711 clones were used for array preparation. Clones were mostly selected from a cDNA library of developing caryopses (517 clones). A smaller number of clones were selected from a library of etiolated seedlings (73 clones) and roots (104 clones), giving a total of 691 and some additional fragments for internal control. In selecting the clones from the cDNA library of etiolated seedlings and roots, special emphasis was given to the carbohydrate metabolism and stress genes. In a second extended program, 1440 clones were used for macroarray preparation. Clones were selected preferentially from a cDNA library of developing caryopsis (1235 clones). Additionally, clones specific for etiolated seedlings (73 clones) and roots (104 clones), which were used in the 711 array were included, giving a total of 1412 and some additional internal control (same EST amplified independently or different EST clones coding for the same gene). All those sequences except a few of minor quality have been deposited in the EMBL sequence database and can also be obtained from a web-server at the IPK (<http://www.pgrc.ipk-gatersleben.de>).

5.1.3.2 Amplification of cDNA inserts: Inserts of cDNA clones (plasmid DNA) were amplified by PCR using slightly modified M13 universal (5'-CGACGTTGTAAAACGACGGCCA) and reverse primers (5'-ACAGGAAACAGCTATGACCTTG) complementary to vector sequences flanking the cDNA inserts. For each cDNA clone, about 5 ng of plasmid DNA was used as template in a 50µl PCR reaction mix containing 10 mM Tris HCl [tris(hydroxymethyl)aminomethane] (pH 9.0), 50mM KCl, 1.5 mM MgCl₂, 0.2 mM of each deoxynucleotide, 1µM of each primer, and 0.6 units of Taq polymerase (Amplitaq Gold). Inserts were amplified (Master Cycler Gradient, Eppendorf, Hamburg, Germany) by using an amplification programme of 1 min denaturation at 94°C and 30 cycles of 30 s at 94°C,

followed by 30 s at 58°C and 2 min at 72°C. 5 µl of each reaction were separated on a 1.5 % agarose gel to evaluate the quality of amplicons. PCR reactions, which yield more than one fragment or resulted in low amounts of product, were repeated at slightly altered annealing temperature. After purification on QIA-quick columns according to the manufacturers protocol (Qiagen, Hilden, Germany) amplification products were again analysed on 1.5% agarose gels to estimate their DNA content and adjusted between 2.0 and 1.8.

5.1.3.3 Spotting of cDNA fragments: Concentration-adjusted PCR products were diluted 1:1 with 1 M NaOH, 5 M NaCl and deposited in duplicates on positively charged 5 x 9 cm nylon membranes (BiodyneB, Pall, Dreieich, Germany) by using a BioGrid robot equipped with spotting pins of 0.4 mm diameter (Biorobotics, Cambridge, UK). Three strokes with the spotting tool were used to transfer approximately 15 nl from each PCR product to the nylon membrane. After spotting was completed, the membranes were washed in 0.4 M NaOH, 1.5 M NaCl, neutralized in 0.5 M Tris, pH 7.5, 1.5 M NaCl and the DNA cross-linked to their surface by a brief UV treatment (120 mJ, Stratalinker, Stratagene, La Jolla, CA, USA). After washing in 2 x SSC arrays were dried for 1 h at 80°C and stored at room temperature until further use.

5.1.4 RNA EXTRACTION AND SYNTHESIS OF ³³P-LABELLED cDNA PROBES

100 – 200 mg of the pericarp and embryo sac fraction were prepared from Barke, Bowman and *seg8* caryopses by hand dissection and used to prepare total RNA as described by Heim *et al.* (1993). For synthesis of ³³P-labelled cDNA, polyA⁺-RNA was extracted from 35 µg of total RNA using oligo(dT)-magnetic beads (Dynal, Hamburg, Germany) according to the manufacturers recommendations. PolyA⁺-RNA bound to the magnetic beads was used directly for synthesis of a covalently bound first strand cDNA library using Superscript reverse transcriptase (Life Technologies, Karlsruhe, Germany). ³³P-labelled second strand cDNA free of unincorporated ³³P-dCTP was obtained through a random priming reaction (Megaprime Labelling Kit, Amersham Pharmacia, Freiburg, Germany) with an increased amount of Klenow polymerase (10 units). After removal of the supernatant, ³³P-labelled cDNA was eluted from the magnetic beads in 50 µl 2 mM EDTA by denaturation (3 min, 95°C) and filtered using a micro-centrifuge tube filter with a 0.2 µm Anapore membrane (Whatman, Göttingen, Germany).

5.1.5 PROCEDURE FOR cDNA MACROARRAY HYBRIDIZATION

Before the first hybridization experiment with labelled cDNA, every cDNA array was cycled through a mock hybridization including a probe removal procedure to detach loosely bound spotted DNA. After wetting the array in 2 x SSC, it was pre-hybridized for at least 3 h at 65°C in Church buffer (0.5 M sodium phosphate, pH 7.2, 7% (w/v) SDS, 1% (w/v) BSA, 1 mM EDTA) containing sheared salmon sperm DNA (10 µg/ml). Heat denatured (3 min, 95°C), labelled cDNA was added together with fresh hybridization buffer, and the filter was hybridized at 65°C for at least 12 h. cDNA arrays were washed three times with 40 mM sodium phosphate pH 7.2, 0.1% (w/v) SDS, 2 mM EDTA for 20 min at 65°C, wrapped in Saran wrap and exposed to an image plate of a Fuji BAS2000 phosphoimager (Fuji Photo Film Co., Tokyo, Japan) from 2 – 4 h. Labelled probes were completely removed from the filter by successive treatments with boiling washing solution, an alkaline treatment (0.4 M NaOH) for 15 min at 45°C and a neutralization reaction in 0.1 × SSC; 0.1 % (w/v) SDS; 0.2 M Tris HCl, pH 7.5. Successful removal of the labelled probe was controlled by long exposure (at least 4 h) of the array to an image plate.

5.1.6 ARRAY EVALUATION

The image data obtained from the phosphoimager were imported into the program package Array Vision (Imaging Research, St. Catharinas, Ontario, Canada) for spot detection and quantification of hybridization signals. Local background was subtracted from spot intensities and signal intensity of the duplicated spots for each cDNA fragment was averaged. In 711-macroarray, the signal intensities were normalized with respect to the total amount of radioactivity bound to the array and the signal intensities of the two spots representing each amplified cDNA fragment were averaged. To allow comparison of signal intensities across experiments in 1412-macroarray, the median of the logarithmically scaled intensity distribution for each experiment was set to zero (median centering of arrays, Eisen *et al.*, 1998). This procedure usually yields similar results like the previously used normalization (711 array) based on the total signal of an array, but improves the comparison of experiments with somewhat higher background values. Thereafter, the logarithmically scaled signal intensities of each gene was centered by its median across all experiments (median centering of genes, Eisen *et al.*, 1998), which emphasize the differential expression of genes irrespective of absolute signal intensities. These two procedures were repeated four more times and the resulting values were used for all clustering algorithms in J-Express (Disvik *et al.*, 2001). Since median centering of genes does not yield information about signal intensity,

we used the data after the first round of median centering of arrays to calculate non-logarithmic, normalized signal intensities. These normalized signal intensities were used to exclude genes with low signal intensities across all experiments for a more detailed analysis (see Results).

5.1.7 DATA FILTERING

For further analysis of the 1412 cDNA array analysis in “Barke” seed development, the complete dataset was reduced to cDNA fragments, which show differential expression across the experiments. Those cDNA fragments were selected based on two criteria. (1) To exclude cDNA fragments with signals always close to the background the normalized non-logarithmic signal intensity should exceed 3 arbitrary units (au) for at least one experiment. This value was compared with the normalized average background of 0.3 au and the maximal signal of 433 au. (2) The ratio between the minimal and the maximal signal for a cDNA fragment across all experiments had to exceed the factor of 10. The data set filtered in this way comprised 337 cDNA fragments, which fulfill both criteria.

5.1.8 CLUSTERING ALGORITHMS

The goal of clustering is to group together genes (objects) with similar properties. J-Express provides a comprehensive set of clustering methods and informative visualizations. Hierarchical clustering and k-mean clustering (Eisen *et al.*, 1998) tools of J-express software (Disvik *et al.*, 2001) were used for clustering the expression profiles.

5.1.8.1 Usage of J-Express: The normalized array data from different experiments were loaded as text files (tab delimited in a spreadsheet format), which allow selection of rows (expression values) and columns (gene identity) of every gene in a series of experiments. The feeded data file can be subjected to one of the analysis methods such as standard hierarchical and k-mean clustering. It represents a graphical user interface that integrates a number of viewing capabilities.

5.1.9 NORTHERN BLOTTING

Total RNA prepared from pericarp and embryo sac tissues of developing caryopses (0-8 DAF) harvested in two-day intervals was separated on a 1% agarose gel containing 15% formaldehyde and blotted overnight onto HybondN⁺ membranes (Amersham Pharmacia, Freiburg, Germany). Various fragments obtained by enzymatic digestions, which excluded

the polyA tail from the cDNAs, were used as probes after labelling with [³²P]dCTP. Membranes were sequentially hybridized with the following probes derived from cDNA clones: HY09N16 (*HvSUS2*) - a 312bp PCR-amplified sequence of the 3'-untranslated region (UTR); HY03B06 (putative transcription factor *FIL*) - a 412bp PstI-fragment; HW02F11 (vacuolar invertase) - a 283 PCR-amplified sequence of the 3'-UTR; HY09L21 (unknown gene called NucPro) - a 1.2kb DraI/PvuI fragment. Hybridizations were performed at 65°C, and the filters were washed at high stringency according to Church and Gilbert (1984). Signals on filters were quantified using a Fuji-BAS phosphoimager (Fuji Photo Film C., Tokyo, Japan). Loading of total RNA in each lane was monitored using a 26S rDNA probe (data not shown).

5.1.10 EXTRACTION AND DETERMINATION OF METABOLIC INTERMEDIATES

Frozen material (*seg8* and wild type caryopses) was extracted with trichloroacetic acid (Herbers *et al.*, 1997). Sugars including standards were determined by ion chromatography (DX-500, Dionex, USA) with pulsed amperometric detection. Separation was carried out on a Carbo-Pac PA1 column (4 x 250 mm) at 25 °C. Purest HPLC water and 0.3 M NaOH were used as eluents A (NaH₂PO₄/Na₂HPO₄, 1:1 molar ratio, 25 mM, pH 2.8) and B (NaH₂PO₄/Na₂HPO₄, 1:1 molar ratio, 125 mM, pH 2.9) respectively. The column was equilibrated with 3 % buffer A at a flow rate of 1 ml per minute. The gradient was produced by the following concentration changes: 15 min 25 % B, 18 min 35 % B, 24 min 83 % B, hold 83 % B for 6 min, return to 3 % B in 2 min. Nucleotides and nucleotide sugars were determined by ion chromatography (DX-500). Separation was carried out on a Vydac 302 IC column (4.6 x 250 mm) at 25 °C and the eluted sugars were photometrically detected at 260 nm. The column was equilibrated with buffer A at a flow rate of 2 ml per minute. The gradient was accomplished with buffer A (NaH₂PO₄/Na₂HPO₄, 1:1 molar ratio, 25 mM, pH 2.8) and buffer B (NaH₂PO₄/Na₂HPO₄, 1:1 molar ratio, 125 mM, pH 2.9). The gradient was produced by the following concentration changes: 2 min 0 % B, 9 min 11 % B, 18 min 100 % B, hold 100 % B for 2 min, return to 0 % B in 1 min.

5.1.11 DETERMINATION OF STARCH

Seeds from *seg8* and wild type plants were freeze-dried and pulverized in a mortar-pestle. Soluble carbohydrates were extracted in 80% ethanol at 80°C for 1 h. After centrifugation, the supernatant was evaporated and dissolved in sterile water for enzymatic carbohydrate determination (Boeringer Mannheim, Germany). The remaining insoluble material was used

for starch determination after solubilising in 1 N KOH and hydrolysis with amyloglucosidase (Heim *et al.*, 1993).

5.2 Methodology adopted for salinity response studies in foxtail millet

5.2.1 PLANT MATERIAL AND SALINITY TREATMENTS

Seeds of foxtail millet (*Setaria italica* L.) cvs. Prasad (salt-tolerant) and Lepakshi (salt-sensitive) were procured from Andhra Pradesh Agricultural Experimental Station, Anantapur, India. Seeds were surface sterilized with 0.1% (w/v) sodium hypo chlorite solution for 5 min, thoroughly rinsed with distilled water and allowed to germinate on filter paper in petri dishes. Seeds were supplied with Hoagland medium supplemented with 0, 50, 100, 150, 200 and 250 mM NaCl. The Petri dishes were incubated at 25°C under aseptic conditions for 5 days in the dark.

5.2.2 GROWTH MEASUREMENTS

The length of the primary shoot was measured for 100 seedlings (5-day-old) from each cultivar grown under control conditions (without NaCl) and different salt concentrations (50, 100, 150, 200 mM NaCl) in three independent experiments. The percentage of relative shoot growth inhibition was calculated from the mean shoot length measurements.

5.2.3 DETERMINATION OF SODIUM CONTENT

Sodium content was determined as described by Dionisio-Sese and Tobita, (1998). Dried seedlings (10 mg) were chopped into pieces of 5 mm length and placed in test tubes containing 20 ml distilled deionized water. The tubes were incubated in boiling water for 1 h and autoclaved at 121°C for 20 min and cooled. The sodium content was determined by using an atomic absorption spectrophotometer (AA-660, Shimadzu; Tokyo, Japan).

5.2.4 ELECTROLYTE LEAKAGE

Electrolyte leakage was determined as described by Dionisio-Sese and Tobita, (1998). Fresh seedlings (200 mg) were cut into pieces of 5 mm length and placed in test tubes containing 10 ml distilled deionized water. The tubes were incubated in a water bath at 32°C for 2 h and the initial electrical conductivity of the medium (EC₁) was measured. Afterwards, the samples were autoclaved at 121°C for 20 min to release all electrolytes. Samples were then cooled to 25°C and the final electrical conductivity (EC₂) was measured. The electrolyte leakage (EL) was calculated by using the formula $EL = EC_1/EC_2 \times 100$.

5.2.5 ESTIMATION OF MALONALDEHYDE (MDA) CONCENTRATION

The MDA content in 5-day-old seedlings was determined by the thio barbituric acid (TBA) reaction as described by Heath and Packer (1968). 100 mg fresh weight of seedlings were homogenised in 500µl of 0.1% (W/V) TCA. The homogenate was centrifuged at 9,000 x g for 5 min and 4 ml of 20% TCA containing 0.5% (W/V) TBA was added to 1 ml of the supernatant. The mixture was incubated at 95°C for 30 min and then quickly chilled on ice. The contents were centrifuged at 9,000 x g for 15 min and the absorbance was measured at 532 nm in a Shimadzu 1601 spectrophotometer. The concentration of MDA was calculated using the MDA extinction coefficient ($155 \text{ mM}^{-1} \text{ cm}^{-1}$).

5.2.6 cDNA ARRAYS

5.2.6.1 Array design: Barley EST's derived from cDNA libraries of developing caryopsis, roots and etiolated seedlings were used to create a cDNA array (Sreenivasulu *et al.*, 2002; materials and methods, section 5.1.3). Among the set of cDNA fragments, approximately 58 stress-related genes are included.

5.2.6.2 Synthesis of ^{33}P hybridization cDNA probe, hybridization and data normalization:

For synthesis of ^{33}P -labelled cDNA probe, 35µg of total RNA was extracted from 5-day-old seedlings of control tolerant, 250 mM NaCl treated tolerant, control sensitive and 250 mM NaCl treated sensitive seedlings. Preparation of ^{33}P -labelled second strand cDNA probes as well as the hybridization procedure has been described previously in the materials and methods (section 5.1.4 and 5.1.5). Pre-hybridization and hybridization was carried out at 60°C. The cDNA arrays were washed three times with 40 mM sodium phosphate pH7.2, 1% SDS, 2mM EDTA for 30 min at 60°C and exposed to the imaging plate of a Fuji BAS2000 phosphoimager (Fuji Photo Film, Tokyo, Japan) for 6 hr. The image data were imported into the program package Array vision (Imaging Research, St. Catharine's Ont., Canada) for spot detection and quantification of hybridization signals. The signal intensities were normalized with respect to the total amount of radioactivity bound to the array.

5.2.7 RT-PCR MEDIATED CLONING OF PHGPX cDNA

Total RNA from salt-tolerant and salt-sensitive seedlings treated with 250 mM NaCl was isolated as described by Heim *et al.*, (1993). RT-PCR was performed under standard conditions using an oligo d(T) primer for amplification of mRNA, followed by a PCR with two combinations of degenerated primers (forward: 5'-GTBAAYGTYGCHMARTGTG-3' / reverse 1: 5'-

TTRTCAAYMARRAAYTTRGWR AAG-3' , reverse 2: 5'-CRGCYTTRAADCKWGTGC-3'), which were designed on conserved regions of known PHGPX genes. A cDNA library from salt-treated seedlings of tolerant foxtail millet (5-day-old) was constructed using the ZAP express cDNA synthesis kit (Stratagene) and screened under low stringency conditions using the $\alpha^{32}\text{P}$ -labelled cDNA fragment (316 bp) obtained by RT-PCR.

5.2.8 SOUTHERN HYBRIDIZATION

Genomic DNA from seedlings was isolated, 10 μg of DNA was digested with BamHI, EcoRI, HindIII, PvuII and XhoI and separated on a 1% agarose gel. The gel was blotted overnight onto a Hybond-N⁺ nylon membrane (Amersham Braunschweig, Germany). The 316 bp RT-PCR PHGPX fragment of the millet was used as probe after labelling with [α -³²P]dCTP. Hybridizations were performed at 65°C, and the filter was washed twice with 2xSSPE / 0.1% SDS, twice with 1xSSC/ 0.1% SDS, and once with 0.5xSSC/0.1% SDS at 65°C for 15 min each.

5.2.9 NORTHERN BLOT ANALYSIS

RNA isolation and gel blot analysis were performed as described in the materials and methods (section 5.1.9). Filters were hybridized to the ³²P-labelled PCR fragment of the PHGPX gene as probe at 55°C according to the method of Church and Gilbert, (1984). The hybridization signals were quantified using the Bio Image Analyser BAS 2000 (Fuji Photo Film Co., Tokyo, Japan). To check the amount of total RNA loaded on each lane, filters were rehybridized with a ³²P-labelled 26S rRNA fragment of potato.

5.2.10 CHARACTERIZATION OF THE SALT-INDUCED 25kD PROTEIN

5.2.10.1 Protein extraction and estimation of protein content: Five-day-old seedlings (100 mg) of both cultivars grown at 250 mM NaCl and control conditions were ground to a fine powder with liquid nitrogen and homogenized with ice-cold 50 mM Tris-HCl buffer (pH 7.4). The extracts were centrifuged for 20 min at 8,000 g at 4°C. Protein concentration was determined by the Dye-binding assay (Bradford, 1976) using bovine serum albumin (BSA) as standard.

5.2.10.2 SDS-PAGE analysis: An equal amount of each protein sample (35 μg) was loaded on 12-15% gradient SDS-PAGE gel. After running, the gels were stained with silver nitrate solution for protein detection (Laemmli, 1970).

5.2.10.3 Purification of 25 kD protein: Five-day-old seedlings (5 g) of the tolerant cultivar grown at 250 mM NaCl were homogenized in liquid nitrogen and extracted with 50 mM Tris-HCl buffer (pH 7.4), containing 1 mM ethylenediamine tetra-acetic acid (EDTA), 2mM phenylmethylsulphonyl fluoride (PMSF), 0.6% insoluble polyvinylpyrrolidone (PVP) and 0.5 M sucrose. The homogenate was filtered through a nylon sieve (40 μ m) and centrifuged at 8,000 g for 10 min. A DEAE-Sepharose (Sigma) column (bed: 10 x 2.5 cm) was pre-equilibrated with Tris-HCl buffer (50 mM pH 7.2) and the supernatant containing proteins were subjected for ion-exchange chromatography. The sample was eluted through a NaCl step-gradient (0.2, 0.4, 0.6, 0.8 and 1.0 M) and 1 ml fractions were collected. The absorbance of each fraction was monitored at 280 nm and total peroxidase activity was determined. The fractions number 12-18 containing peroxidases were pooled, lyophilised and subjected to FPLC (Superose) to achieve higher purity. The column was pre-equilibrated and eluted with PBS buffer (pH 7.4) as flow-through. The salt-induced 25 kD protein defined by the major peak was collected and purified to the maximum extent.

5.2.10.4 Amino acid sequencing: The purified protein (salt-induced 25 kD protein) was electrophorated on a 12% SDS-PAGE (Laemmli, 1970) and electroblotted onto polyvinylidene difluoride (PVDF) membrane (Millipore) using the Multiphor II (LKB, Pharmacia) electrophoretic transfer apparatus according to the manufacturer's protocol. 10 mM 3-[cyclohexylamino]-1-propane-sulphonic acid (CAPS; pH 11) was used as transfer buffer. The membrane was stained by coomassie blue, and that part of the membrane containing the purified protein was subjected to the sequencer LF3400 (Beckman Instruments Fullerton, Ca, USA).

References

- Adams MD, Dubnick M, Kerlavage AR, Moreno R, Kelley JM, Utterback TR, Nagle JW, Fields C, Venter JC** (1992) Sequence identification of 2,375 human brain genes. *Nature* **355**: 632-634.
- Adams S, Vinkenoog R, Spielman M, Dickinson HG, Scott RJ** (2000) Parent-of-origin effects on seed development in *Arabidopsis thaliana* require DNA methylation. *Development* **127**: 2493-2502.
- Ahn S, Tanksley SD** (1993) Comparative linkage maps of the rice and maize genomes. *Proc Natl Acad Sci USA* **90**: 7980-7984.
- Altschul SF, Madden TL, Schaffer AA, Zhang J, Zhang Z, Miller W, Lipman DJ** (1997) Gapped BLAST and PSI-BLAST: a new generation of protein database search programs. *Nucleic Acids Res* **25**: 3389-3402.
- Avsian-Kretchmer O, Eshdat Y, Gueta-Dahan Y, Ben-Hayyim G** (1999) Regulation of stress-induced phospholipid hydroperoxide glutathione peroxidase expression in citrus. *Planta* **209**: 469-477.
- Bairoch A, Apweiler R** (2000) The SWISS-PROT protein sequence database and its supplement TrEMBL in 2000. *Nucleic Acids Res* **28**: 45-48.
- Bateman A, Birney E, Cerruti L, Durbin R, Etwiller L, Eddy SR, Griffiths-Jones S, Howe KL, Marshall M, Sonnhammer ELL** (2002) The Pfam Protein Families Database *Nucleic Acids Res* **30**: 276-280.
- Beeor-Tzahar T, Ben-Hayyim G, Holland D, Faltin Z, Eshdat Y** (1995) A stress-associated citrus protein is a distinct plant phospholipid hydroperoxide glutathione peroxidase. *FEBS letters* **366**: 151-155.
- Ben-Hayyim G, Faltin Z, Gepstein S, Camoin L, Strosberg AD, Eshdat Y** (1993) Isolation and characterisation of salt-associated protein in citrus. *Plant Sci* **88**:129-140.
- Bhave MR, Lawrence S, Barton C, Hannah LC** (1990) Identification and molecular characterization of *Shrunken-2* cDNA clones of maize. *Plant Cell* **2**: 581-588.
- Boguski MS, Schuler GD** (1995) Establishing a human transcript map. *Nat Genet* **10**: 369-371.
- Bohnert HJ, Jensen RG** (1996) Metabolic engineering for increased salt tolerance. The next step. *Aust J Plant Physiol* **23**: 661-667.
- Bohnert HJ, Ayoubi P, Borchert C, Bressan RA, Burnap RL, Cushman JC, Cushman MA, Deyholos M, Fischer R, Galbraith DW, Hasegawa PM, Jenks M, Kawasaki S, Koiwa H, Kore-eda S, Lee BH, Michalowski CB, Misawa E, Nomura M, Ozturk N, Postier B, Prade R, Song CP, Tanaka Y, Wang H, Zhu JKA** (2001) Genomics approach towards salt stress tolerance. *Plant Physiol Biochem* **39**: 295-311.

- Boyer JS** (1982) Plant productivity and environment. *Science* **218**: 443-448.
- Borisjuk L, Walenta S, Rolletschek H, Mueller-Klieser W, Wobus U, Weber H** (2002a) Spatial analysis of plant metabolism: Sucrose imaging within *Vicia faba* cotyledons reveals specific developmental patterns. *Plant J* **29**: 521-530.
- Borisjuk L, Wang TL, Rolletschek H, Wobus U, Weber H** (2002b) A pea seed mutant affected in the differentiation of the embryonic epidermis is impaired in embryo growth and seed maturation. *Development* **129**: 1595-1607.
- Bosnes M, Weideman F, Olsen OA** (1992) Endosperm differentiation in barley wild-type and sex mutants. *Plant J* **2**: 661-674.
- Bowman JL, Smyth DR** (1999) CRABS CLAW, a gene that regulates carpel and nectary development in *Arabidopsis*, encodes a novel protein with zinc finger and helix-loop-helix domains. *Development* **126**: 2387-2396.
- Bradford MN** (1976) A rapid and sensitive method for the quantitation of microgram quantities of protein utilizing the principle of protein-dye binding. *Anal Biochem* **72**: 248-254.
- Brown RC, Lemon BE, Olsen OA** (1994) Endosperm development in barley: microtubule involvement in the morphogenetic pathway. *Plant Cell* **6**: 1241-1252.
- Bueno P, Piqueras A, Kurepa J, Savoure A, Verbruggen N, Van Montagu M, Inzé D** (1998) Expression of antioxidant enzymes in response to abscisic acid and high osmoticum in tobacco BY-2 cell cultures. *Plant Sci* **138**: 27-34.
- Chao S, Sharp PJ, Gale MD** (1988) A linkage map of wheat homeologous group 7 chromosomes using RFLP markers. In: Miller TE, Koebner RMD (eds) Proc 7th Int Wheat Genet Symp. Bath, UK, 493-498.
- Chaudhury AM, Ming L, Miller C, Craig S, Dennis ES, Peacock WJ** (1997) Fertilization-independent seed development in *Arabidopsis thaliana*. *Proc Natl Acad Sci USA* **94**: 4223-4228.
- Cheng W, Taliercio EW, Chourey PS** (1996) The *Miniature1* seed locus of maize encodes a cell wall invertase required for normal development of endosperm and maternal cells in the pedicel. *Plant Cell* **8**: 971-983.
- Christoffels A, Miller R, Hide W** (1999) STACK_PACK and STACK (Sequence Tag Alignment and Consensus Knowledgebase): A novel, comprehensive, hierarchical EST clustering and consensus generation and analysis system providing unique insight into the human genome. *American J Human Genet* **65**: 477.
- Chourey PS, Nelson OE** (1976) The enzymatic deficiency conditioned by the *shrunk-en-1* mutations in maize. *Biochem Genet* **14**: 1041-1055.
- Chu FF, Doroshov JH, Esworthy RS** (1993) Expression, characterization and tissue distribution of a new cellular selenium-dependent glutathione peroxidase, GSHPx-GI. *J Biol Chem* **268**: 2571-2576.

- Churin Y, Schilling S, Börner T** (1999) A gene family encoding glutathione peroxidase homologues in *Hordeum Vulgare* (barley). *FEBS letters* **459**: 33-38.
- Church GM, Gilbert W** (1984) Genomic sequencing. *Proc Natl Acad Sci USA* **81**: 1991-1995.
- Cowan AK, Cripps RF, Richings EW, Taylor NJ** (2001) Fruit size: Towards an understanding of the metabolic control of fruit growth using avocado as a model system. *Physiol Plant* **111**: 127-136.
- Cramer GR, Alberico GJ, Schmidt C** (1994) Salt tolerance is not associated with the sodium accumulation of two maize hybrids. *Aust J Plant Physiol* **21**: 675-692.
- Criqui M.C, Jamet E, Parmentier Y, Marbach J, Durr A, Fleck J** (1992) Isolation and characterization of plant cDNA showing homology to animal glutathione peroxidases. *Plant Mol Biol* **18**: 623-627.
- Cummins I, Cole DJ, Edwards R** (1999) A role for glutathione transferases functioning as glutathione peroxidases in resistance to multiple herbicides in black-grass. *Plant J* **18**: 285-292.
- Cushman JC, Bohnert HJ** (2000) Genomic approaches to plant stress tolerance. *Curr Opin Plant Biol* **3**: 117-124.
- Del Río LA, Sevilla F, Scandalio LM, Palma JM** (1991) Nutritional effect and expression of superoxide dismutases: Induction and gene expression diagnostics, prospective protection against oxygen toxicity. *Free Radical Res Commun* **12-13**: 819-828.
- Depège N, Drevet J, Boyer N** (1998) Molecular cloning and characterization of tomato cDNAs encoding glutathione peroxidase-like proteins. *European J Biochem* **253**: 445-451.
- Depège N, Varenne M, Boyer N** (2000) Induction of oxidative stress and GPX-like protein activation in tomato plants after mechanical stimulation. *Physiol Plant* **110**: 209-214.
- Desikan R, Mackerness SAH, Hancock JT, Neill SJ** (2001) Regulation of the *Arabidopsis* transcriptome by oxidative stress. *Plant Physiol* **127**: 159-172.
- Dionisio-Sese ML, Tobita S** (1998) Antioxidant responses of rice seedlings to salinity stress. *Plant Sci* **135**: 1-9.
- Disvik B, Jonassen I** (2001) J-Express: exploring gene expression data using Java. *Bioinformatics* **17**: 369-370.
- Djarot I, Peterson DM** (1991) Seed development in a shrunken endosperm barley mutant. *Ann Bot* **68**: 495-499.
- Doehlert DC, Felker FC** (1987) Characterization and distribution of invertase activity in developing maize (*zea mays*) kernels. *Physiol Plant* **70**: 51-57.

- Doehlert DC** (1990) Distribution of enzyme-activities within the developing maize (*zea mays*) kernel in relation to starch, oil and protein accumulation. *Physiol Plant* **78**: 560-567.
- Doehlert DC, Kuo TM** (1990) Sugar metabolism in developing kernels of starch-deficient endosperm mutants of maize. *Plant Physiol* **92**: 990-994.
- Eckermann C, Eichel J, Schroder J** (2000) Plant methionine synthase: New insights into properties and expression. *Biol Chem* **381**: 695-703.
- Eichel J, Gonzalez JC, Hotze M, Matthews RG, Schroder J** (1995) Vitamin-B-12-independent methionine synthase from a higher-plant (*Catharanthus roseus*) – Molecular characterization, regulation, heterologous expression and enzyme properties. *European J Biochem* **230**: 1053-1058.
- Eisen MB, Spellman PT, Brown PO, Botstein D** (1998) Cluster analysis and display of genome-wide expression patterns. *Proc Natl Acad Sci USA* **95**: 14863-14868.
- Eshdat Y, Holland D, Faltin Z, Ben-Hayyim G** (1997) Plant glutathione peroxidases. *Physiol Plant* **100**: 234-240.
- Felker FC, Peterson DM, Nelson OE** (1985) Anatomy of immature grains of eight maternal effect shrunken endosperm barley mutants. *American J Bot* **72**: 248-256.
- Falquet L, Pagni M, Bucher P, Hulo N, Sigrist CJA, Hofmann K, Bairoch A** (2002) The PROSITE database, its status in 2002. *Nucleic Acids Res* **30**: 235-238.
- Flohé L, Günzler WA** (1984) Assays of glutathione peroxidase. *Methods Enzym* **105**: 114-121.
- Foyer CH, Descourvieres P, Kunert KJ** (1994) Protection against oxygen radicals: an important defence mechanism studied in transgenic plants. *Plant Cell Environ* **17**: 507-523.
- Girke T, Todd J, Ruska S, White J, Benning C, Ohlrogge J** (2000) Microarray analysis of developing *Arabidopsis* seeds. *Plant Physiol* **124**: 1570-1581.
- Gossett DG, Millhollon EP, Lucas MC** (1994) Antioxidant response to NaCl stress in salt-tolerant and salt-sensitive cultivars of cotton. *Crop Sci* **34**: 706-714.
- Goto S, Bono H, Ogata H, Fujibuchi T, Nishioka T, Sato K, Kanehisa M** (1997) *Proc Pacific Symp On Biocomputing World Scientific, Singapore*. 175-186.
- Grimes HD, Tranbarger TJ, Franceschi VR** (1993) Expression and accumulation patterns of nitrogen-responsive lipoxygenase in soybeans. *Plant Physiol* **103**: 457-466.
- Gueta-Dahan Y, Yaniv Z, Zilinskas BA, Ben-Hayyim G** (1997) Salt and oxidative stress: similar and specific responses and their relation to salt tolerance in citrus. *Planta* **203**: 460-469.

- Guerasimova A, Nyarsik L, Girnus I, Steinfath M, Wruck W, Griffiths H, Herwig R, Wierling CO, Brien J, Eickhoff H, Lehrach H, Radelof U** (2001) New tools for oligonucleotide fingerprinting. *Biotechniques* **31**: 490-495.
- Gupta PK, Roy JK Prasad M** (1999) DNA chips, microarrays and genomics. *Curr Sci* **77**: 875-884.
- Halliwell B, Gutteridge JMC** (1989) *Free radicals in biology and medicine*, London: Oxford University Press.
- Hannah LC, Nelson OE** (1976) Characterization of ADP-glucose pyrophosphorylase from *shrunk-2 and brittle-2* mutants of maize. *Biochem Genet* **14**: 547-560.
- Harrison CJ, Hedley CL, Wang TL** (1998) Evidence that the *rug3* locus of pea (*Pisum sativum* L.) encodes plastidial phosphoglucomutase confirms that the imported substrate for starch synthesis in pea amyloplasts is glucose-6-phosphate. *Plant J* **13**: 753-762.
- Hasegawa M, Bressan A, Zhu JK, Bohnert HJ** (2000) Plant cellular and molecular responses to high salinity. *Annu Rev Plant Physiol Plant Mol Biol* **51**: 463-499.
- Hattori T, Nakagawa S, Nakamura K** (1990) High-level expression of tuberous root storage protein genes of sweet potato in stems of plantlets grown *in vitro* on sucrose medium. *Plant Mol Biol* **14**: 595-604.
- Heath RL, Packer L** (1968) Photoperoxidation in isolated chloroplasts. 1. Kinetics and stoichiometry of fattyacid peroxidation. *Arch Biochem Biophys* **125**: 189-198.
- Heim U, Weber H, Bäumlein H, Wobus U** (1993) A sucrose-synthase gene of *Vicia faba* L: Expression pattern in developing seeds in relation to starch synthesis and metabolic regulation. *Planta* **191**: 394-401.
- Herbers K, Meuwly P, Frommer WB, Metraux JP, Sonnewald U** (1996) Systemic acquired resistance mediated by the ectopic expression of invertase: Possible hexose sensing in the secretory pathway. *Plant Cell* **8**: 793-803.
- Herbers K, Tacke E, Hazirezaei M, Krause KP, Melzer M, Rohde W, Sonnewald U** (1997) Expression of a luteoviral movement protein in transgenic plants leads to carbohydrate accumulation and reduced photosynthetic capacity in source leaves. *Plant J* **2**: 1045-1056.
- Hernandez JA, Corpas FJ, Gomez M, de Rio LA, Sevilla F** (1993) Salt-induced oxidative stress mediated by activated oxygen species in pea leaf mitochondria. *Physiol Plant* **89**: 103-110.
- Hernández JA, Jiménez A, Mullineaux P, Sevilla F** (2000) Tolerance of pea (*Pisum sativum* L.) to long-term salt stress is associated with induction of antioxidant defences. *Plant Cell Environ* **23**: 853-862.
- Herwig R, Aanstad P, Clark M, Lehrach H** (2001) Statistical evaluation of differential expression on cDNA nylon arrays with replicated experiments. *Nucleic Acids Res* **29**: 1-9.

- Hofestädt R, Scholz U** (1998) Information processing for the analysis of metabolic pathways and inborn errors. *Biosystems* **47**: 91-102.
- Holland D, Ben-Hayyim G, Faltin Z, Camoin L, Strosberg AD, Eshdat Y** (1993) Molecular characterisation of salt-stress-associated protein in citrus: protein and cDNA sequence homology to mammalian glutathione peroxidase. *Plant Mol Biol* **21**: 923-927.
- Houlgatte R, Mariage-Samson R, Duprat S, Tessier A, Bentolilal S, Lamy B, Aufray C** (1995) The genexpress index – A resource for gene discovery and the genic map of the human genome. *Genome Res* **5**: 272-304.
- Huang XQ, Madan A** (1999) CAP3: A DNA sequence assembly program. *Genome Res* **9**: 868-877.
- Jarvi AJ, Eslick RF** (1975) Shrunken endosperm mutants in barley. *Crop Sci* **15**: 363-366.
- Kawasaki S, Borchert C, Deyholos M, Wang H, Brazille S, Kawai K, Galbraith D, Bohnert HJ** (2001) Gene expression profiles during the initial phase of salt stress in rice. *Plant Cell* **13**: 889-905.
- Koch KE** (1996) Carbohydrate-modulated gene expression in plants. *Ann Rev Plant Physiol Plant Mol Biol* **47**: 509-540.
- Kohchi T, Fujisige K, Ohyama K** (1995) Construction of an equalized cDNA library from *Arabidopsis thaliana*. *Plant J* **8**: 771-776.
- Koßmann J, Visser RGF, Müller-Röber BT, Willmitzer L, Sonnewald U** (1991) Cloning and expression analysis of a potato cDNA that encodes branching enzyme: evidence for coexpression of starch biosynthetic genes. *Mol Gen Genet* **230**: 39-44.
- Laemmli UK** (1970) Cleavage of structural proteins during the assembly of the head of bacteriophage T4. *Nature* **227**: 680-685.
- Leprince O, Harren FJ, Buitink J, Alberda M, Hoekstra FA** (2000) Metabolic dysfunction and unabated respiration precede the loss of membrane integrity during dehydration of germinating radicles. *Plant Physiol* **122**: 597-608.
- Levine A, Tenhaken R, Dixon R, Lamb C** (1994) H₂O₂ from oxidative burst orchestrates the plant hypersensitive disease resistance response. *Cell* **79**: 583-593.
- Li W, Feng H, Fan J, Zhang R, Zhao N, Liu J** (2000) Molecular cloning and expression of a phospholipid hydroperoxide glutathione peroxidase homolog in *Oryza sativa*. *Biochim Biophys Acta* **1493**: 225-230.
- Lindorff-Larsen K, Winther JR** (2001) Surprisingly high stability of barley lipid transfer protein, LTP1, towards denaturant, heat and proteases. *FEBS letters* **488**: 145-148.
- Maheshwari P** (1950) An introduction to the embryology of angiosperms. McGraw-Hill, New York, NY.

- Maitz M, Santandrea G, Zhang Z, Lal S, Hannah C, Salamini F, Thompson RD** (2000) *rgf1*, a mutation reducing grain filling in maize through effects on basal endosperm and pedicel development. *Plant J* **23**: 29-42.
- McDonald AML, Stark JR, Morrison WR, Ellis RP** (1991) The composition of starch granules from developing barley genotypes. *J cereal sci* **13**: 93-112.
- Michal G** (1993) (Ed.), *Biochemical Pathways*. Boehringer Mannheim, Germany.
- Michalek W, Weschke W, Pleissner KP, Graner A** (2002) EST analysis in barley defines a unigene set comprising 4,000 genes. *Theor Appl Genet* **104**: 97-103.
- Miller ME, Chourey PS** (1992) The maize invertase-deficient *miniature-1* seed mutation is associated with aberrant pedicel and endosperm development. *Plant Cell* **4**: 297-305.
- Miller RT, Christoffels AG, Gopalakrishnan C, Burke J, Ptitsyn AA, Broveak TR, Hide WA** (1999) A comprehensive approach to clustering of expressed human gene sequence: The sequence tag alignment and consensus knowledge base. *Genome Res* **9**: 1143-1155.
- Mita S, Suzuki-Fujii K, Nakamura K** (1995) Sugar-inducible expression of a gene for β -amylase in *Arabidopsis thaliana*. *Plant Physiol* **107**: 895-904.
- Miyamoto Y** (2000) *Trends Glycosc Gly* **12**: 351-360.
- Murray DR** (1987) Nutritive role of seed coats in developing legume seeds. *American J Bot* **74**: 1122-1137.
- Müller-Röber BT, Koßmann J, Hannah LC, Willmitzer L, Sonnewald U** (1990) One of two different ADP-glucose pyrophosphorylase genes from potato responds strongly to elevated levels of sucrose. *Mol Gen Genet* **224**: 136-146.
- Mullineaux MP, Karpinski S, Jiménez A, Cleary SP, Robinson C, Creissen GP** (1998) Identification of cDNAs encoding plastid-targeted glutathione peroxidase. *Plant J* **13**: 375-379.
- Noctor G, Foyer C** (1998) Ascorbate and glutathione: keeping active oxygen under control. *Ann Rev Plant Physiol Plant Mol Biol* **49**: 249-279.
- Ohlrogge J, Benning C** (2000) Unraveling plant metabolism by EST analysis. *Curr Opin Plant Biol* **3**: 224-228.
- Ohto M, Hayashi K, Isobe M, Nakamura K** (1995) Involvement of Ca^{2+} - signalling in the sugar-inducible expression of genes coding for sporamin and β -amylase of sweet potato. *Plant J* **7**: 297-307.
- Olmos E, Hernandez JA, Sevilla F, Hellin E** (1994) Induction of several antioxidant enzymes in the selection of a salt-tolerant cell line of *Pisum sativum*. *J Plant Physiol* **144**: 594-598.
- Olsen OA, Potter RH, Kalla R** (1992) Histo-differentiation and molecular biology of developing cereal endosperm. *Seed Sci Res* **2**: 117-131.

- Paterson AH, Lin Y-R, Li Z, Schertz KF, Doebley JF, Pinson SRM, Liu S-C, Stansel JW, Irvine JE** (1995) Convergent domestication of cereal crops by independent mutations at corresponding genetic loci. *Science* **269**: 1714-1718.
- Patrick JW, Offler CE** (1995) Post-sieve element transport of sucrose in developing seeds. *Australian J Plant Physiol* **22**: 681-702.
- Patrick JW** (1997) Phloem unloading: Sieve element unloading and post-sieve element transport *Ann Rev Plant Physiol* **48**: 191-222.
- Patrick JW and Offler CE** (2001) Compartmentation of transport and transfer events in developing seeds. *J Exper Bot* **52**: 551-564.
- Pego JV, Smeekens SCM** (2000) Plant fructokinases: a sweet family get-together. *Trends Plant Sci* **5**: 531-536.
- Potokina E, Sreenivasulu N, Altschmied L, Michalek W, Graner A** (2002) Differential gene expression during seed germination in barley (*Horedum vulgare* L.) *Funct Integr Genomics* **2**: 28-39.
- Ramage RT, Crandall CR** (1981) Shrunken endosperm mutant *seg8*. *Barley Genet Newslett* **11**: 34.
- Ramage RT** (1983) Chromosome location of shrunken endosperm mutants *seg6g* and *seg8k*. *Barley Genet Newslett* **13**: 64-65.
- Richmond T, Somerville S** (2000) Chasing the dream: plant EST microarrays. *Curr Opin Plant Biol* **3**: 108-116.
- Ritchie S, Swanson SJ, Gilroy S** (2000) Physiology of the aleurone layer and starchy endosperm during grain development and early seedling growth: new insights from cell and molecular biology. *Seed Sci Res* **10**: 193-212.
- Rounsley SD, Glodek A, Sutton G, Adams MD, Somerville CR, Venter JC, Kerlavage AR** (1996) The construction of *Arabidopsis* expressed sequence tag assemblies - A new resource to facilitate gene identification. *Plant Physiol* **112**: 1177-1183.
- Sadka A, Dewald DB, May GD, Park WD, Mullet JE** (1994) Phosphate modulates transcription of soybean *vspB* and other sugar-inducible genes. *Plant Cell* **6**: 737-749.
- Schaffer AA, Petreikov M** (1997) Inhibition of fructokinase and sucrose synthase by cytosolic levels of fructose in young tomato fruit undergoing transient starch synthesis. *Physiol Plant* **101**: 800-806.
- Schena M, Shalon D, Davis RW, Brown PO** (1995) Quantitative monitoring of gene-expression patterns with a complementary-DNA microarray. *Science* **270**: 467-470.

- Schoof H, Zaccaria P, Gundlach H, Lemcke K, Rudd S, Kolesov G, Arnold R, Schomburg I, Chang A, Schomburg D** (2002) BRENDA, enzyme data and metabolic information. *Nucleic Acids Res* **30**: 47-49.
- Schomburg I, Chang AJ, Hofmann O, Ebeling C, Ehrentreich F, Schomburg D** (2002) BRENDA: a resource for enzyme data and metabolic information. *Trends Biochem Sci* **27**: 54-56.
- Schulman AH, Ahokas H** (1990) A novel shrunken endosperm mutant of barley. *Physiol Plant* **78**: 583-589.
- Sen-Gupta A, Webb RP, Holladay AS, Allen RD** (1993) Overexpression of superoxide dismutase protects plants from oxidative stress. Induction of ascorbate peroxidase in superoxide dismutase overexpressing plants. *Plant Physiol* **103**: 1067-1073.
- Singha S, Choudhuri MA** (1990) Effect of salinity (NaCl) stress on H₂O₂ metabolism in *Vigna* and *Oryza* seedlings. *Biochemie und Physiologie der Pflanzen* **186**: 69-74.
- Smeekens S** (2000) Sugar-induced signal transduction in plants. *Ann Rev Plant Physiol Plant Mol Biol* **51**: 49-81.
- Smirnoff N** (1993) The role of active oxygen in the response of plants to water deficit and desiccation. *New Phytol* **125**: 27-58.
- Sreenivasulu N, Ramanjulu S, Ramachandra-Kini K, Prakash HS, Shetty HS, Savithri HS, Sudhakar C** (1999) Peroxidase activity and peroxidase isoforms as modified by salt stress in two cultivars of *foxtail millet*. *Plant Sci* **141**: 1-9.
- Sreenivasulu N, Grimm B, Wobus U, Weschke W** (2000) Differential response of antioxidant compounds to salinity stress in salt-tolerant and salt-sensitive seedlings of foxtail millet (*Setaria italica*). *Physiol plant* **109**: 435-442.
- Sreenivasulu N, Altschmied L, Panitz R, Hähnel U, Michalek W, Weschke W, Wobus U** (2002) Identification of genes specifically expressed in maternal and filial tissues of barley caryopses: A cDNA array analysis. *Mol Genet Genomics* **266**: 758-767.
- Stoesser G, Baker W, van den Broek A, Camon E, Garcia-Pastor M, Kanz C, Kulikova T, Leinonen R, Lin Q, Lombard V, Lopez R, Redaschi N, Stoehr P, Tuli Tzouvara K, Vaughan R** (2002) The EMBL Nucleotide Sequence Database. *Nucleic Acids Res* **30**: 21-26.
- Sturm A** (1999) Invertases. Primary structures, functions, and roles in plant development and sucrose partitioning. *Plant Physiol* **121**: 1-7.
- Sturm A, Tang GQ** (1999) The sucrose-cleaving enzymes of plants are crucial for development, growth and carbon partitioning. *Trends Plant Sci* **4**: 401-407.
- Sugimoto M., Furui S, Suzuki Y** (1997a) Molecular cloning and characterization of a cDNA encoding putative phospholipid hydroperoxide glutathione peroxidase from spinach. *Biosci Biotech Biochem* **61**: 1379-1381.

- Sugimoto M, Sakamoto W** (1997b) Putative phospholipid hydroperoxide glutathione peroxidase gene from *Arabidopsis thaliana* induced by oxidative stress. *Genes Genetic Systematics* **72**: 311-316.
- Tavazoie S, Hughes JD, Campbell MJ, Cho RJ, Church GM** (1999) Systematic determination of genetic network architecture. *Nat Genet* **22**: 281-285.
- Tamayo P, Slonim D, Mesirov J, Zhu Q, Kitareewan S, Dmitrovsky E, Lande, ES, Golub TR** (1999) Interpreting patterns of gene expression with self-organizing maps: Methods and application to hematopoietic differentiation. *Proc Natl Acad Sci USA* **96**: 2907-2912.
- Takeda S, Mano S, Ohto M, Nakamura K** (1994) Inhibitors of protein phosphatases I and 2A block the sugar-inducible gene expression in plants. *Plant Physiol* **106**: 567-574.
- Takeda T, Toyofuku K, Matsukura C, Yamaguchi J** (2001) Sugar transporters involved in flowering and grain development of rice. *J Plant Physiol* **158**: 465-470.
- Tanaka TS, Jaradat SA, Lim MK, Kargul GJ, Wang XH, Grahovac MJ, Pantano S, Sano Y, Piao Y, Nagaraja R, Doi H, Wood WH, Becker KG, Ko MSH** (2000) Genome-wide expression profiling of mid-gestation placenta and embryo using a 15,000 mouse developmental cDNA microarray. *Proc Natl Acad Sci USA* **97**: 9127-9132.
- Tepperman JM, Zhu T, Chang HS, Wang X, Quail PH** (2001) Multiple transcription-factor genes are early targets of phytochrome A signaling. *Proc Natl Acad Sci USA* **98**: 9437-9442.
- Tobias RB, Boyer CD, Shannon JC** (1992) Alterations in carbohydrate intermediates in the endosperm of starch-deficient maize (*Za mays* L.) genotypes. *Plant Physiol* **99**: 146-152.
- Tran L, Inoue Y, Kimura A** (1993) Oxidative stress response in yeast: purification and some properties of a membrane-bound glutathione peroxidase from *Hansenula mrakii*. *Biochim Biophys Acta* **1164**: 166-172.
- Tsugane K, Kobayashi K, Niwa Y, Ohba Y, Wada K, Kobayashi H** (1999) A recessive *Arabidopsis* mutant that grows photoautotrophically under salt stress shows enhanced active oxygen detoxification. *Plant Cell* **11**: 1195-1206.
- Tyynelä J, Stitt M, Lönneborg A, Smeekens S, Schulman AH** (1995) Metabolism of starch synthesis in developing grains of the *shx* shrunken mutant of barley (*Hordeum vulgare*). *Physiol Plant* **93**: 77-84.
- Ursini F, Maiorino M, Brigelius-Flohé R, Aumann KD, Roveri A, Schomburg D, Flohé L** (1995) Diversity of glutathione peroxidase. *Methods Enzym* **252**: 38-53.
- Van de Loo FJ, Turner S, Somerville C** (1995) Expressed sequence tags from developing castor seeds. *Plant Physiol* **108**: 1141-1150.

- Weber H, Borisjuk L, Heim U, Buchner P, Wobus U** (1995) Seed coat-associated invertases of fava-bean control both unloading and storage functions – cloning and cell-type-specific expression. *Plant Cell* **7**: 1835-1846.
- Weber H, Borisjuk L, Wobus U** (1996) Controlling seed development and seed size in *Vicia faba*: A role for seed coat-associated invertases and carbohydrate state. *Plant J* **10**: 823-834.
- Weber H, Borisjuk L, Wobus U** (1997) Sugar import and metabolism during seed development. *Trends Plant Sci* **2**: 169-174.
- Weber H, Heim U, Golombek S, Borisjuk L, Wobus U** (1998) Assimilate uptake and the regulation of seed development. *Seed Sci Res* **8**: 331-345.
- Weber H, Rolletschek H, Heim U, Golombek S, Gubatz S, Wobus U** (2000) Antisense-inhibition of ADP-glucose pyrophosphorylase in developing seeds of *Vicia narbonensis* moderately decreases starch but increases protein content and affects seed maturation. *Plant J* **24**: 33-43.
- Weschke W, Panitz R, Sauer N, Wang Q, Neubohn B, Weber H, Wobus U** (2000) Sucrose transport into barley seeds: molecular characterization of two transporters and implications for seed development and starch accumulation. *Plant J* **21**: 455-467.
- Weschke W, Panitz R, Gubatz S, Wang Q, Sreenivasulu N, Weber H, Wobus U** (2002) The role of invertases and hexose transporters in controlling sugar ratios in maternal and filial tissues of barley caryopses during early development. (submitted)
- Wingender E, Chen X, Hehl R, Karas H, Liebich I, Matys V, Meinhardt T, rüß M, Reuter I, Schacherer F** (2000) TRANSFAC: an integrated system for gene expression regulation *Nucleic Acids Res* **28**: 316-319.
- Wobus U, Weber H** (1999) Sugars as signal molecules in plant seed development. *Biol Chem* **380**: 937-944.
- White JA, Todd T, Newman T, Focks N, Girke T, de Ilarduya OM, Jaworski JG, Ohlrogge JB, Benning C** (2000) A new set of *Arabidopsis* expressed sequence tags from developing seeds. The metabolic pathway from carbohydrates to seed oil. *Plant Physiol* **124**: 1582-1594.
- Whitkus R, Doebley J, Lee M** (1992) Comparative genome mapping of sorghum and maize. *Genetics* **132**: 1119-1130.
- Xu FX, Chye ML** (1999) Expression of cysteine proteinase during developmental events associated with programmed cell death in brinjal. *Plant J* **17**: 321-327.
- Yeo AR, Flowers TJ** (1983) Varietal differences in the toxicity of sodium ions in rice leaves. *Physiol Plant* **59**: 189-195.

Young TE, Gallie DR, DeMason DA (1997) Ethylene-mediated programmed cell death during maize endosperm development of wild-type and *shrunken2* genotypes. *Plant Physiol* 115: 737-751.

ACKNOWLEDGEMENTS

I am particularly grateful to Prof. Dr. Ulrich Wobus, Director of the IPK, for giving me the opportunity to join his research group “Gene Expression”, for his careful supervision, guidance, helpful and stimulating discussions, for critical reading of the dissertation and providing his valuable time during this work.

I deem it a great pleasure to express my sincere thanks to Dr. Winfriede Weschke for constant encouragement, guidance, valuable suggestions during the methodology adopted during the course of this work, for cDNA library construction of foxtail millet and critical reading of the dissertation.

I am thankful to Dr. Lothar Altschmied, who introduced me to bioinformatic tools and also for the performance of annotation of ESTs and clustering analysis and helpful suggestions for dissertation writing. I want to extend my gratitude to Mr. Urs Hähnel to introduce me to handling of Robots used in spotting techniques. I am thankful to Dr. Wolfgang Michalek for providing EST clones and Dr. Volodymyr Radchuk for probe preparation. I am indebted to Dr. Reinhard Panitz and Dr. Hardy Rolletchek for their carrying out histological analyses of *seg8* mutant and sugar measurements, respectively. I am thankful to Dr. Manoela Miranda for isolation of PHGPX clone and its alignment. I am thankful to Dr. C. Horstman for help in FPLC purification and Dr. H.S. Prakash for peptide sequencing. I am grateful to Mrs. Gabi Einert for her technical assistance in tissue separation and Mrs. Angela Stegman and Mrs. Elsa Fessel for support in laboratory matters. I would also like to thank Mrs. Tiemann for the quality help in graphic work. For help in web page creation I thank Mr. Vasudeva Chari and proof reading of draft I thank Dr. Perisamy Theriappan. I would like to thank all the coworkers of the “Genwirkung” group for the scientifically stimulating environment and constant support that has promoted this work.

I wish to express my heartfelt thanks to Prof. D. Frankowiak, NDSU, USA for providing *seg8* mutant transferred to the genetic background of Bowman. I thank Andhra Pradesh Agricultural Experimental Station, India, for providing salt-tolerant and salt-sensitive cultivars of foxtail millet.

I am grateful to the financial support from the Land Sachsen Anhalt (FKZ: 2687/0087B) and BMBF (Functional genomics of developing and germinating barley seeds GABI-SEED).

Finally, I thank the authorities of the Institute of Plant Genetics and Crop Plant Research (IPK), Gatersleben, Germany for providing the facilities to carry out this work.

Erklärung

Hiermit erkläre Ich, daß diese Arbeit von mir abgefertigt wurde. Es wurden keine anderen als die in der Literatur zitierten Hilfsmittel benutzt. Diese Arbeit wurde weder für vergebliche Promotionsversuche verwendet noch irgendwo sonst zur Promotion eingereicht.

Nese Sreenivasulu

Gatersleben, im May 2002

CURRICULUM-VITAE

- 1. Name** Nese Sreenivasulu
- 2. Address** Department of Molecular Genetics
Institut für Pflanzengenetik und
Kulturpflanzenforschung (IPK)
Corrensstraße 03
Gatersleben 06466
- 3. Place of Birth** Anantapur
- 4. Date of Birth** 01- 05- 1973
- 5. Nationality** Indian

6. Academic record

Name of the University	Examination	Year	Division	Marks(%)	Subject
Govt. Science College Chitradurga	B.Sc., (graduate)	1990-93	First	61.66	Chemistry, Botany, Zoology
S.K. University Anantapur	M.Sc., (post-graduate)	1994-95	First	73.58	Botany
Mysore University Mysore	M.Phil (pre-Ph.D)	1996	First	71.75	Seed Tech.
Institute of Plant Genetics And Crop Plant Research (IPK) Gatersleben, Germany		1998-2002	Doctoral fellow		

7. Research Experience

M.Sc., Project work- ‘Studies on Effect of Salt stress on groundnut cultivars’ under the guidance of Dr. C. Sudhakar, Department of Botany, S.K. University, Anantapur.

Short-term research programme- working in association with Dr. C. Sudhakar on ‘Differential sensitivity of mulberry cultivars to water stress on photosynthetic parameters’

M.Phil Dissertation work- ‘Laboratory procedures for genetic purity assessment of maize genotypes’ under the guidance of Prof. H.S. Prakash and Prof. H.S. Shetty, Department of Applied Botany and Biotechnology, Mysore University, Mysore.

Ph.D thesis- ‘Construction and use of cDNA arrays in studying barley seed development and foxtail millet salt tolerance’ under the guidance of Prof. U. Wobus, Institute of Plant Genetics and Crop Plant Research (IPK), Gatersleben, Germany.

8. Teaching Experience

Engaged both theory and practical classes for Master’s students in S.K. University, Anantapur.

9. Awards/Fellowships

- a. Third Rank in M.Sc., Botany, 1995
- b. DST Senior Research Fellow, 1996
- c. DAAD Fellow, 1998

Carried out an DST-sponsored major research project as a Senior Research Fellow entitled **‘Purification and Characterization of a salt stress induced protein (23 kDa) in *Setaria italica* L. (Foxtail millet)’**.

Scientific work carried out on the basis of DAAD fellowship, project entitled **‘Screening and Characterization of a gene coding for a 23kDa salt stress induced protein’** under the guidance of Prof. Ulrich Wobus, Department of Molecular Genetics, IPK, Gatersleben, Germany.

10. Papers published

N. Sreenivasulu, P.B. Kavi Kishor, R.K. Varshney and L. Altschmied. Mining functional information from cereal genomes- the utility of expressed sequence tags (ESTs). **Current Science** 83: 965-973, 2002a

N. Sreenivasulu, L. Altschmied, R. Panitz, U. Hähnel, W. Michalek, W. Weschke and U. Wobus. Identification of genes specifically expressed in maternal and filial tissues of barley caryopses: a cDNA array analysis. **Molecular Genetics and Genomics** 266: 758-767, 2002b.

E. Potokina, **N. Sreenivasulu**, L. Altschmied, W. Michalek, A. Graner. Differential gene expression during seed germination in barley (*Hordeum vulgare* L). **Functional and Integrative Genomics** 2: 28-39, 2002.

N. Sreenivasulu, B. Grimm, U. Wobus and W. Weschke. Differential response of antioxidant compounds to salinity stress in salt-tolerant and salt-sensitive seedlings of foxtail millet (*Setaria italaica*). **Physiologia plantarum** 109: 435-442, 2000.

S. G. Kumar, K.V. Madhusudhan, **N. Sreenivasulu** and C. Sudhakar. Stress responses in two genotypes of mulberry (*Morus alba* L.) under NaCl salinity. **Indian Journal of Experimental Biology** 38: 192-195, 2000.

N. Sreenivasulu, S. Ramanjulu, K.R. Kini, H.S. Prakash, H.S. Shetty, H.S. Savithri and C. Sudhakar. Peroxidase activity and peroxidase isoforms as modified by salt stress in two cultivars of foxtail millet with differential salt tolerance. **Plant Science** 141: 1-9, 1999.

S. Ramanjulu, **N. Sreenivasulu**, S. Giridhara Kumar and C. Sudhakar. Photosynthetic characteristics in mulberry during water stress and rewatering. **Photosynthetica** 35(2): 259-263, 1998.

S. Ramanjulu, **N. Sreenivasulu** and C. Sudhakar. Effect of Water stress on photosynthesis in two mulberry genotypes with differential drought tolerance. **Photosynthetica** **35(2)**: 279-283, 1998.

N. Sreenivasulu, K. R. Kini, K.T. Pandurange Gowda, H.S. Prakash and H. S. Shetty. Protein and peroxidase markers of a maize hybrid Ganga-11 hybrid and its parental lines. **Tropical Agricultural Research and Extension** (in press)

11. Papers submitted

W. Weschke, R. Panitz, S. Gubatz, Q Wang, **N. Sreenivasulu**, H. Weber and U. Wobus. The role of invertases and hexose transporters in controlling sugar ratios in maternal and filial tissues of barley caryopses during early development. (submitted)

N. Sreenivasulu, L. Altschmied, V. Radchuk, U. Wobus and W. Weschke. Delineating distinct metabolic and developmental patterns in developing barley caryopses by DNA macroarray analysis. (manuscript in preparation)

N. Sreenivasulu, M. Miranda, H.S. Prakash, U. Wobus and W. Weschke. Molecular characterization of phospholipid hydroperoxide glutathione peroxidase gene and its corresponding protein in salt-tolerant cultivar of *Setaria italica* L. (manuscript in preparation)

12. Proceedings published

E. Potokina, M. Caspers, **N. Sreenivasulu**, M. Wang, L. Altschmied and A. Graner. Functional Genomics bei Gerste: Vom Erkenntnisgewinn zur züchterischen Nutzung. **Vorträge für Pflanzenzüchtung** 54: 173-181, 2002.

W. Weschke, **N. Sreenivasulu**, R. Panitz, H. Weber and U. Wobus. Wechselwirkung von maternalen and filialen Geweben in der frühen Entwicklung des Gerstenkorns – eine cDNA Array Analyse. **Vorträge für Pflanzenzüchtung** 52: 69-74, 2001.

N. Sreenivasulu, L. Altschmied, V. Radchuk, R. Panitz, W. Weschke and U. Wobus. Chasing the dream: Genomic approaches to barley seed development. **Proceedings of Seed Science and Technology in the New Millennium – Vistas and Vision** 27-28, 2001.

N. Sreenivasulu, M. Miranda, L. Altschmied, U. Wobus and W. Weschke. Differential expression of protective antioxidant components to NaCl stress in foxtail millet genotypes. **Proceedings of the 4th International Triticeae Symposium** 399-403, 2001.

N. Sreenivasulu, M. Siefken, U. Hähnel, W. Weschke, U. Wobus and L. Altschmied. (Authors **N.S** and **M.S** are contributed equally) Multiparallel expression analysis using EST-Clones from Barley. **Proceedings of Barley Genetics VIII** 196-198, 2000.

16. Abstracts Published

N. Sreenivasulu, L. Altschmied, V. Radchuk, U. Wobus and W. Weschke. Delineating distinct expression patterns of metabolic pathways in developing barley caryopses by DNA macroarray analysis. Published at 17th Long Ashton International Symposium, “New frontiers in plant development: From genes to phenotype” Bristol, England (page no. 83), 2002.

U. Wobus, L. Borisjuk, **N. Sreenivasulu**, S. Gubatz, H. Weber and W. Weschke. Carbon metabolism in developing seeds: the dual role of sugars. Published in Comparative Biochemistry and Physiology Part A (P2. 12b) 132: 2002.

N. Sreenivasulu, H. Rolletschek, S. Gubatz, V. Radchuk, U. Wobus and W. Weschke. The barley endosperm mutant *seg8*: Histological analysis, expression profiling and characteristic changes in metabolite profiles. Published at 6th Gatersleben Research Conference, "Plant Genetic Resources in the Genomic Era: Genetic diversity, Genome evolution and New Applications (Abstract no. P53, page no. 97), IPK, Gatersleben, Germany, 2002.

E. Potokina, M. Caspers, **N. Sreenivasulu**, M. Wang, A. Sorensen and A. Graner. Malting quality of barley cultivars in terms of gene expression. Published at 6th Gatersleben Research Conference, "Plant Genetic Resources in the Genomic Era: Genetic diversity, Genome evolution and New Applications (Abstract no. P44, page no. 88), IPK, Gatersleben, Germany, 2002.

N. Sreenivasulu, U. Wobus, M. Miranda, W. Weschke. A set of salt-induced genes identified in tolerant foxtail millet seedlings by using a barley cDNA macroarray. Published at 4th International Triticeae Symposium (page no. 137), Madrid, Spain.

N. Sreenivasulu, R. Panitz, V. Radchuk, L. Altschmied, U. Wobus and W. Weschke. Coordinated gene expression in maternal and filial seed organs analysed by cDNAarrays and insitu hybridization. Published at 14. Tagung Molekularbiologie der Pflanzen, Dabringhausen (Abstract no. 57), 2001

N. Sreenivasulu, W. Michalek, L. Altschmied, U. Hähnel, U. Wobus and W. Weschke. Using the cDNAarray technique in barley: identification of genes exclusively expressed in the maternal and filial tissue of the young caryopsis. Published at 8th International symposium on plant Seeds (Abstract no. P4), IPK, Gatersleben, Germany, 2000

N. Sreenivasulu, W. Weschke, B. Grimm and U. Wobus. The acidic guaicol peroxidase and ascorbate peroxidase responses modified by salt stress in two cultivars of foxtail millet (*Setaria italica* L.) differed in salt tolerance. Published at Peroxidase conference abstracts (Abstract no. 54), Columbus, Ohio, USA, 1999